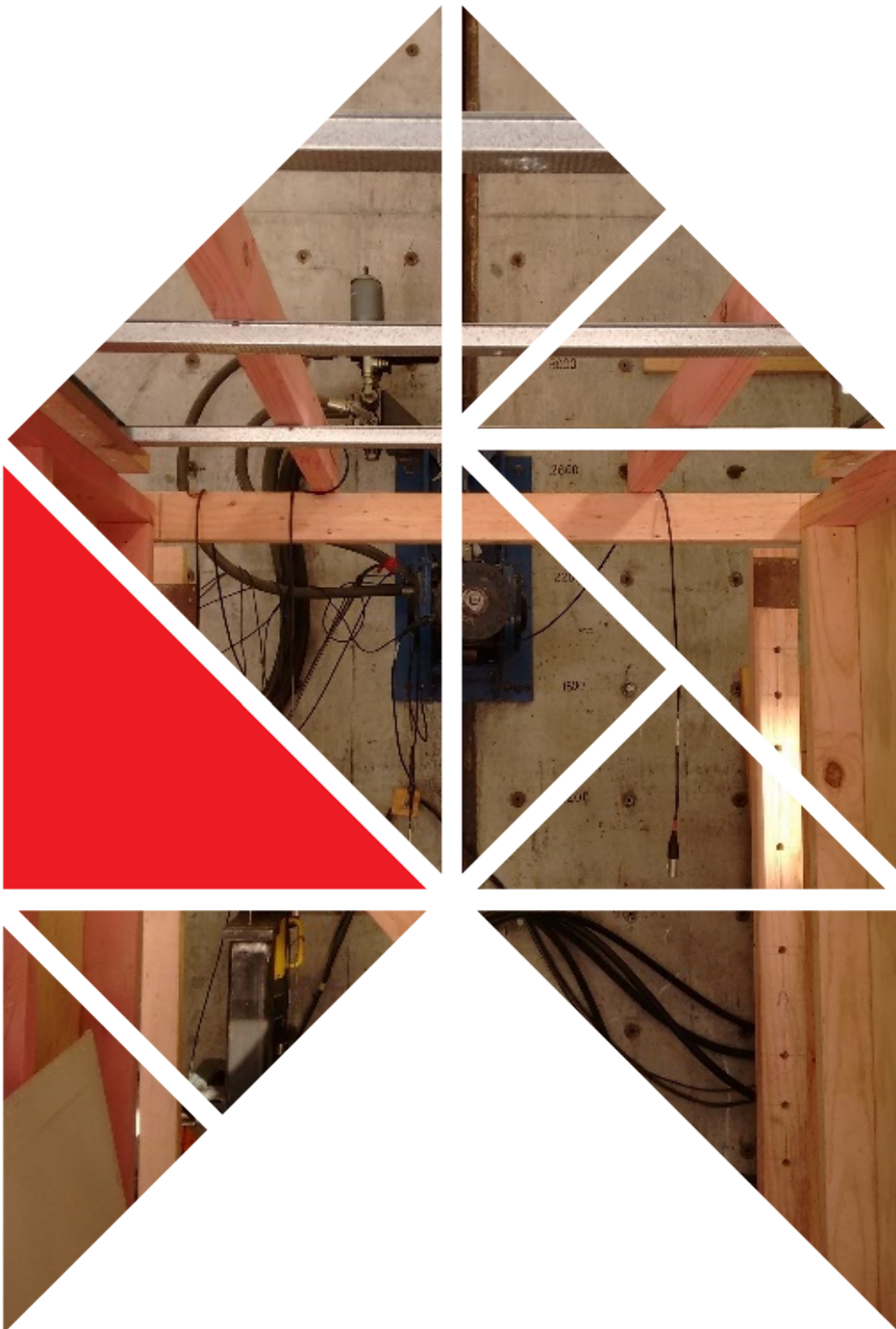


# Seismic effects of structural irregularity of light timber-framed buildings

Angela Liu and Roger Shelton





1222 Moonshine Rd  
RD1, Porirua 5381  
Private Bag 50 908  
Porirua 5240  
New Zealand  
[branz.nz](http://branz.nz)



Funded from the  
**Building Research Levy**

## Acknowledgements

We would like to thank:

- Dr David Carradine at BRANZ, who made the racking test data on plasterboard walls available for this study
- BRANZ Structures Lab for conducting the tests on plasterboard ceiling diaphragms.

# Seismic effects of structural irregularity of light timber-framed buildings

## BRANZ Study Report SR404

### Authors

Angela Liu and Roger Shelton

### Reference

Liu, A. & Shelton, R. (2018). *Seismic effects of structural irregularity of light timber-framed buildings*. BRANZ Study Report SR404. Judgeford, New Zealand: BRANZ Ltd.

### Abstract

The majority of residential buildings in New Zealand are low-rise light timber-framed (LTF) buildings, and their gravity load and lateral load-resisting systems are universally plasterboard-sheathed walls. Construction of residential LTF buildings in New Zealand largely follows a prescriptive standard – NZS 3604:2011 *Timber-framed buildings* – which specifies not only the seismic demand but also the seismic bracing provisions. Designers need to ensure the provided total seismic bracing capacity is at least equal to the total seismic bracing demand. NZS 3604:2011 also specifies the irregularity limits of bracing arrangements within a floor plan, which were established based on engineering rules of thumb rather than scientific evidence. Earthquake damage observed in the 2010/11 Canterbury earthquake sequence demonstrated that simple regular LTF houses performed well while irregular houses often had significant damage that was uneconomical to repair. This suggested that the irregularity of LTF buildings was an important factor responsible for the exacerbated earthquake damage. The objectives of this study were to quantify seismic effects of permissible irregularities of single-storey buildings in NZS 3604:2011 and to provide scientific evidence for elaborating irregularity limits in NZS 3604:2011.

A literature review of research efforts on seismic behaviour of irregular buildings was conducted. The review revealed that three-dimensional analyses with adequate modelling of lateral seismic-resisting systems and diaphragms are essential to capture the necessary seismic behaviour of irregular building structures. To adequately model lateral seismic-resisting elements (plasterboard walls) of LTF buildings, many sets of test data collected from past racking tests on plasterboard walls were studied. Subsequently, a racking model of plasterboard bracing wall elements was developed, and the degrading behaviour of plasterboard walls was simulated by the degrading shear modulus. Similarly, in-plane rigidity performance of ceiling diaphragms of LTF buildings was experimentally studied in this project. The test programme consisted of two-stage ceiling diaphragm tests, including a full-scale ceiling diaphragm test and four small-scale ceiling diaphragms with different construction details as often used in different applications. Consequently, a mathematical model was developed to simulate

the in-plane rigidity of plasterboard ceiling diaphragms as typical of New Zealand practice.

To study the seismic effects of permissible plan irregularities from NZS 3604:2011 on LTF buildings, six case study buildings with different permissible bracing irregularities were seismically designed to NZS 3604:2011. Three-dimensional non-linear push-over analyses were conducted of these model buildings where LTF walls and ceiling diaphragms were modelled using the models developed in this project.

The study revealed that permissible irregular bracing arrangements in NZS 3604:2011 could amplify lateral deflections by 500% compared with regular counterparts. The consequence is that irregular LTF buildings within the scope of NZS 3604:2011 could be unacceptably flexible in earthquakes, implying the need for tightening the irregularity limits in NZS 3604:2011.

## Keywords

LTF buildings, plasterboard walls, racking performance, seismic bracing, plasterboard ceiling diaphragms, residential buildings, in-plane irregularity.

## Contents

|           |  |           |
|-----------|--|-----------|
| <b>1.</b> | <b>INTRODUCTION .....</b>  | <b>1</b>  |
| 1.1       | Background and objectives.....   | 1         |
| 1.2       | Research design and report organisation.....   | 2         |
| <b>2.</b> | <b>RESEARCH REVIEW ON SEISMIC EFFECTS OF STRUCTURAL IRREGULARITY .....</b>                 | <b>3</b>  |
| 2.1       | Structural irregularities and relevant standards .....                                     | 3         |
| 2.2       | Research review of seismic effects of structural irregularities in concrete buildings..... | 4         |
| 2.3       | Research review of seismic effects of structural irregularities in LTF buildings.....      | 5         |
| 2.4       | Summary.....   | 6         |
| <b>3.</b> | <b>SEISMIC BEHAVIOUR OF LTF BRACING WALLS .....</b>  | <b>7</b>  |
| 3.1       | Characteristics of bracing behaviour of LTF walls .....                                    | 7         |
| 3.2       | Racking model of plasterboard walls .....  | 10        |
| 3.2.1     | Outlines of the model development .....  | 10        |
| 3.2.2     | Mathematical model development .....   | 10        |
| 3.3       | Summary.....   | 12        |
| <b>4.</b> | <b>RIGIDITY STUDY OF ROOF/CEILING DIAPHRAGMS.....</b>                                      | <b>13</b> |
| 4.1       | In-plane behaviour of diaphragms in LTF buildings.....                                     | 13        |
| 4.2       | Tests of plasterboard ceiling diaphragms.....  | 14        |
| 4.2.1     | Tests of plasterboard ceiling diaphragms .....   | 14        |
| 4.2.2     | Test observations and findings.....  | 14        |
| 4.3       | In-plane rigidity of plasterboard ceiling diaphragms.....                                  | 15        |
| 4.3.1     | Engineering basis of the model development.....  | 15        |
| 4.3.2     | Mathematical model development .....   | 16        |
| 4.4       | Summary.....   | 18        |
| <b>5.</b> | <b>SEISMIC PERFORMANCE OF PERMISSIBLE DESIGNS AND IMPROVEMENTS.....</b>                    | <b>19</b> |
| 5.1       | Case study LTF buildings.....  | 19        |
| 5.1.1     | Rectangular case study buildings.....  | 19        |
| 5.1.2     | L-shaped case study buildings.....   | 23        |
| 5.1.3     | Summary .....  | 26        |
| 5.2       | Structural modelling and seismic analyses .....  | 26        |
| 5.2.1     | Modelling techniques of LTF walls and ceiling diaphragms .....                             | 27        |
| 5.2.2     | Equivalent static push-over analyses.....  | 28        |
| 5.2.3     | Results of analysis .....  | 29        |
| 5.3       | Discussion .....   | 32        |
| 5.3.1     | Seismic performance of permissible earthquake designs.....                                 | 32        |
| 5.3.2     | Effect of boosting minimum bracing provisions.....   | 33        |
| 5.3.3     | Effects of ceiling diaphragm rigidity .....  | 33        |
| 5.3.4     | Overall seismic demand.....  | 33        |
| <b>6.</b> | <b>CONCLUSIONS AND RECOMMENDATIONS.....</b>  | <b>35</b> |
|           | <b>REFERENCES .....</b>  | <b>37</b> |
|           | <b>APPENDIX A: SEISMIC BEHAVIOUR OF LTF BRACING WALLS .....</b>                            | <b>41</b> |

## APPENDIX B: RIGIDITY STUDY OF ROOF/CEILING DIAPHRAGMS..... 49

### Figures

|   |    |
|---|----|
| Figure 1. The sheathing (two plasterboard sheets) worked as one plate. Deformation is mainly due to slips. .... | 8  |
| Figure 2. Final appearance after racking on a plasterboard wall of 2.4 m long. ....                             | 8  |
| Figure 3. The sheathing (two plasterboard sheets) worked as one plate. Deformation is mainly due to slips. .... | 9  |
| Figure 4. Final appearance after racking on a plasterboard wall of 2.4 m long. ....                             | 9  |
| Figure 5. Floor plan of single-level rectangular case study buildings.....                                      | 20 |
| Figure 6. Bracing arrangement of case study building RR.....  | 21 |
| Figure 7. Bracing arrangement of case study building RIR1.....  | 22 |
| Figure 8. Bracing arrangement of case study building RIR2.....  | 22 |
| Figure 9. Plan of L-shaped case study buildings. ....   | 23 |
| Figure 10. Bracing distribution of case study building LR.....  | 24 |
| Figure 11. Bracing distribution of case study building LIR1.....  | 25 |
| Figure 12. Bracing distribution of case study building LIR2.....  | 25 |
| Figure 13. Deflections obtained for case study building RR. ....  | 30 |
| Figure 14. Deflections obtained for case study building RIR1. ....  | 30 |
| Figure 15. Deflections obtained for case study building RIR2. ....  | 30 |
| Figure 16. Deflections obtained for building LR. ....   | 31 |
| Figure 17. Deflections obtained for building LIR1. ....   | 31 |
| Figure 18. Deflections obtained for building LIR2. ....   | 31 |
| Figure 19. P21 test arrangement. ....   | 42 |
| Figure 20. Hysteresis loops of a 1.2 m long plasterboard wall. ....   | 43 |
| Figure 21. Wall rocking mode. ....  | 46 |
| Figure 22. Test results versus the model developed. ....  | 47 |
| Figure 23. Construction of dwanged and battened ceilings (Shelton, 2004). ....                                  | 52 |
| Figure 24. Common diaphragm construction practice (Winstone Wallboards, 2014). ..                               | 53 |
| Figure 25. Plan of the full-scale ceiling test specimen and test set-up. ....                                   | 54 |
| Figure 26. Edge details of the test specimen and the support details ....                                       | 55 |
| Figure 27. Mitek 6T10 Tylok connector at corners of diaphragm.....  | 55 |
| Figure 28. Framing of the full-scale ceiling test specimen. ....  | 56 |
| Figure 29. Full-scale test specimen prior to testing.....   | 56 |
| Figure 30. Arrangement of slip gauges.....  | 57 |
| Figure 31. Arrangement of frame displacement gauges. ....   | 58 |
| Figure 32. Plot of applied and adjusted loads.....  | 59 |
| Figure 33. Damage associated with screw failures.....   | 59 |
| Figure 34. Disengagement of linings at southwest corner due to screw fixing failure. .                          | 60 |
| Figure 35. Hysteresis loops obtained from the full-scale ceiling diaphragm test. ....                           | 61 |
| Figure 36. Absolute deflections at different locations of plasterboard sheet (mm) ....                          | 61 |
| Figure 37. Contribution of screw slips to the total diaphragm deflection. ....                                  | 62 |
| Figure 38. Screw slip model. ....   | 63 |
| Figure 39. Validation of predicted deflection versus measured deflection.....                                   | 63 |

|  |    |
|--|----|
| Figure 40. Test set up for the small-scale ceiling tests. ....                                   | 65 |
| Figure 41. Hysteresis behaviour of screw slips of four small-scale ceiling diaphragm tests. .... | 66 |

## Tables

|   |    |
|---|----|
| Table 1. Equivalent shear modulus ( $G_{eq}$ ). ....  | 11 |
| Table 2. $G_v$ of virtually solid LTF walls. ....   | 12 |
| Table 3. Slip-related ceiling diaphragm rigidity. ....  | 15 |
| Table 4. Equivalent shear modulus, $G_e$ , of the full-scale ceiling diaphragm test. ....               | 17 |
| Table 5. Estimated equivalent shear modulus, $G_e$ . ....   | 17 |
| Table 6. $G_e$ of virtually solid plasterboard ceiling diaphragms. ....                                 | 18 |
| Table 7. Rectangular case study buildings. ....   | 20 |
| Table 8. Summary of seismic bracing designs of rectangular case study buildings RR, RIR1 and RIR2. .... | 23 |
| Table 9. Summary of the bracing designs of case study buildings LR, LIR1 and LIR2. ....                 | 26 |
| Table 10. $G$ of virtual solid LTF walls. ....  | 27 |
| Table 11. $G$ of virtual solid plasterboard ceiling diaphragm as for the full-scale test. ....          | 27 |
| Table 12. Range of shear modulus, $G$ , of plasterboard ceiling diaphragms. ....                        | 28 |
| Table 13. Seismic actions. ....   | 28 |
| Table 14. $G$ of wall elements of rectangular buildings (MPa). ....                                     | 29 |
| Table 15. $G$ of wall elements of L-shaped buildings (MPa). ....  | 29 |
| Table 16. $G$ for ceiling diaphragms of rectangular and L-shaped buildings (MPa) ....                   | 29 |
| Table 17. Lateral deflections along different grid lines (rectangular buildings). ....                  | 30 |
| Table 18. Lateral deflections along different grid lines (L-shaped buildings). ....                     | 32 |
| Table 19. Fundamental periods $T$ (s). ....   | 34 |
| Table 20. Attainment of racking strength at the same deflection level. ....                             | 43 |
| Table 21. Equivalent damping levels, $\xi_{eq}$ . ....  | 44 |
| Table 22. Equivalent shear modulus ( $G$ ). ....  | 47 |
| Table 23. Dimensional limits of ceiling diaphragms in NZS 3604:2011. ....                               | 51 |
| Table 24. Provisions in NZS 3604:2011 for floor and ceiling diaphragms. ....                            | 51 |
| Table 25. Small-scale ceiling diaphragm tests. ....   | 64 |
| Table 26. Slip-related ceiling diaphragm rigidity. ....   | 66 |
| Table 27. Equivalent shear modulus, $G_e$ , of the full-scale ceiling diaphragm test. ....              | 68 |
| Table 28. Estimated equivalent shear modulus, $G_e$ . ....  | 68 |



# 1. Introduction

## 1.1 Background and objectives

The majority of residential buildings in New Zealand are light timber-framed (LTF) buildings. By definition, LTF buildings refers to low-rise residential buildings, which contain a suspended timber floor/roof and have sheathed LTF walls as the gravity load and lateral load-resisting systems. Construction of residential LTF buildings in New Zealand largely follows a prescriptive standard – NZS 3604:2011 *Timber-framed buildings*.

Although a descriptive standard, the development of NZS 3604:2011 has an engineering basis (Shelton, 2013). The seismic engineering basis in NZS 3604:2011 used a force-based approach in deriving the seismic design actions (demand). The force-based approach was the equivalent static method with a fundamental period of  $T_1 = 0.45$  second and a ductility of  $\mu = 3.5$  as in NZS 1170.5:2004 *Structural design actions – Part 5: Earthquake actions – New Zealand*. In using NZS 3604:2011, the seismic demand is determined by reading from a predefined table, based on the soil classification, seismic hazard zone, house foundation type (concrete slab on ground or suspended timber floor) and building envelope weight. NZS 3604:2011 also specifies that the P21 test and evaluation procedure developed and published by BRANZ be used to evaluate the seismic bracing capacity of proprietary LTF wall elements. Designers need to ensure the provided bracing capacity is at least equal to the bracing demand.

Apart from matching the provided total bracing capacity with the overall bracing demand, NZS 3604:2011 also specifies the rule for distributing bracing elements within a floor plan. Bracing lines are required to be spaced at no more than 6 m in each direction, and the bracing arrangements can be irregular but shall be within certain limits. The irregularity limits specified in NZS 3604:2011 are:

- the minimum bracing provision in each bracing line should be greater than 100 bracing units (BUs) or 50% of the total bracing demand divided by the number of bracing lines in the direction being considered
- the minimum bracing provision in each bracing line should be not less than 15 BUs/m of external wall length for external walls.

It is noted that these irregularity limits were established based on engineering rules of thumb. There has been neither any scientific research work to quantify the adverse seismic effects of structural irregularity for NZS 3604:2011 buildings nor any work to justify the appropriateness of the irregularity allowance in NZS 3604:2011.

Earthquake damage observed in the 2010/11 Canterbury earthquake sequence demonstrated that residential LTF buildings all achieved the New Zealand Building Code objective of “safeguarding people from injury caused by structural failure”. However, the observed earthquake damage in Christchurch showed significant discrepancies. Some houses had no damage at all while others had damage well beyond repair (Liu, 2015). What stood out was that simple regular LTF houses performed well while irregular houses often had significant damage that was uneconomical to repair. This suggested that the irregularity of LTF buildings was an important factor responsible for the exacerbated earthquake damage.

The objectives of this study were to:

- to study quantitatively the seismic effects of permissible plan irregularities within the scope of NZS 3604:2011 on the seismic performance of LTF buildings
- provide a scientific basis for adjusting the current irregularity limits in NZS 3604:2011 if necessary.

## 1.2 Research design and report organisation

Section 2 describes a literature search on seismic effects of structural irregularities in a broad structural engineering context. As a result of this review, some critical considerations in studying seismic effects of plan irregularity of low-rise LTF buildings were identified. In detail, this review has highlighted that an essential part in studying seismic effects of structural irregularity of low-rise LTF buildings is a three-dimensional analysis with adequate modelling techniques capable of capturing the non-linear performance of lateral load-resisting systems (timber bracing walls in this case) and diaphragms.

As part of the modelling development of timber bracing walls, a literature search was conducted on seismic performance of LTF walls, which is described in section 3 and Appendix A. The review revealed that most of these research efforts on modelling technique of bracing performance of LTF walls were based on overseas practices, which were different from New Zealand practice. To develop a model capable of capturing the racking performance of timber walls as typical of New Zealand practice, results of many racking tests of LTF walls typical of New Zealand residential construction were collected and studied. Subsequently, the racking model of LTF walls as typical of New Zealand residential construction was developed for the study conducted in this project.

Similar to LTF bracing walls, proper modelling of in-plane behaviour of timber diaphragms is a necessary part of the intended three-dimensional analyses for LTF buildings with plan irregularities. Section 4 describes a literature review of in-plane structural performance of timber diaphragms that was conducted, and the available methods were found not suitable for New Zealand residential construction practice. As such, current roof diaphragm construction practice in New Zealand was surveyed. A test programme on roof ceiling diaphragms as typical of New Zealand practice was designed and a series of tests were conducted. Subsequently, the in-plane stiffness model of roof ceiling diaphragms as typical of New Zealand residential construction was developed, based on the test results, and the developed model was used for the study conducted in this project. This part of the work is summarised in Appendix B.

The studies on seismic performance conducted for LTF buildings with permissible plan irregularities from NZS 3604:2011 are presented in section 5. Several case study buildings are described that were seismically designed to NZS 3604:2011 and had different permissible bracing irregularities. Following descriptions of these case study buildings, the modelling techniques in evaluating the seismic performance of each of these buildings and the analysis results are presented. The effects of permissible bracing irregularities from NZS 3604:2011 and other design aspects on the expected seismic performance of LTF residential buildings are also discussed.

Section 6 summarises the findings and recommendations from the study.

## 2. Research review on seismic effects of structural irregularity

### 2.1 Structural irregularities and relevant standards

Irregularities in building structures cannot be avoided and occur for various reasons. A few examples are:

- irregular shapes of floor plans because of the functional requirements or restrictions of available sites or something else
- non-symmetrical arrangements of lateral load-resisting systems in a building structure within a floor plan or along the elevation
- significant mass variation within a floor plan or from floor to floor.

Irregularities in building structures can be broadly classified into two categories – vertical and horizontal (plan) irregularities. Vertical irregularity arises due to the change of the stiffness and/or strength of the lateral load-resisting systems along the building height. Horizontal irregularity arises when the distance between the centre of rigidity and the centre of the applied storey shear force at any level of the building becomes significant.

When a building structure has vertical irregularities, deformation/damage of the building in earthquakes could concentrate in one level, leading to undesirable earthquake performance. When a building structure has plan irregularities, the building will have torsional responses in earthquakes. The translational seismic responses will be coupled with the torsional responses, leading to significantly sophisticated seismic behaviour.

Past earthquake observations have frequently demonstrated that simple and regular structures perform a lot better in earthquakes compared to similar but irregular buildings (Arnold & Reitherman, 1982; Paulay & Priestley, 1992). How to make appropriate allowance for the detrimental effects of structural irregularity in designing buildings for earthquakes is one of the most challenging tasks (Paulay & Priestley, 1992). The rule of thumb is the greater the irregularities of a structure, the harder it is to predict its seismic performance.

To address adverse seismic effects of structural irregularities, the current seismic design standards around the world are based on the same principles. Typically, the standards specify certain irregularity limits, and these limits are used to classify a building structure as either regular or irregular. Such irregularity limits are intended to determine the sophistication of the analysis method used for seismically designing the building structures. While the specified irregularity limits provide some insights on the likely undesirable effects due to the presence of irregularity, these limits were developed by consensus, rather than being based on quantitative data (SEAOC, 1999). Earthquake damage observed in recent earthquakes shows that the specified requirements are inadequate to address the uncertainties associated with structural irregularities (Canterbury Earthquakes Royal Commission, 2012). As such, our understanding of the effects of structural irregularities on seismic performance of building structures needs to be significantly advanced.

In New Zealand, the seismic loading standard relating to seismic designs of all types of structures is NZS 1170.5:2004. This standard classifies a building structure as either

regular or irregular according to the specified vertical and horizontal irregularity limits. With regards to the seismic analysis, NZS 1170.5:2004 specifies the application limits of different analysis methods, based on structural irregularity classification of the buildings as well as the sizes of the buildings. For instance, the standard specifies that the equivalent static method of analysis, which is the simplest analysis method, shall be used only when at least one of the following criteria is satisfied:

- The height between the base and the top of the structure is less than 10 m.
- The largest translational period calculated is less than 0.4 seconds.
- The structure is not classified as irregular and the largest translational period is less than 2.0 seconds.

For structures that do not satisfy at least one of these application criteria, a more sophisticated analysis method is required – for example, the modal response spectrum method or numerical integration time history analysis.

Similar to overseas standards, the New Zealand seismic design standard NZS 1170.5:2004 implies that the seismic performance analyses of irregular and/or taller buildings require significantly more sophisticated analysis tools than regular (simple) and small buildings.

## 2.2 Research review of seismic effects of structural irregularities in concrete buildings

There have been significant research efforts made in understanding the effects of structural irregularity on seismic performance of building structures. However, significant work at the University of Canterbury by Paulay in the 1990s and early 2000s brought about realisation that current methods addressing the irregularity-related seismic torsional responses were a fundamental mismatch with the modern seismic design philosophy of capacity design (Paulay, 1996, 1997, 2000; Paulay & Priestley, 1992). In summary, current seismic code provision for structural irregularity was based on an elastic approach, while seismic design philosophy of modern codes relies on inelastic deformations in well defined regions to dissipate the energy.

In recent years, there have been renewed research interests in the seismic effects due to structural irregularities. Research was mainly limited to the seismic effects of large and heavy building structures, such as reinforced concrete (RC)-framed buildings and RC wall buildings, ranging from the seismic effects of in-plan irregularities to the seismic effects of vertical irregularities. The studies on in-plan irregularities included in-plan irregularities due to either non-uniform distribution of mass or strength and stiffness of lateral seismic-resisting systems within the building plan (Chopra & Goel, 2004; Fajfar, Marusic & Perus, 2006). The studies on vertical irregularities included vertical irregularities due to the variation of masses (FEMA, 2012; Valmundsson & Nau, 1997; Al-Ali & Krawinkler, 1998) and/or the variation of stiffness and strength of lateral load-resisting systems along the building height. In New Zealand, more recent work in this area included the parametric study at the University of Canterbury by Sadashiva (2010) where the effects of various irregularities on seismic demands were quantified by employing a single-degree-of-freedom model – a significantly simplified analysis model.

The research on seismic effects of structural irregularities in building structures remains at the development stages, and currently there are no elaborate methods

developed. Nevertheless, some fundamental principles revealed from these studies are applicable to the study of structural irregularity in LTF buildings:

- Global analyses (three-dimensional analyses) with adequate stiffness modelling of the lateral seismic-resisting systems and the floor diaphragms are necessary in studying the seismic performance of building structures with structural irregularities.
- Flexibility of floor diaphragms plays an important role when structural irregularity exists (FEMA, 2012; Liu, 2011).

## 2.3 Research review of seismic effects of structural irregularities in LTF buildings

LTF residential buildings in New Zealand are usually low rise and they are constructed using a platform construction technique, which is different from that used in concrete structures or steel structures. For heavy structures (RC or steel structures), seismic-resisting systems commonly continue from the base to the top of the buildings. In contrast, LTF buildings are constructed using a platform technique and have no requirements for bracing elements at one level to be aligned with bracing elements at the level below or above. As such, timber-framed residential buildings are characterised by frequent offsets of seismic bracing wall elements from level to level. This is one of the most important factors considered in classifying buildings as irregular buildings in NZS 1170.5:2004, meaning that LTF buildings potentially have more significant structural irregularities.

As the lateral seismic-resisting systems in an LTF building have offsets from floor to floor, diaphragms play greater roles for transmitting seismic loads between bracing systems compared with structures without offsets of lateral load-resisting systems. However, the floor and roof diaphragms of LTF buildings are of timber construction and they are not as rigid as concrete floors. As a consequence, the seismic effects of structural irregularities in LTF buildings are expected to be different from those of RC or steel buildings.

The seismic design requirements for LTF residential buildings are traditionally less rigorous than other structures. There is no evidence of research efforts made in New Zealand on seismic effects of structural irregularities in LTF buildings. Limited research activities on the seismic effects of specific structural aspects on irregular LTF buildings have been undertaken overseas and are reviewed below.

Lucksiri et al. (2012) studied the effect of plan irregularity due to irregular plan configurations on seismic performance of single-storey wood-frame dwellings by employing many surrogate building models. In this study, the modelling technique of the roof diaphragm was not explicitly explained, and it appeared that the roof diaphragm was considered as rigid. A focus of the study was the occurrences of maximum drifts exceeding the 3% collapse prevention limit. The study concluded that irregular configuration tends to induce eccentricity and results in one wall to exceed the allowable drift limit, and fail, earlier than others. Square-like buildings usually perform better than long, thin rectangular ones.

Research effort has been made overseas to quantify the effects of diaphragm rigidity on seismic performance of irregular LTF buildings. For example, Kirkham, Gupta and Miller (2015) studied the modelling techniques of roof diaphragm (as typical of USA practice) stiffness (rigid, semi-rigid or flexible horizontal diaphragm analyses) in

relation to the plan configurations. The analysis results were compared with historical earthquake damage reports. The study concluded that semi-rigid modelling or an envelope method is prudent. Chen et al. (2014) also studied the influences of diaphragm stiffness on seismic load distribution among different lateral load-resisting systems of timber buildings by conducting a numerical study using a multiple-spring model. For the multiple-spring model, the translational springs are used to model the diaphragm stiffness and the stiffness of the different lateral load-resisting systems. The model was validated with test results and finite element analysis results of a specific benchmark building. The lateral load distribution between different lateral load-resisting systems with varying stiffness ratios of diaphragm to lateral load-resisting systems was also investigated. The results show that, contrary to common belief, the forces transferred by a semi-rigid diaphragm to supporting lateral load-resisting systems may be higher than those predicted by flexible and rigid-diaphragm assumptions. Therefore, using the envelope force approach could lead to underestimation of the design forces in the shear walls.

In summary, research efforts on seismic effects of structural irregularities in LTF residential buildings have been predominantly carried out overseas, based on overseas construction practice. The method for properly modelling LTF buildings with irregularities, including modelling the in-plane rigidity of the floor/roof diaphragms, is still under development. LTF construction practice in New Zealand is significantly different from overseas practice. As such, the findings based on overseas practice should not be used directly in New Zealand.

## 2.4 Summary

A review of research efforts on seismic responses of building structures with structural irregularities has revealed that structural irregularities in building structures cause the buildings to respond in a much more sophisticated manner than regular buildings. Findings relevant to LTF buildings are summarised as follows:

- Seismic response characteristics of an LTF building with in-plan irregularity is likely to have some variations from those of a concrete building with structural irregularities.
- In-plane rigidity of roof/floor diaphragms is crucial for an LTF building with in-plan irregularity to mobilise lateral load-resisting systems in both directions in resolving the torsional response.
- 3D global analyses are required to adequately capture the seismic performance when LTF buildings have structural irregularity.
- 3D global analyses would require adequate stiffness/strength modelling of the seismic bracing timber walls and the floor diaphragms.



### 3. Seismic behaviour of LTF bracing walls

As stated in section 2, when a building structure has in-plan structural irregularities, its translational responses will be coupled with its torsional responses in earthquakes. It is thus essential that three-dimensional analyses with adequate modelling of bracing elements and diaphragms are conducted in studying seismic performance of building structures with in-plan structural irregularities.

This section outlines the study on racking behaviour of LTF walls (the detailed study is presented in Appendix A) and describes the mathematical model developed for representing bracing behaviour of LTF walls as typical of New Zealand residential construction.

#### 3.1 Characteristics of bracing behaviour of LTF walls

Residential buildings in many countries including USA and Canada are low-rise LTF buildings that are braced by LTF bracing walls. For overseas practice, the sheathing sheets for LTF bracing walls are often engineered timber panels, such as plywood or oriented stranded boards. In comparison, the sheathing materials in constructing LTF bracing walls in New Zealand are often plasterboard sheets.

A significant amount of research effort has been applied to quantify the bracing performance of LTF bracing walls both in overseas and in New Zealand. Results have revealed that bracing behaviour of LTF bracing walls is highly dependent on the sheathing materials and the fixing details from the sheathing sheets to the timber frames.

Most of the overseas research effort on the bracing behaviour of LTF walls deals with LTF walls with wood-based panel sheathing. It was found that dominant deformation sources of LTF walls with wood-based panel sheathing included the slips of fasteners and the relative movements between sheathing sheets if wall uplifts are prevented.

A large proportion of studies on bracing behaviour of LTF walls with plasterboard sheathing have been conducted mainly in New Zealand because LTF residential buildings overseas generally do not rely on plasterboard walls (LTF walls with plasterboard sheathing) as seismic bracing elements. Racking tests on plasterboard walls conducted in New Zealand frequently reveal that plasterboard walls have different cyclic responses from wood-based timber walls and that plasterboard walls generally behave in a more brittle manner. The common observation is that there is no visible relative deformation between plasterboard sheets, and the sheathing of a plasterboard wall behaves like a monolithic plate element during a racking test.

Figure 1 to Figure 4 show the final appearances of two racking tests of plasterboard walls of 2.4 x 2.4 m, where two plasterboard sheets of 1.2 x 2.4 m were used for each test.

With the uplifts being suppressed, the dominant deformation source of LTF walls with plasterboard sheathing was found to be the slips between plasterboard sheets and fasteners, which are universally screws. The proper modelling of fastener slips is therefore the most important aspect in developing hysteresis models of plasterboard walls.



**Figure 1. The sheathing (two plasterboard sheets) worked as one plate. Deformation is mainly due to slips.**



**Figure 2. Final appearance after racking on a plasterboard wall of 2.4 m long.**





**Figure 3. The sheathing (two plasterboard sheets) worked as one plate. Deformation is mainly due to slips.**

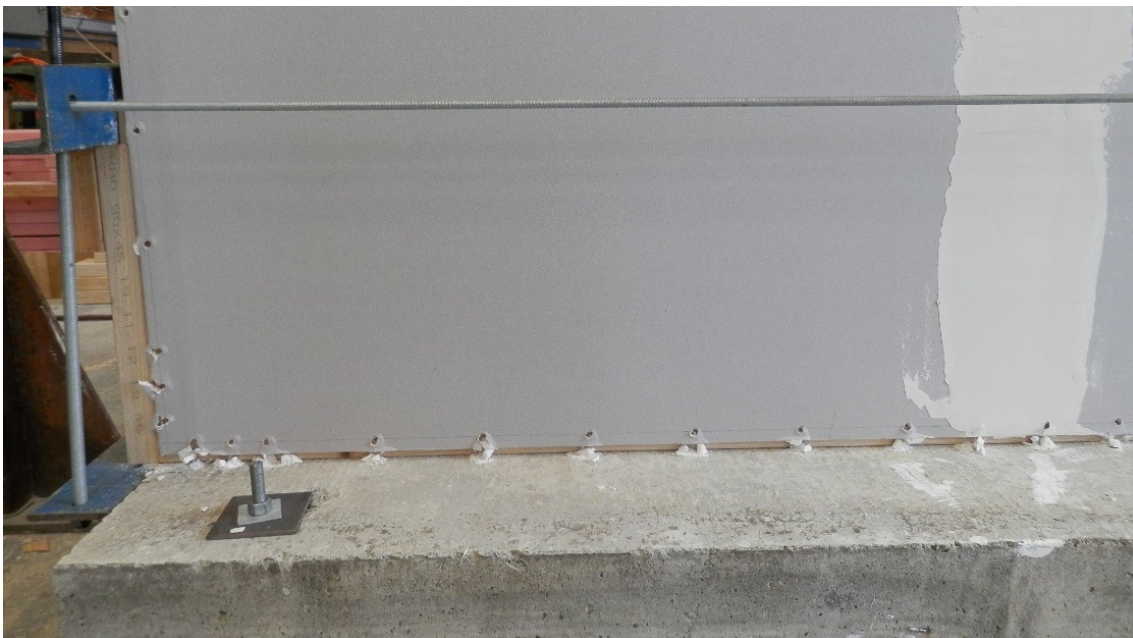


**Figure 4. Final appearance after racking on a plasterboard wall of 2.4 m long.**

## 3.2 Racking model of plasterboard walls

### 3.2.1 Outlines of the model development

A mathematical model representing bracing behaviour of plasterboard walls as typical of New Zealand practice has been developed and calibrated, based on test results and test observations (see Appendix A). The development is described below.

BRANZ Structures Lab has conducted many racking tests on plasterboard bracing walls on either a commercial basis or a research basis and thus there is a good internal source on bracing performance of plasterboard walls typical of New Zealand house construction practice. To inform the development of the racking model of plasterboard bracing walls, many sets of racking test results of plasterboard walls were collected and analysed. Meanwhile the damage state images taken during the racking tests were studied. Findings revealed from studying the test results are:

- entire sheathing over a plasterboard wall behaves like a monolithic plate during racking
- the primary deformation source of a plasterboard wall, when subjected to racking, is the slips of fasteners
- the non-linear behaviour and significant performance degradation of a plasterboard wall is associated with the non-linear behaviour of fastener slips.

As such, the development of the mathematical model for the bracing behaviour of plasterboard walls focuses on the modelling of the fastener slips. The sheathing of a plasterboard wall behaves as a monolithic plate. As suggested by test evidence, the contribution of fastener slips to the lateral deformation of the wall has a similar expression to the contribution of shear deformation. In engineering, shear deformation of a plate element is a function of shear modulus ( $G$ ) and the plate's geometrical dimensions. As such, the mathematical model developed uses a degrading shear modulus to represent the degrading bracing performance of plasterboard walls.

The developed mathematical model is intended to be used when plasterboard walls are modelled as shell elements.

### 3.2.2 Mathematical model development

#### Test data calibration

Racking test results on plasterboard walls as typical of New Zealand practice were collected, from the recent projects conducted at BRANZ (Appendix A). The collected test results were calibrated to inform the model development (Appendix A), and this is described as follows:

Assuming that wall uplift is suppressed, the lateral deflection,  $\Delta_{total}$ , at the top of a cantilever plasterboard wall consists of three components – flexural deformation ( $\Delta_f$ ), shear deformation ( $\Delta_s$ ) and fastener slip ( $\Delta_{sl}$ ).

The primary contribution to flexural rigidity of an LTF wall is attributed to the chords of the wall, and the shear resistance is primarily provided by sheathing. With regards to the fastener slips, fasteners used for constructing plasterboard walls are universally screws. The slips of fasteners then are dependent on the properties of the sheathing materials and thickness of the sheathing.

Considering that the sheathing of a plasterboard wall behaves as a monolithic board with fixings around the wall edges,  $\Delta_{sl}$  is proportional to the wall aspect ratio (H/L) and disproportional to the thickness of sheathing (t), a similar expression to  $\Delta_s$ . As a result,  $\Delta_s$  and  $\Delta_{sl}$  are combined as one component,  $\Delta_{ss}$ .

The total lateral deflection of a plasterboard wall when subjected a racking load, V, is then expressed as follows:

$$\Delta_{total} = \Delta_f + \Delta_{ss} \quad \text{Eq. 1}$$

Where:  $\Delta_f$  is the contribution of flexural deformation to the total lateral deflection

$$\Delta_f = 2VH^3/(3EAL^2) \quad \text{Eq. 2}$$

Where: V is the lateral seismic action applied at the top of the wall, H is the wall height, E is the elastic modulus of the chord, A is the sectional area of one chord and L is the length of the wall.

$$\Delta_{ss} = VH/(G_{eq} L t) \quad \text{Eq. 3}$$

Where:  $G_{eq}$  is the equivalent shear modulus in relation to the combined effect of shear deformation and fastener slip deformation and t is thickness of sheathing.

In calibrating  $G_{eq}$ , E was taken as 8,000 MPa as per NZS 3603:1993 *Timber structures standard* for SG8, A was taken as the sectional area of one chord member (90 x 45 mm) and t was taken as the total thickness of the sheathing.

The values of  $G_{eq}$  in relation to the lateral deflection,  $\Delta_{total}$ , were calibrated against the test results and are summarised in Table 1. This data was used to simulate the degrading behaviour of plasterboard walls in earthquakes. It is to be noted that the derivation of  $G_{eq}$  in Table 1 considers plasterboard walls as hollow walls.

**Table 1. Equivalent shear modulus ( $G_{eq}$ ).**

|                | $\Delta_{total}$ (mm) |    |    |    |    |    |
|----------------|-----------------------|----|----|----|----|----|
|                | 8                     | 15 | 22 | 29 | 36 | 43 |
| $G_{eq}$ (MPa) | 90                    | 50 | 35 | 25 | 18 | 15 |

### Conversion of hollow walls to virtually solid walls

To simplify the computer modelling, the mathematical model developed in this project modelled the walls as virtually solid wall elements, and the mechanical engineering properties of wall elements were correspondingly adjusted, based on the values in Table 1.

In conducting conversion of hollow plasterboard walls to virtually solid walls, the assignment of the thickness of virtually solid walls was arbitrary. Virtual thickness of singly lined plasterboard walls was taken as the overall thickness of the walls, which was the sum of the depth of a stud (90 mm) and the thickness of a sheathing sheet (10 mm). The virtual thickness of doubly lined plasterboard walls was taken as 165 mm. This was a mathematical number for convenience because such an assignment would enable the use of same material properties for singly lined and doubly lined plasterboard walls.

The engineering properties representing the solid shell elements are modulus of elasticity ( $E_v$ ) and shear modulus ( $G_v$ ). The two parameters derived for the virtually solid wall sections are  $E_v$  and  $G_v$ .

By assuming  $E_v$  of the virtually solid section as 2,500 MPa, the converted shear modulus,  $G_v$ , in relation to the lateral deflection levels, is listed in Table 2 for plasterboard walls. The model developed matches the test results well, as reported in Appendix A.

**Table 2.  $G_v$  of virtually solid LTF walls.**

|             | $\Delta_{total}$ (mm) |      |      |      |      |      |
|-------------|-----------------------|------|------|------|------|------|
|             | 8                     | 15   | 22   | 29   | 36   | 43   |
| $G_v$ (MPa) | 9.00                  | 5.00 | 3.50 | 2.75 | 2.00 | 1.50 |

### 3.3 Summary

This section outlines the development of the mathematical model that represents the bracing behaviour of plasterboard walls reported in Appendix A.

Key elements of the model development are:

- the mathematical model was developed based on the in-house test results on plasterboard bracing walls
- plasterboard walls are represented using solid shell elements
- two mechanical engineering properties – modulus of elasticity ( $E_v$ ) and shear modulus ( $G_v$ ) – of the assigned materials to the solid shell elements are determined by conducting calibration against test results of plasterboard walls
- degrading behaviour of plasterboard walls is simulated through a degrading shear modulus,  $G_v$ .



## 4. Rigidity study of roof/ceiling diaphragms

A diaphragm (either a floor diaphragm or a roof diaphragm) is an important structural component. In the case of earthquakes, diaphragms are responsible for distributing the lateral seismic actions across the building to lateral load-resisting systems, maintaining the structural integrity by tying structural elements together and providing lateral restraints to slender vertical elements so on.

For LTF buildings constructed to NZS 3604:2011, there is no requirement for bracing elements at one level to be aligned vertically with bracing elements at the level below or above. Thus, a diaphragm is essential to transfer the concentrated lateral loads from bracing elements above to bracing elements below. In this case, the strength and stiffness of the diaphragms of an LTF building will directly affect the effectiveness of the load transfer from the bracing elements at the level above to the bracing elements at the level below in earthquakes.

NZS 3604:2011 also allows for the bracing elements to be arranged in an irregular manner within a specified limit. As stated in section 3, when a building structure has in-plan structural irregularities, its translational responses will be coupled with its torsional responses in earthquakes. The coupling effect of translational and torsional responses is dependent on the rigidity of the diaphragms.

The diaphragms in timber buildings are timber diaphragms, and they are neither rigid nor flexible. The semi-rigid nature of timber diaphragms significantly complicates the analysis and the assessment of the actions resisted by lateral bracing elements (Pang & Rosowsky, 2010; Christovasilis, Filiatrault & Wanitkorkul, 2007). It is therefore essential to quantify the in-plane rigidity of the diaphragms in order to adequately study the seismic performance of timber buildings with structural irregularities.

This section outlines the literature review and experimental study conducted on plasterboard ceiling diaphragms as typical of New Zealand residential construction practice and the mathematical model developed for simulating in-plane rigidity of plasterboard ceiling diaphragm.

### 4.1 In-plane behaviour of diaphragms in LTF buildings

Numerous studies have been conducted overseas on quantifying the in-plane stiffness of timber floor and ceiling diaphragms. Similar to the bracing performance of LTF walls, in-plane behaviour of floor/roof diaphragms was found to be dependent on many factors. These factors include sheathing sheets, fixing details from sheathing to the frames, aspect ratios of diaphragms, construction details of diaphragm framings, connection details between diaphragms and vertical bracing elements.

For New Zealand residential buildings, the construction techniques of diaphragms are different from overseas practices. Examples of these differences include the framing, lining sheet materials and/or the fixing details from linings to the framings or at junctions of ceiling to walls. Consequently, it is expected that the in-plane behaviour of roof/floor diaphragms typical of New Zealand construction is different from that of their overseas counterparts. This means that the in-plane behaviour of ceiling and floor diaphragms of LTF residential buildings typical of New Zealand practice needs to be studied based on New Zealand practice. There are no reported studies on in-plane behaviour of floor/ceiling diaphragms with plasterboard linings typical of New Zealand

residential construction. A test programme was designed as part of this research effort to inform the model development of in-plane rigidity of plasterboard ceiling diaphragms (Appendix B).

## 4.2 Tests of plasterboard ceiling diaphragms

Diaphragms in LTF buildings constructed to NZS 3604:2011 are often classified into two categories – normal diaphragms and structural diaphragms – depending on the spacing of bracing lines. Typically, the structural diaphragms are needed only in the situation where the bracing lines in the storey below are spaced at more than 6 m, according to NZS 3604:2011. The requirements in constructing structural diaphragms are significantly more stringent than these for non-structural diaphragms. As a result, the in-plane rigidity of structural diaphragms could be significantly different from that of non-structural diaphragms. One of the objectives of the test programme (Appendix B) was to quantify the in-plane stiffness of plasterboard ceiling diaphragms in different applications in order to establish the variation range of the in-plane rigidity of ceiling diaphragms.

### 4.2.1 Tests of plasterboard ceiling diaphragms

In designing the experimental programme, a review of typical New Zealand practice of timber ceiling diaphragms was conducted. As a result of the review, four different ceiling diaphragm construction details in different applications were deemed to be sufficient to establish upper and lower bounds of the in-plane rigidity of ceiling diaphragms. These four types of construction details of plasterboard ceiling diaphragms were included in the ceiling diaphragm test programme.

The experimental programme on plasterboard ceiling diaphragms included one full-scale ceiling diaphragm test and four small-scale ceiling diaphragm tests by subjecting the diaphragms to in-plane loading. The full-scale test specimen was 3.6 x 7.2 m in plan, and it had the same construction details as recommended by Winstone Wallboards (2014), which is the commonly used practice in constructing structural diaphragms in New Zealand. The full-scale test was used as a benchmark test for quantifying the in-plane rigidity of plasterboard ceiling diaphragms. For the four small-scale tests, they had identical plan dimension (1.2 x 1.2 m) and test set-ups. The differences between the four small-scale tests were the edge fixing details from plasterboard to framing and the batten orientation for different applications and practice. Among the four small-scale tests, one had identical diaphragm construction details to the full-scale test while the other three represented the variations of construction details in different applications. The small-scale tests were conducted to quantify the relative in-plane rigidity of other ceiling diaphragm details to that of the ceiling diaphragm with identical detail to the full-scale test. Ultimately, the small-scale tests, with the aid of the benchmark in-plane rigidity obtained from the full-scale test, enabled the estimation of the in-plane rigidities of plasterboard ceiling diaphragms with different construction details.

### 4.2.2 Test observations and findings

#### Full-scale test

For the full-scale test, instrumentation was installed to give the necessary information needed to quantify different deformation components. The obtained test results led to the following conclusions:

- There are insignificant relative movements between plasterboard sheet joints when the diaphragms are subjected to in-plane loading.
- The dominant contribution to the in-plane flexibility of plasterboard ceiling diaphragms is due to the slips of screws from plasterboard linings to the framing. The deformation component of screw slips could reach up to 75% of the total deflection of a diaphragm.
- The beam analogy method in NZS 3603:1993, although developed mainly based on timber-based panel sheathing, could be used for modelling the plasterboard ceiling diaphragm, provided that the screw slip model is adequate.

### Small-scale tests

Observations from the four small-scale tests of plasterboard ceiling diaphragms confirmed that the screw slip was the major contributor to the flexibility of plasterboard ceiling diaphragms.

Analyses of the test results from the four small-scale tests were conducted. Assuming that flexibility of the plasterboard ceiling diaphragms is proportional to magnitudes of screw slips, the relative in-plane rigidity,  $K_R$ , of ceiling diaphragms with different details could be derived. The obtained relative in-plane rigidity of ceiling diaphragms with different details is summarised in Table 3.

**Table 3. Slip-related ceiling diaphragm rigidity.**

| Test ID | $K_R$ | Comments of diaphragm construction details   |
|---------|-------|--|
| A       | 1.0   | Same details as the full-scale test (structural diaphragm)   |
| B       | 0.85  | Same as test A except that batten orientation changed  |
| C       | 17.0  | Same as test A except that the reinforcing tapes were used along the joints at wall-ceiling junctions.         |
| D       | 0.22  | Same as test A except that screw spacing was 600 mm instead of 150 mm as for test A (non-structural diaphragm) |

## 4.3 In-plane rigidity of plasterboard ceiling diaphragms

### 4.3.1 Engineering basis of the model development

As an essential part of the intended 3D seismic analyses of LTF buildings, a mathematical model representing in-plane rigidity of plasterboard ceiling diaphragms typical of New Zealand practice has been developed, based on test results (see Appendix B).

The developed mathematical model is intended to be used when diaphragms are modelled as shell elements. The model development is based on the test evidence that plasterboard sheathing within a plasterboard ceiling diaphragm behaves as a monolithic plate and there are no visible relative movements between plasterboard sheets. The primary deformation source of plasterboard ceiling diaphragms, when subjected to in-plane loading such as earthquake actions, is the slips of screws. This is to say that the non-linear behaviour and significant performance degradation of plasterboard ceiling diaphragms are associated with the non-linear behaviour of screw slips.

As such, a degrading shear modulus is used to represent the degrading in-plane performance of plasterboard ceiling diaphragms. This is similar to the approach used in developing a racking model of timber walls.

### 4.3.2 Mathematical model development

#### Model calibration

It is well known that the racking performance of timber bracing walls shares many similarities to the in-plane responses of timber diaphragms.

In NZS 3603:1993, the total lateral deflection of a timber wall when subjected to racking has four deformation components – flexural, shear, screw slip and base uplift. Meanwhile, the total in-plane deflection of a timber diaphragm has three components – flexural, shear and screw slip. Clearly, the only difference in the in-plane rigidity of a timber wall and a timber diaphragm is that timber walls need to allow for the contribution of uplift at the wall base, but the diaphragms do not have such a deformation component.

The mathematical model for representing the in-plane rigidity of ceiling diaphragms is developed based on the formulae in NZS 3603:1993, similar to that of timber walls.

In NZS 3603:1993, timber diaphragms are analysed using a girder analogy method, where the sheathing is the web of the girder and the top plate of the wall or a continuous joist is the flange. Most diaphragms are deep beams, and they are considered as simply supported beams.

According to NZS 3603:1993, the total deflection of a timber diaphragm sheathed by plywood sheets could be estimated as follows:

$$\Delta_{\text{total}} = \Delta_f + \Delta_s + \Delta_{\text{slip}} \quad \text{Eq. 4}$$

Where:

$\Delta_f = 5PL^3/(192EAB^2)$  – the deflection contribution due to in-plane bending deformation of the diaphragm. The primary contribution of a timber diaphragm to bending rigidity is attributed to the chords of the diaphragm. E is the elastic modulus of the chords.

$\Delta_s = PL/(8GBt)$  – the deflection contribution due to shear deformation where the shear resistance is primarily provided by the web of the diaphragm, G is the shear modulus of the web and t is the thickness of the plasterboard.

$\Delta_{\text{slip}}$  is the contribution of the screw slips, between fasteners and the sheathing, to the total deflection of the diaphragm.

As for the mathematical model development of timber plasterboard walls, the shear and slip deformation components,  $\Delta_s$  and  $\Delta_{\text{slip}}$ , are combined as  $\Delta_{\text{ss}}$ .

Hence, Eq. 4 becomes:

$$\Delta_{\text{total}} = \Delta_f + \Delta_{\text{ss}} \quad \text{Eq. 5}$$

Where:

$$\Delta_{\text{ss}} = PL/(8G_e Bt) \quad \text{Eq. 6}$$

Where:  $G_e$  is the equivalent shear modulus in relation to the effect of shear deformation and screw slips.  $G_e$  will degrade as loading progresses, leading to non-linear performance of ceiling diaphragms.



The equivalent shear modulus at the loading peaks is derived using Eq. 4–6, based on the test results obtained from the full-scale ceiling diaphragm test.

The calibrated equivalent shear modulus is listed in Table 4.

**Table 4. Equivalent shear modulus,  $G_e$ , of the full-scale ceiling diaphragm test.**

| V (kN/m) | $\Delta$ (mm) | $G_e$ (MPa) |
|----------|---------------|-------------|
| 1.1      | 0.5           | 450         |
| 1.9      | 1             | 370         |
| 2.5      | 1.6           | 300         |
| 3.6      | 2.75          | 220         |
| 3.6      | 4.5           | 160         |
| 3.6      | 5             | 140         |
| 4.0      | 6             | 110         |

- V is the shear action in the two sides of the diaphragm, parallel to the loading direction.
- $\Delta$  is the translational deflection at mid-span of the diaphragm relative to the support.

As shown in Table 4, equivalent shear modulus,  $G_e$ , degrades as the deformation progresses, as revealed from the full-scale plasterboard ceiling diaphragm test.

The equivalent shear modulus of plasterboard ceiling diaphragms with different details is estimated based on the relative rigidity values derived from small-scale ceiling diaphragm test.

Table 5 lists the estimated equivalent shear modulus for various joint details in ceiling diaphragms.

**Table 5. Estimated equivalent shear modulus,  $G_e$ .**

| In-plane translation (mm) | $G_e$ of full-scale test (MPa) | $G_e$ (detail B) (MPa) | $G_e$ (detail C) (MPa) | $G_e$ (detail D) (MPa) |
|---------------------------|--------------------------------|------------------------|------------------------|------------------------|
| 0.5                       | 450                            | 397                    | 7500                   | 97                     |
| 1                         | 370                            | 326                    | 6167                   | 80                     |
| 1.6                       | 300                            | 265                    | 5000                   | 65                     |
| 2.75                      | 220                            | 194                    | 3667                   | 47                     |
| 4.5                       | 160                            | 141                    | 2667                   | 35                     |
| 5                         | 140                            | 124                    | 2333                   | 30                     |
| 6                         | 110                            | 97                     | 1833                   | 24                     |

### Mathematical model for a virtually solid section

To simplify the computer modelling, the mathematical model developed in this project models the diaphragms as virtually solid shell elements of 100 mm in thickness, and the mechanical engineering properties of diaphragm elements are correspondingly adjusted, based on the values in Table 5.

By assuming  $E_v$  of the virtual solid section is 2,500 MPa, the converted shear modulus,  $G_v$ , in relation to the in-plane mid-span deflection levels is listed in Table 6 for plasterboard ceiling diaphragms.

**Table 6.  $G_e$  of virtually solid plasterboard ceiling diaphragms.**

| In-plane translation (mm) | $G_e$ of full-scale test (MPa) | $G_e$ (detail B) (MPa) | $G_e$ (detail C) (MPa) | $G_e$ (detail D) (MPa) |
|---------------------------|--------------------------------|------------------------|------------------------|------------------------|
| 0.5                       | 40                             | 35                     | 670                    | 8.5                    |
| 1                         | 35                             | 31                     | 583                    | 7.5                    |
| 1.6                       | 28                             | 25                     | 467                    | 6.0                    |
| 2.75                      | 21                             | 18                     | 350                    | 4.5                    |
| 4.5                       | 16                             | 14                     | 267                    | 3.5                    |
| 5                         | 14                             | 12                     | 233                    | 3.0                    |
| 6                         | 10                             | 9                      | 165                    | 2.2                    |

## 4.4 Summary

This section summarises the experimental study conducted on plasterboard ceiling diaphragms typical of New Zealand practice and describes the mathematical model developed to represent the in-plane rigidity of plasterboard ceiling diaphragms (Appendix B).

Highlights of the study reported in this section include the following:

- Plasterboard linings behave like one monolithic plate over the entire diaphragm under consideration when the plasterboard ceiling diaphragm is subjected to in-plane loading.
- About 80% of total in-plane deformation of plasterboard ceiling diaphragms, when subjected to in-plane loading, is from slips of screws from plasterboard linings to the frames.
- The beam analogy method in predicting in-plane deflection of floor diaphragms as in NZS 3603:1993 can be used in estimating the rigidity of plasterboard ceiling diaphragms if the screw slip model is adequate.
- Stiffness degradation of the plasterboard ceiling diaphragm is very significant as the loading progresses and the non-linear deformation mechanism is limited to screw slips.
- A mathematical model in simulating the in-plane rigidity of plasterboard ceiling diaphragms was developed based on the test results, and the degrading characteristics of the plasterboard ceiling diaphragms is represented by a degrading shear modulus.
- The developed model is easy to use when diaphragms are modelled as shell elements of a solid section.

## 5. Seismic performance of permissible designs and improvements

The current design standard for timber-framed buildings, NZS 3604:2011, allows irregular distribution of bracing elements across the building plan to certain limits, as described in section 2. According to NZS 3604:2011, designers do not need to allow for the adverse consequences of in-plan structural irregular arrangements of bracing elements as far as the irregular limits in NZS 3604:2011 are met. However, the limits of irregular distribution of bracing elements within a plan were not established based on robust scientific studies.

The earthquake damage observed in recent earthquakes demonstrated that irregular LTF buildings had significantly more damage than simple regular counterparts, indicating that structural irregularity exacerbated the seismic effects significantly.

To fulfil the objective stated in section 1, single-storey LTF buildings with varying degrees of irregularities permissible in NZS 3604:2011 were designed, and their seismic performance was studied.

### 5.1 Case study LTF buildings

Six case study LTF buildings were designed according to NZS 3604:2011. It was assumed that all these buildings were constructed on a site that has a seismic hazard factor of  $Z = 0.46$  and is classified as subsoil class D according to NZS 1170.5:2004. All these case study buildings had RC rib-slab foundations.

Among these six buildings, three LTF buildings were rectangular in plan and the structural irregularity was caused by irregular arrangements of bracing elements within the floor plan.

The other three buildings were L-shaped in plan and had some degree of irregular bracing arrangement within each wing of the floor plan.

These six buildings were selected to:

- evaluate seismic effects of permissible irregular distribution of bracing resistance within the scope of NZS 3604:2011
- determine the appropriate irregularity limits required for controlling earthquake damage.

#### 5.1.1 Rectangular case study buildings

The three rectangular LTF buildings share an identical floor plan of 12 x 15 m. The benchmark building, RR, is perfectly regular in both directions, and its seismic bracing provision is just equal to the seismic demand as calculated from NZS 3604:2011.

The other two rectangular case study buildings – RIR1 and RIR2 – have the same total bracing provisions as building RR but irregular bracing arrangements, which are still allowable in NZS 3604:2011.

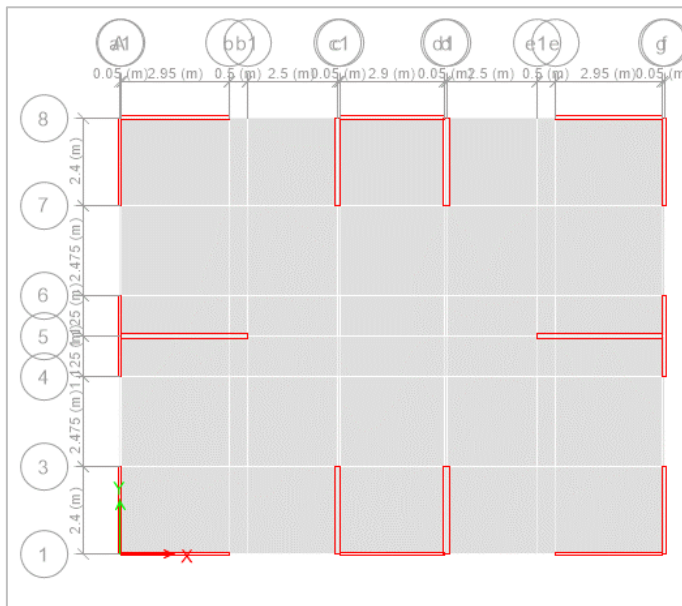
The three rectangular case study buildings are summarised in Table 7.

**Table 7. Rectangular case study buildings.**

|   | RR  | RIR1 | RIR2 |
|---|-----|------|------|
| Total bracing provision to minimum NZS 3604:2011? | Yes | Yes  | Yes  |
| In how many directions does irregularity exist?   | 0   | 1    | 1    |
| Irregularity magnitude (%)*                       | 0   | 100  | 50   |

100% means that the bracing arrangements are very irregular and the irregular arrangements reach the specified limits. In comparison, 50% means less irregularity and the bracing arrangements are between 100% irregularity and perfectly regular.

Figure 5 shows the plan of the rectangular case study buildings.


**Figure 5. Floor plan of single-level rectangular case study buildings.**

### Building RR

Case study building RR is designed to be perfectly regular and is considered as the benchmark building for the first group of buildings. Building RR is a single-level rectangular building measuring 12 x 15 m with a corrugated metal roof and heavy cladding. The roof pitch is less than 25° and the storey height is 2.4 m. The building has a concrete slab foundation and is situated on a site that is classified as subsoil class D and has a hazard factor of 0.46 according to NZS 1170.5:2004.

The seismic demand for this case study building is 9 BUs/m<sup>2</sup>, according to NZS 3604:2011. This was derived based on a seismic coefficient of 0.4 (Shelton, 2013) where the lumped seismic mass at roof level equals 1.125 kPa or 20,642 kg in total. The total seismic demand for this building is 1,620 BUs for both directions.

For the seismic bracing design, it is assumed that the bracing rating of the perimeter LTF walls, which are lined on one face, is 60 BUs/m, which is in the middle range of the bracing capacitor of singly lined bracing walls. Similarly, the bracing rating of the internal bracing walls, which are lined on both faces, is assumed to be 85 BUs/m, which is a close match to the seismic rating given to doubly lined proprietary bracing walls without hold-down devices.

Figure 6 shows the bracing schedule of case study building RR. In x direction, the total length of external LTF walls is 17.6 m and the total length of internal LTF walls is

6.9 m. As a consequence, the total seismic bracing in x direction is 1,640 BUs, about equal to the demand. In y direction, the total length of external LTF walls is 14.1 m and the total length of internal LTF walls is 9.6 m. The total seismic bracing provision in y direction is 1,660 BUs, again about equal to the demand. Therefore, the seismic design of building RR meets the current seismic design standard NZS 3604:2011.

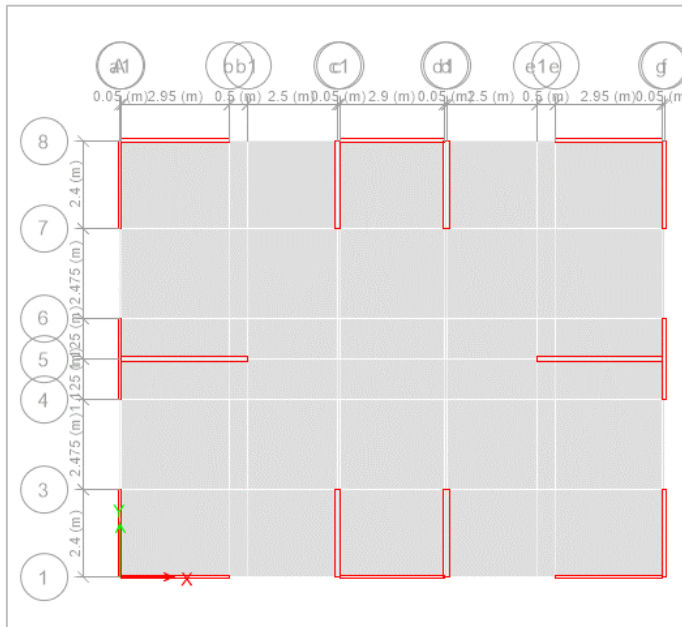


**Figure 6. Bracing arrangement of case study building RR.**

### Building RIR1

Case study building RIR1 is identical to case study building RR except that the bracing arrangement in y direction is towards the extreme end (the scenario with an irregularity magnitude of 100%) of allowable irregularity by NZS 3604:2011.

With regards to the bracing distribution across a building plan, NZS 3604:2011 has the following specifications:

- Bracing lines in any storey shall be at no more than 6 m in each direction.
- Minimum bracing resistance for each bracing line shall be the greater of 100 BUs or 50% of the total bracing demand divided by the number of bracing lines in the direction being considered.
- Apart from the above two requirements, minimum bracing resistance for each external wall in any storey shall be no less than 15 BUs/m of external wall length.

For case study building RIR1, the number of bracing lines in y direction is four and the building length in y direction is 12 m. Therefore, the above bracing distribution specifications in NZS 3604:2011 are translated as follows:

- Minimum bracing provision for each internal bracing line is 202 BUs, which is the larger of IB1 and IB2 where  $IB1 = 100$  BUs and  $IB2 = 203$  BUs, which is calculated as  $1,620 \text{ BUs} \times 0.5 / 4$  as specified in clause 2.
- Minimum bracing provision for each external wall line is 202 BUs, which is the larger of EB1 and EB2, where  $EB1 = 203$  BUs, calculated as  $1,620 \text{ BUs} \times 0.5 / 4$  as specified in clause 2 and  $EB2 = 15 \text{ BUs/m} \times 12 \text{ m} = 180$  BUs.

Figure 7 shows the bracing distribution across the floor plan of case study building RIR1. The irregular bracing provision in y direction is close to the maximum allowable irregularity in NZS 3604:2011.

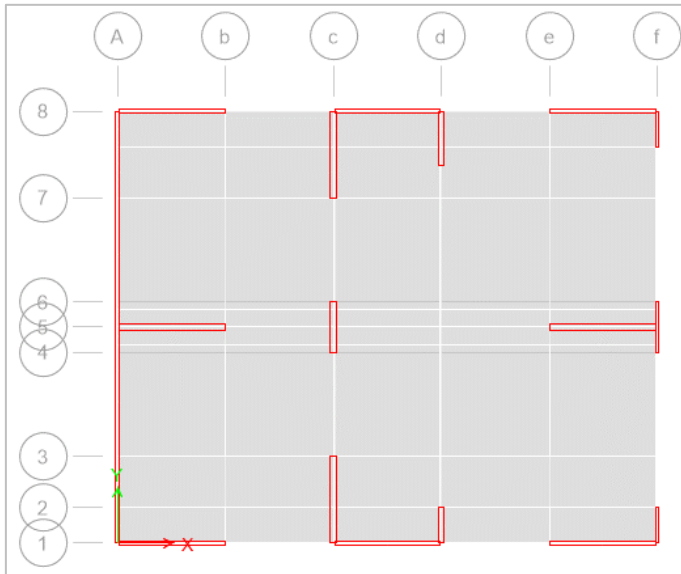


**Figure 7. Bracing arrangement of case study building RIR1.**

#### Building RIR2

Case study building RIR2 is identical to case study building RIR1 except that the bracing arrangement in y direction is less irregular. Specifically, the minimum bracing provision in each bracing line is determined to be 75% total demand divided by the number of bracing lines.

Figure 8 shows the bracing distribution across the floor plan of case study building RIR2. The irregularity of bracing arrangement in y direction is moderate.

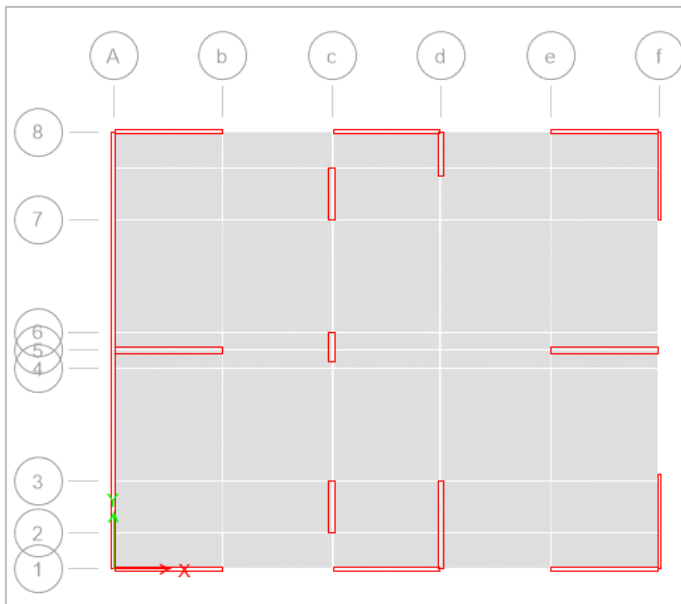


**Figure 8. Bracing arrangement of case study building RIR2.**

The seismic bracing design information for the three rectangular case study buildings is summarised in Table 8.

**Table 8. Summary of seismic bracing designs of rectangular case study buildings RR, RIR1 and RIR2.**

|  |  | x direction |     |     | y direction |     |     |     |
|--|--|-------------|-----|-----|-------------|-----|-----|-----|
| Bracing line #                                     |  | 1           | 2   | 3   | 1           | 2   | 3   | 4   |
| Minimum bracing requirement in NZS 3604:2011 (BUs) |  | 270         | 270 | 270 | 202         | 202 | 202 | 202 |
| RR   | Bracing provision at each bracing line (BUs) | 531         | 587 | 531 | 423         | 408 | 408 | 423 |
|  | Total bracing provision (BUs)                | 1650        |     |     | 1662        |     |     |     |
| RIR1   | Bracing provision at each bracing line (BUs) | 531         | 587 | 531 | 720         | 527 | 212 | 204 |
|  | Total bracing provision (BUs)                | 1650        |     |     | 1665        |     |     |     |
| RIR2   | Bracing provision at each bracing line (BUs) | 531         | 587 | 531 | 720         | 305 | 305 | 300 |
|  | Total bracing provision (BUs)                | 1650        |     |     | 1630        |     |     |     |

### 5.1.2 L-shaped case study buildings

Three L-shaped single level case study buildings – LR, LIR1 and LIR2 – were designed and studied in this project.

These three buildings are identical except for their bracing arrangements across the floor plan. The first is regular in both directions, the second is irregular in one direction only and the third is irregular in both directions.

All three buildings have corrugated metal roofs and heavy cladding. The roof pitch is less than 25° and the storey height is 2.4 m. The buildings have concrete slab foundations and situated on a site classified as subsoil class D with a hazard factor of 0.46 according to NZS 1170.5:2004.

Figure 9 shows the floor plan of the L-shaped buildings.

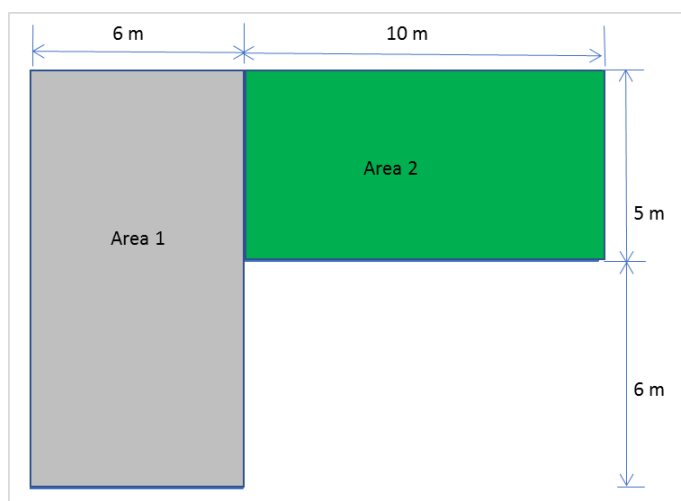


**Figure 9. Plan of L-shaped case study buildings.**



### Building LR

Case study building LR is the benchmark L-shaped building, which is considered to be regular. Although it has an L-shaped floor plan (geometrical irregularity), the seismic design is intended to produce reasonably regular bracing arrangements. The building has a wing of 5 x 10 m (area 2 as marked in Figure 9) extending more than 6 m from the remainder of the building and the bracing elements within the wing are designed to provide sufficient bracing capacity for the seismic actions associated with the wing, as required by NZS 3604:2011.

The seismic demand for the building is 9 BUs/m<sup>2</sup>, according to NZS 3604:2011, and this corresponds to a seismic coefficient of 0.4. The total seismic demand for this building is 594 BUs for area 1 and 450 BUs for area 2. The total seismic demand for the whole building is 1,044 BUs. The lumped seismic mass at roof level of this case study building is 13,305 kg.

As in section 5.1.1, the seismic bracing designs here assume that seismic bracing ratings of the perimeter LTF walls and the internal bracing walls are 60 BUs/m and 85 BUs/m, respectively.

Figure 10 shows the bracing schedule of case study building LR.

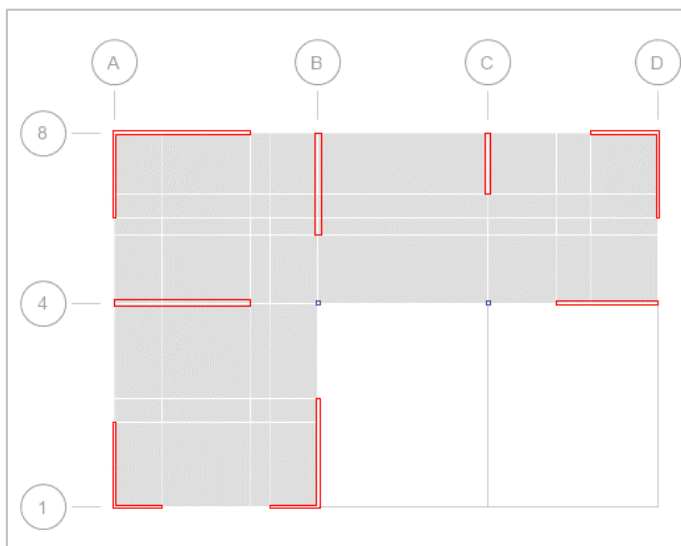


**Figure 10. Bracing distribution of case study building LR.**

In x direction, the total length of external LTF walls is 11.8 m and the total length of internal LTF walls is 4 m. As a consequence, the total seismic bracing provision in x direction is 1,048 BUs, about the same as the demand. In y direction, the total length of external LTF walls is 10.7 m and the total length of internal LTF walls is 4.8 m. As a consequence, the total seismic bracing provision in y direction is 1,050 BUs, about equal to the demand. Therefore, the seismic design of building LR meets the current seismic design standard NZS 3604:2011.

### Building LIR1

Case study building LIR1 is identical to case study building LR except that the bracing arrangement in y direction is close to the allowable irregularity limit in NZS 3604:2011, i.e. 50% total demand divided by the number of bracing lines in this case.



Figure 11 shows the bracing distribution across the floor plan of case study building LIR1. Noted is that the irregularity of the bracing arrangement is only in one direction but the magnitude of irregularity is towards the extreme end of allowable irregularity limits in NZS 3604:2011.

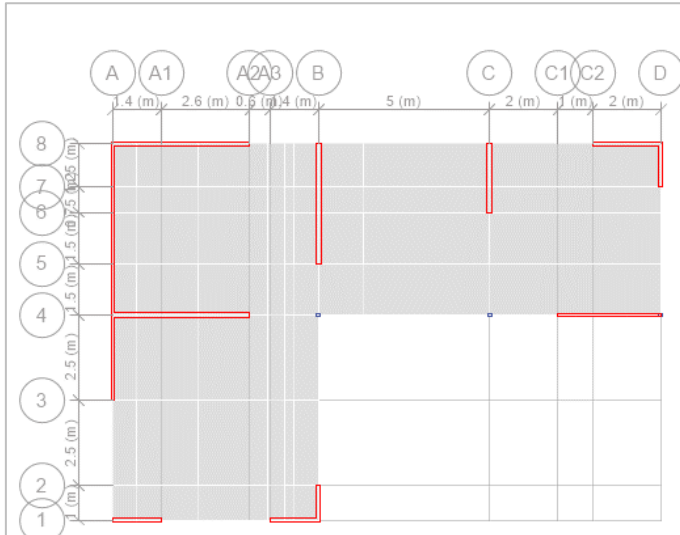


**Figure 11. Bracing distribution of case study building LIR1.**

### Building LIR2

Case study building LIR2 is identical to case study building LIR1 except that the bracing arrangement in x direction is also irregular but still within the irregularity requirements of NZS 3604:2011.

Figure 12 shows the bracing distribution across the floor plan of case study building LIR2

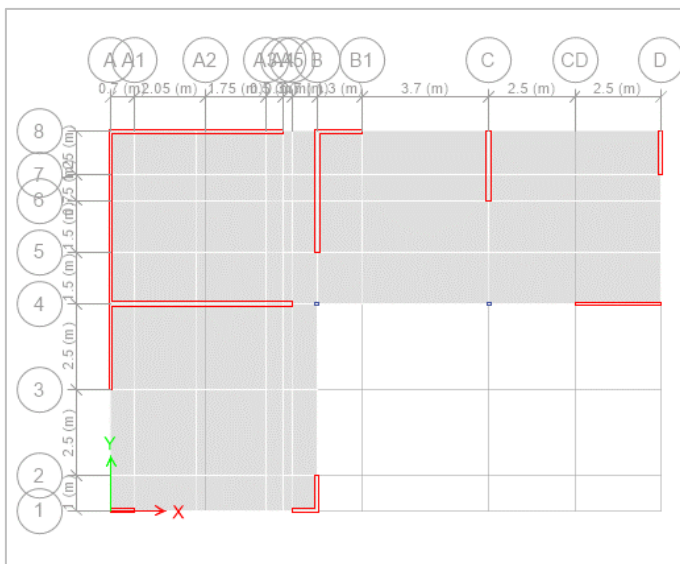


**Figure 12. Bracing distribution of case study building LIR2.**

Table 9 summarises the minimum earthquake bracing demands and the earthquake bracing provisions along bracing lines for case study buildings LR, LIR1 and LIR2.

**Table 9. Summary of the bracing designs of case study buildings LR, LIR1 and LIR2.**

|  |  | x direction |     |     | y direction |     |     |     |
|--|--|-------------|-----|-----|-------------|-----|-----|-----|
| Bracing line #                                     |  | 1           | 2   | 3   | 1           | 2   | 3   | 4   |
| Minimum bracing requirement in NZS 3604:2011 (BUs) |  | 90*         | 174 | 240 | 165         | 130 | 130 | 75* |
| LR   | Bracing provision at each bracing line (BUs) | 168         | 520 | 360 | 300         | 447 | 153 | 150 |
|  | Total bracing provision (BUs)                | 1048        |     |     | 1050        |     |     |     |
| LIR1   | Bracing provision at each bracing line (BUs) | 168         | 520 | 360 | 450         | 358 | 170 | 75  |
|  | Total bracing provision (BUs)                | 1064        |     |     | 1053        |     |     |     |
| LIR2   | Bracing provision at each bracing line (BUs) | 90          | 596 | 378 | 450         | 358 | 170 | 75  |
|  | Total bracing provision (BUs)                | 1064        |     |     | 1053        |     |     |     |

\* Minimum bracing requirement if bracing demand is derived based on each building wing.

### 5.1.3 Summary

In summary, two groups of single-storey LTF buildings were seismically designed according to NZS 3604:2011. One group of case study buildings was rectangular in plan, and the other group of case study buildings were L-shaped in plan where one wing extends more than 6 m from the remaining building.

The case study buildings were assumed to be situated in a site with a subsoil class D according to NZS 1170.5:2004 and a hazard factor of 0.46 as per the upper limit of earthquake zone 3 as specified in NZS 3604:2011.

Each group contained three case study LTF buildings. The three buildings of each group had identical floor plans, and the only differences between each other were that the buildings had different allowable irregular distributions of the bracing elements across the building floor plan.

## 5.2 Structural modelling and seismic analyses

Earthquake performance of irregular building structures is significantly more complicated than that of regular counterparts. In the case of a perfectly regular building, a 2D seismic analysis could adequately capture the seismic performance characteristics of a regular building. In contrast, an irregular building is expected to have torsional responses in earthquakes, which will be coupled with translational responses.

In this latter case, seismic actions will be transmitted by the floor diaphragms into the lateral load-resisting systems in both directions across the entire building. The seismic performance of an irregular building thus depends not only on the racking behaviour of primary lateral load-resisting systems but also the in-plane rigidities of floor/roof diaphragms.

Three-dimensional global analyses with adequate modelling of the lateral seismic-resisting systems and the floor diaphragms are essential to adequately capture the seismic performance of buildings with structural irregularities.

For LTF residential buildings in New Zealand, the primary lateral seismic-resisting systems are typically plasterboard-lined LTF walls, and roof/floor diaphragms are not

rigid. It is important to adequately model racking behaviour (stiffness, strength and energy-dissipating capacity) of LTF walls and model in-plane rigidity performance of floor/roof diaphragms.

In evaluating the seismic performance of the case study buildings, a 3D mathematical model for each case study building as designed in section 5.1 was created using ETABS software.

## 5.2.1 Modelling techniques of LTF walls and ceiling diaphragms

In constructing 3D ETABS models, LTF walls and plasterboard ceiling diaphragms were modelled as virtually solid shell elements with orthotropic material properties. The thickness of virtual solid wall sections was taken as 100 mm for singly lined LTF walls as typical of perimeter walls and 165 mm for doubly lined LTF walls as for internal walls, as described in section 3. The thickness of virtual solid ceiling diaphragm sections was taken as 100 mm for plasterboard ceiling diaphragms, as described in section 4.

Two important engineering properties representing the shell elements are modulus of elasticity ( $E$ ) and shear modulus ( $G$ ), and these two parameters were the values derived and calibrated based on test results, as described in sections 3 and 4 for walls and diaphragms respectively.

In detail, modulus of elasticity was defined as constant, that is,  $E = 2,500$  MPa for both wall shell elements and ceiling diaphragm shell elements. Meanwhile, shear modulus,  $G$ , which is the other important material property of the shell elements, is a degrading parameter, and it varies in relation to the imposed deformations, as reported in sections 3 and 4. Values of  $G$  in relation to the imposed deflection are reproduced in Table 10 and Table 11 respectively for wall shell elements and ceiling shell elements.

In Table 11, the relationships between shear stress levels at ceiling diaphragm sides and equivalent  $G$  values are also reproduced from Appendix B, for the purpose of calibrating the used shear modulus in the model.

**Table 10.  $G$  of virtual solid LTF walls.**

|           | Magnitude of lateral storey deflection (mm) |      |      |      |      |      |
|-----------|---|------|------|------|------|------|
|           | 8   | 15   | 22   | 29   | 36   | 43   |
| $G$ (MPa) | 9.00  | 5.00 | 3.50 | 2.75 | 2.00 | 1.50 |

$G$  is the shear modulus derived for LTF bracing walls in association with the use of  $E = 2,500$  MPa,  $t_e = 100$  mm for singly lined walls and  $t_e = 165$  mm for doubly lined LTF walls.

**Table 11.  $G$  of virtual solid plasterboard ceiling diaphragm as for the full-scale test.**

|            | $\Delta$ (mm) |      |      |      |      |      |      |
|------------|---------------|------|------|------|------|------|------|
|            | 0.5           | 1.0  | 1.6  | 2.75 | 4.5  | 5.0  | 6.0  |
| $G$ (MPa)  | 40            | 35   | 28   | 21   | 16   | 14   | 10   |
| $v$ (kN/m) | 1.05          | 1.78 | 2.37 | 3.08 | 3.75 | 3.67 | 3.51 |

- $\Delta$  is the magnitude of deformation at mid-span relative to supports.
- Thickness of the virtually solid shell member is 100 mm.
- $v$  is shear stress level (kN/m) along each side (parallel to seismic directions).

As discussed in section 4, ceiling diaphragms have different construction details in the different application situations. The virtual solid ceiling diaphragm's shear modulus will

vary from the highest values, 17 times the values for the full-scale test in Table 11, to the softest case, which is only 21% of the values for the full-scale test in Table 11.

Table 12 lists the shear modulus of virtual solid shell elements representing ceiling diaphragms in relation to the deformations for the possible stiffest and softest cases respectively.

**Table 12. Range of shear modulus, G, of plasterboard ceiling diaphragms.**

|                       | $\Delta$ (mm) |      |      |      |      |      |      |
|-----------------------|---------------|------|------|------|------|------|------|
|                       | 0.5           | 1.0  | 1.6  | 2.75 | 4.5  | 5.0  | 6.0  |
| Stiffest case G (MPa) | 670           | 583  | 467  | 350  | 267  | 233  | 165  |
| Softest case G (MPa)  | 8.5           | 7.5  | 6.0  | 4.5  | 3.5  | 3.0  | 2.2  |
| v (kN/m)              | 1.05          | 1.78 | 2.37 | 3.08 | 3.75 | 3.67 | 3.51 |

- $\Delta$  is the magnitude of deformation at mid-span relative to supports.
- Thickness of the virtually solid shell member is 100 mm.
- v is shear stress level (kN/m) along each side (parallel to seismic directions).

## 5.2.2 Equivalent static push-over analyses

### Seismic actions

For the static structural analysis conducted on each case study building, only y directional seismic responses were studied. The seismic action applied for each case is derived from NZS 3604:2011 and considered at ultimate limit state (ULS).

It needs to be appreciated that actual seismic actions expected in the modelled LTF structures could be significantly higher than the applied seismic actions derived from NZS 3604:2011, as revealed in previous studies. However, this study is limited to quantifying the effect of irregularity on the seismic performance of NZS 3604:2011 constructions and the determination of the appropriate seismic actions for NZS 3604:2011 construction is beyond the scope of this study.

The design seismic actions applied to the case study buildings are listed in Table 13.

**Table 13. Seismic actions.**

|                       | Total seismic action in either direction (kN) | Seismic action in terms of load/unit area (KPa) |
|-----------------------|---|---|
| Rectangular buildings | 81  | 0.45  |
| L-shaped buildings    | 52  | 0.45  |

### Calibrations of shear modulus of walls and diaphragms

In conducting the 3D static analyses, assignments of E and G for each shell element representing an LTF wall were adjusted iteratively to ensure that the assigned stiffness parameters were compatible with the deformation levels experienced.

Similarly, assignments of E and G for each shell element representing the roof diaphragm were adjusted in iteration to ensure that the assigned stiffness parameters were compatible with the deformation levels experienced.

Table 14 summarises the calibrated engineering parameters of the shell elements representing LTF walls in the ETABS models of rectangular buildings, when the buildings were subjected to lateral seismic actions as shown in Table 13.

**Table 14. G of wall elements of rectangular buildings (MPa).**

| Case study buildings | x direction grid # |      |      | y direction grid # |      |      |      |
|----------------------|--------------------|------|------|--------------------|------|------|------|
|                      | 1                  | 5    | 8    | A                  | C    | D    | F    |
| RR                   | 9.00               | 9.00 | 9.00 | 9.00               | 9.00 | 9.00 | 9.00 |
| RIR1                 | 9.00               | 9.00 | 9.00 | 5.00               | 2.75 | 2.00 | 1.50 |
| RIR2                 | 9.00               | 9.00 | 9.00 | 5.00               | 5.00 | 5.00 | 3.50 |

Table 15 summarises the calibrated engineering parameters of the shell elements representing LTF walls in the ETABS models of L shaped buildings.

**Table 15. G of wall elements of L-shaped buildings (MPa).**

| Case study building | x direction grid # |      |      | y direction grid # |      |      |      |
|---------------------|--------------------|------|------|--------------------|------|------|------|
|                     | 1                  | 4    | 8    | A                  | B    | C    | D    |
| LR                  | 9.00               | 9.00 | 9.00 | 5.00               | 5.00 | 5.00 | 5.00 |
| LIR1                | 9.00               | 9.00 | 9.00 | 2.75               | 2.75 | 2.00 | 2.00 |
| LIR2                | 9.00               | 9.00 | 9.00 | 2.75               | 2.75 | 2.00 | 2.00 |

In the analyses, the ceiling diaphragms were assumed to contain the same construction details as the full-scale ceiling test. The shear modulus of solid shell elements for ceiling diaphragm were calibrated, based on the shear actions.

The used virtual shear modulus of roof ceiling diaphragm for the static analysis is summarised in Table 16.

**Table 16. G for ceiling diaphragms of rectangular and L-shaped buildings (MPa)**

| Case study building | Virtual shear modulus of ceiling diaphragm |
|---------------------|--|
| RR                  | 36   |
| RIR1                | 21   |
| RIR2                | 28   |
| LR                  | 41   |
| LIR1                | 34   |
| LIR2                | 34   |

### 5.2.3 Results of analysis

The 3D ETABS analyses provided seismic response information on static deformations, shear stress concentrations, dynamic responses and so on. The discussion presented here focuses on the induced lateral deflections identified as being closely related to the damage observed in past earthquakes.

Figure 13 to Figure 15 show the obtained lateral deflections at roof eave level for three rectangular case study buildings when subjected to y directional seismic actions derived from NZS 3604:2011.

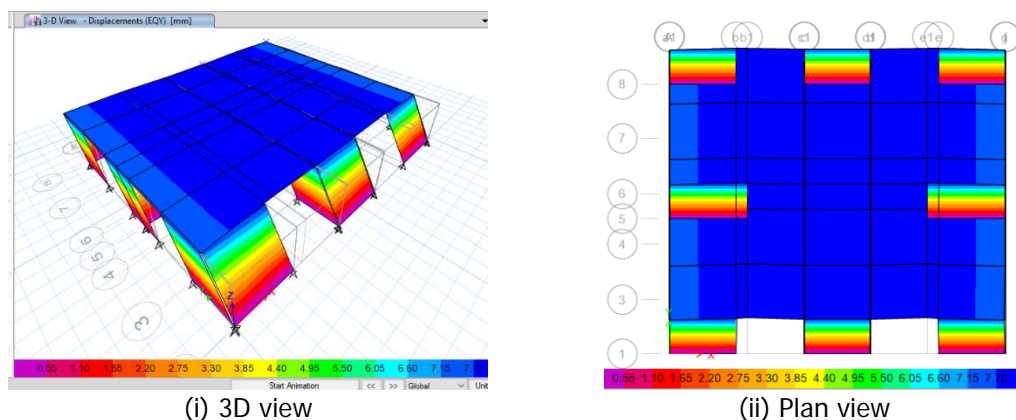


Figure 13. Deflections obtained for case study building RR.

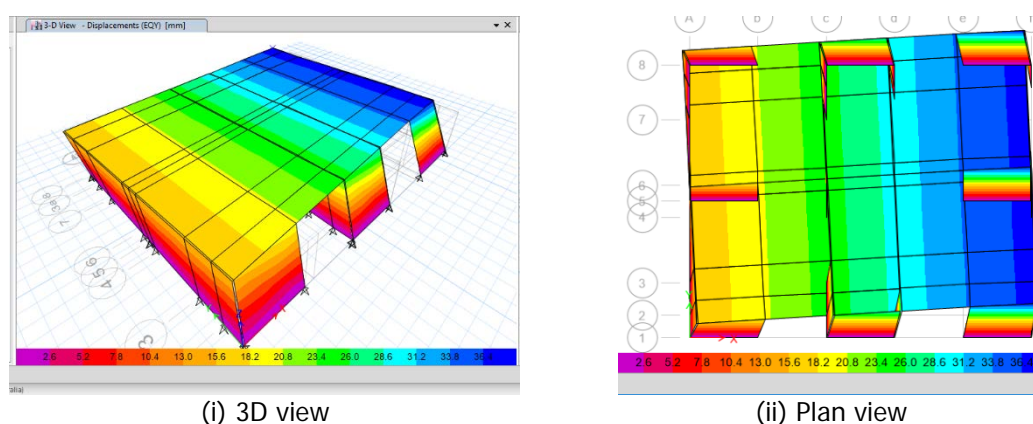


Figure 14. Deflections obtained for case study building RIR1.

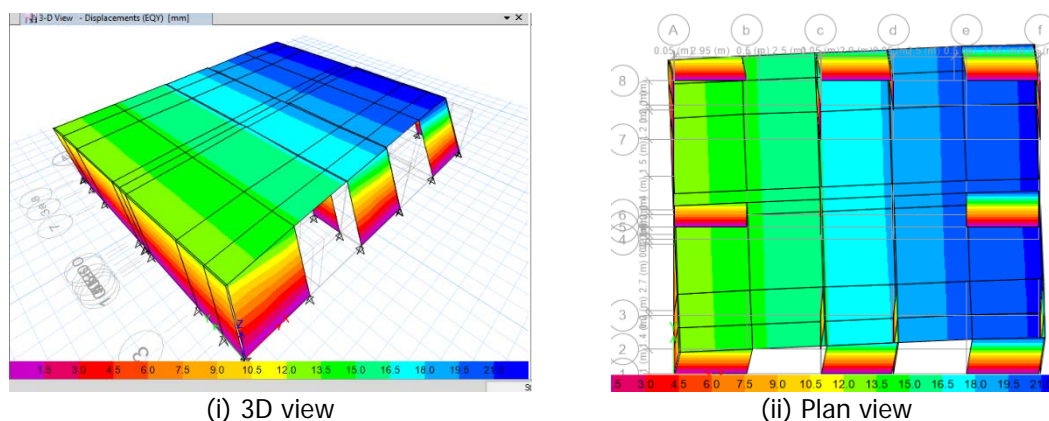


Figure 15. Deflections obtained for case study building RIR2.

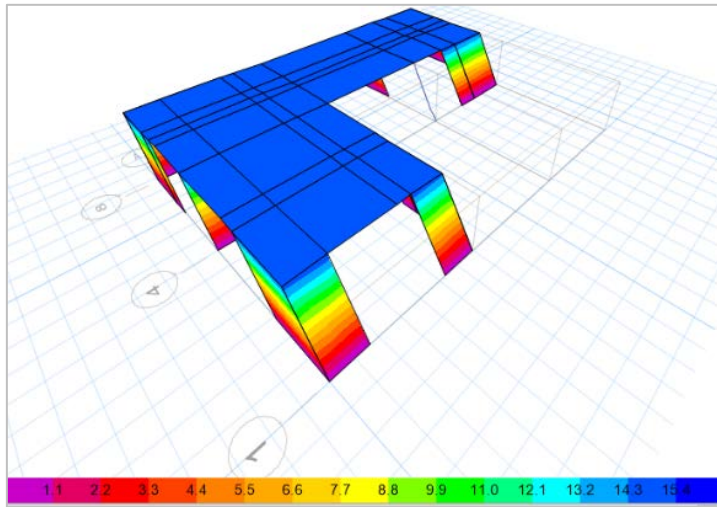
Table 17 lists the obtained deflection results of the rectangular buildings at roof level.

Table 17. Lateral deflections along different grid lines (rectangular buildings).

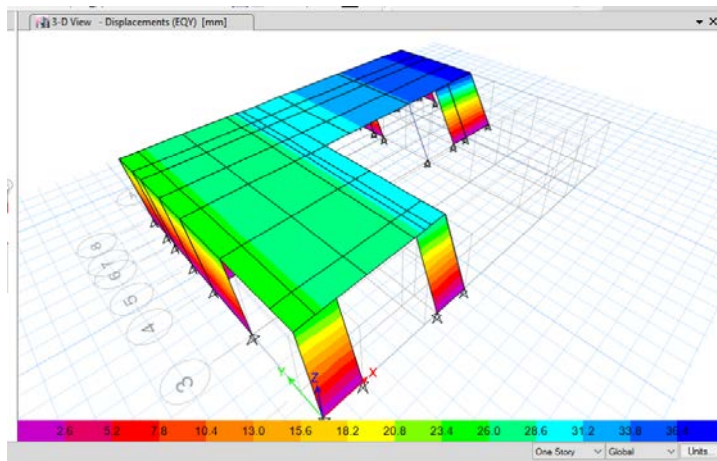
| Case study building | Grid line ID |         |         |         |         |         |
|---------------------|--------------|---------|---------|---------|---------|---------|
|                     | A            | B       | C       | D       | E       | F       |
| RR                  | 7.5 mm       | 7.5 mm  | 7.5 mm  | 7.5 mm  | 7.5 mm  | 7.5 mm  |
| RIR1                | 16.0 mm      | 20.5 mm | 25.0 mm | 29.7 mm | 34.3 mm | 37.8 mm |
| RIR2                | 12.5 mm      | 14.8 mm | 16.6 mm | 18.5 mm | 20.5 mm | 21.6 mm |



Figure 16 to Figure 18 show the obtained lateral deflections at roof eave level for three L-shaped case study buildings when subjected to y directional seismic actions derived from NZS 3604:2011.



**Figure 16. Deflections obtained for building LR.**



**Figure 17. Deflections obtained for building LIR1.**

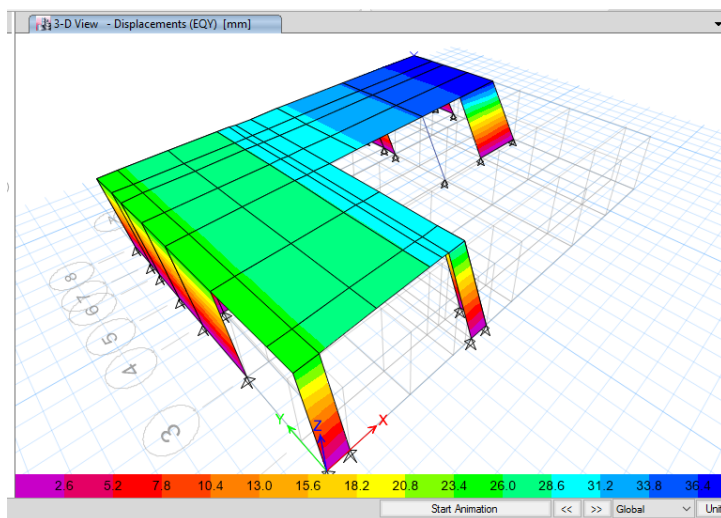


**Figure 18. Deflections obtained for building LIR2.**

Table 18 lists the obtained deflection results of the L-shaped buildings at roof level.

**Table 18. Lateral deflections along different grid lines (L-shaped buildings).**

| Case study building | Grid line ID |         |         |         |
|---------------------|--------------|---------|---------|---------|
|                     | A            | B       | C       | D       |
| LR                  | 14.1 mm      | 14.1 mm | 14.1 mm | 13.6 mm |
| LIR1                | 25.0 mm      | 29.4 mm | 34.0 mm | 38.3 mm |
| LIR2                | 25.1 mm      | 29.2 mm | 33.6 mm | 38.6 mm |

## 5.3 Discussion

For typical LTF buildings, plasterboard-lined LTF walls are the lateral seismic-resisting systems, and therefore, LTF buildings perform in earthquakes in a similar way to other wall structures. The plasterboard-lined shear walls are also the gravity load-carrying elements of LTF buildings. The lateral deflections experienced by these walls in design earthquakes would be small in comparison with the wall lengths. In addition, low-rise LTF residential buildings are light in nature, and subsequently,  $P-\Delta$  effects usually are not significant enough to cause instability problems after the buildings have undergone significant earthquake-induced lateral deflections. Therefore, the LTF buildings of mainly NZS 3604:2011 construction could easily achieve life safety requirements in design earthquakes, as reported in past studies (Liu, 2015, 2017).

The reported collapse limit state for low-rise wooden buildings overseas could reach a storey drift of 7% or even more (Paevere, Foliente & Kasal, 2003; Bahmani & van de Lindt, 2013). A storey drift of 7% is significantly higher than the ULS deflection limit of 2.5%, as specified in the New Zealand seismic loading standard NZS 1170.5:2004. This means that the life safety requirement at ULS as per NZS 3604:2011 is not meaningful for LTF buildings. Instead, damage control would be a much more meaningful ULS seismic performance criterion for LTF buildings. Earthquake damage to LTF buildings is a result of differential deformations between different parts within a plan.

Studies of many P21 tests at BRANZ (Liu, 2015) show that an LTF plasterboard-sheathed wall of reasonable length is expected to experience significant strength degradation and softening after a lateral deflection of 22 mm over a 2.4 m storey height. Thus 22 mm over a 2.4 m storey height (or a storey drift of 1%) at an ULS earthquake event is established as the assessment criterion in evaluating the seismic performance of our case study buildings.

### 5.3.1 Seismic performance of permissible earthquake designs

As described previously, all the case study buildings met the irregularity requirement limits specified by NZS 3604:2011. How have the irregular bracing arrangements affected the lateral deflections experienced by different parts of the buildings?

Comparison of the induced lateral deflections of case study building RR and case study building RIR1, as the values in tables, shows that extreme irregular bracing arrangements as allowed by NZS 3604:2011 could result in significant amplification of lateral deflections. In detail, the largest induced lateral deflection for the studied extremely irregular LTF building was 37.8 mm. This is five times that induced in the perfectly regular building under an ULS seismic action as specified by NZS 3604:2011.



A lateral deflection of 7.5 mm over a storey height of 2.4 m of an LTF building is well within the established damage control limit, which is 22 mm in terms of lateral deflection over a storey height of 2.4 m. In contrast, a lateral deflection of 37.8 mm over a storey height of 2.4 m of an LTF building (as for case study building RIR1) means that the building will no longer be repairable in a major earthquake and will need to be demolished afterwards.

This indicates that the current irregularity limits in NZS 3604:2011 are not robust enough to achieve reasonably consistent seismic performance of LTF buildings.

### 5.3.2 Effect of boosting minimum bracing provisions

Case study building RIR2 was less irregular than case study building RIR1, although both buildings have exactly the same total bracing resistance. For RIR2, the minimum bracing capacity along the perimeters was calculated using 75% rather than 50% of total seismic bracing demand divided by bracing line numbers.

As shown in Table 17, this adjustment resulted in a significantly reduced lateral deflection, and the maximum induced lateral deflection became under 22 mm – the established damage control limit.

This implies that the current irregularity limits in NZS 3604:2011 should be tightened and the minimum bracing provision along the bracing lines, especially the perimeter lines, should be boosted significantly.

### 5.3.3 Effects of ceiling diaphragm rigidity

Effects of ceiling diaphragm rigidity on the seismic performance of LTF buildings are investigated in this study. For a case study building, two ETABS models were constructed. The two ETABS models were identical except for the rigidity of the ceiling diaphragm. The study revealed that a 50% reduction of the ceiling diaphragm rigidity only led to an increase of 5% of maximum induced lateral deflection. An 80% reduction of the ceiling diaphragm rigidity (the low end of the ceiling rigidity) led to an increase of 15% of maximum induced lateral deflection.

These findings suggest that rigidity of ceiling diaphragms without openings has no significant effect on the seismic performance of LTF buildings, provided that the spacing of bracing lines is not greater than 6 m.

### 5.3.4 Overall seismic demand

The seismic action inputs for the static structural analysis conducted on each case study building were derived according to NZS 3604:2011, and the equivalent seismic coefficient was 0.4 for all the case study buildings.

It remains a question whether or not the seismic inputs used are appropriate.

#### Dynamic properties

For each case study building with the members modelled using the calibrated stiffness as described in section 5.2.2, the dynamic responses are calculated.

Obtained fundamental periods associated with the first and second modes are summarised in Table 19.

**Table 19. Fundamental periods T (s).**

| Case study building | T <sub>1</sub>       | T <sub>2</sub>       |
|---------------------|----------------------|----------------------|
| RR                  | 0.29 (X translation) | 0.28 (Y translation) |
| RIR1                | 0.28 (X translation) | 0.14 (torsion)       |
| RIR2                | 0.21 (Y translation) | 0.14 (torsion)       |
| LR                  | 0.45 (Y translation) | 0.35 (torsion)       |
| LIR1                | 0.56 (Y translation) | 0.37 (torsion)       |
| LIR2                | 0.56 (Y translation) | 0.37 (torsion)       |

### Adequacy of current code specifications

As shown in Table 19, the fundamental periods are shorter than 0.45 seconds for all rectangular buildings and about 0.45–0.55 seconds for L-shaped buildings.

For the assumed site where the subsoil class is D as defined in NZS 1170.5:2004 and the seismic hazard is  $Z = 0.46$ , the design seismic coefficient could be expressed as:

$$C_d = S_p C_h(T) Z R_\xi \quad \text{Eq. 7}$$

Where:

$S_p$  is the structural performance factor, which is related to the ductility of the structure

$C_h(T)$  is the spectral shape factor

$Z$  is the hazard factor

$R_\xi$  is the seismic action reduction factor due to the damping

$$R_\xi = \sqrt{\frac{7}{2+\xi}} \quad \text{Eq. 8}$$

Where:  $\xi$  is the damping ratio of the whole building system, including bracing wall elements, floor diaphragms and other important contributors.

For a seismic coefficient of 0.4, the required damping level is 41% for rectangular buildings and 38% for L-shaped buildings.

As reported in Appendix A and previous studies, the damping capacity of plasterboard bracing walls as specified in ordinary LTF residential buildings is less than 20%. This means that, unless other factors (floors and other system factors) could significantly contribute to the overall energy-dissipating capacity of LTF buildings in earthquakes, the current seismic design actions specified by NZS 3604:2011 might have significantly underestimated the seismic actions that are expected to be induced in the buildings.

Study on the breakdowns of other contributors (floors and others) to overall damping levels is beyond the scope of this project but will be required to appropriately evaluate the adequacy of the seismic actions as recommended in NZS 3604:2011.

## 6. Conclusions and recommendations

LTF residential buildings in New Zealand are constructed according to NZS 3604:2011, and their lateral seismic-resisting systems are nearly universally plasterboard walls. With regards to the bracing element distributions across the building plans, NZS 3604:2011 specifies irregular arrangement limits of bracing elements. However, these limits were not based on scientific evidence.

In the Canterbury earthquake sequence, LTF residential buildings all achieved life-safety, but some had unacceptable earthquake damage. It was apparent that presence of irregular bracing arrangements in LTF buildings exacerbated the earthquake damage significantly.

The objective of this study was to quantify the seismic effects of allowable irregularity limits in current design standard NZS 3604:2011 towards developing new rules to control earthquake damage to LTF buildings.

A literature review of research efforts on seismic behaviour of irregular buildings was conducted. The review revealed that structural irregularity complicates seismic performance predictions significantly, and three-dimensional analyses with adequate modelling of lateral seismic-resisting systems and diaphragms are essential to capture the necessary seismic behaviour.

Six single-level LTF case study buildings were designed to NZS 3604:2011 containing different degrees of allowable structural irregularities. Three-dimensional static non-linear push-over seismic analyses were conducted, using the ETABS program, on each case study building.

To adequately model the lateral seismic-resisting elements (plasterboard walls), many sets of test data collected from past racking tests on plasterboard walls were studied. Subsequently, a racking model representing the bracing behaviour of plasterboard bracing wall elements was developed and the degrading behaviour of plasterboard walls was simulated by the degrading shear modulus. The developed mathematical model for plasterboard walls matches the test results reasonably well. With regards to the development of the in-plane rigidity model of ceiling diaphragms, a two-stage test programme was carried out as part of this project. The ceiling diaphragm test programme included a full-scale ceiling diaphragm test and four small-scale ceiling diaphragms with different construction details in different applications. As a result, a mathematical model was developed to simulate the in-plane rigidity of plasterboard ceiling diaphragms as typical of New Zealand practice.

Static push-over analyses were conducted for each case study building in this project where a 3D ETABS model was constructed for each building. The walls and the ceiling diaphragms were modelled using the mathematical models developed in this project. The findings obtained from these studies are summarised below.

### Findings on modelling techniques of LTF buildings as typical of New Zealand practice

- Racking behaviour of plasterboard walls has many similarities to the in-plane performance of plasterboard ceiling diaphragms. Both racking behaviour of plasterboard walls and in-plane performance of plasterboard ceiling diaphragms are strongly dependent on the fixing details from plasterboard sheets to the framing.
- Racking performance of plasterboard walls and in-plane rigidities of plasterboard ceiling diaphragms could be mathematically modelled by a plate member

associated with a material that has a constant elastic modulus and a degrading shear modulus.

#### Findings on seismic bracing arrangement clauses of NZS 3604:2011

- Current permissible irregular seismic bracing arrangements in NZS 3604:2011 could potentially amplify the lateral deflections by 500% in comparison with the regular buildings. LTF buildings with minimum bracing provision along the perimeters could sustain earthquake damage well beyond repair.
- In-plane rigidity of plasterboard ceiling diaphragms varies a lot, depending on the adopted construction practice. In general, plasterboard ceiling diaphragms are relatively rigid in comparison with cantilever plasterboard bracing walls. The higher the in-plane rigidity, the better the overall performance of an irregular building.
- The expected seismic actions induced in LTF buildings could be significantly higher than the specified action in NZS 3604:2011. This occurs because of a mismatch of the assumed energy-dissipating capacity in NZS 3604:2011 and the capable energy-dissipating capacity of plasterboard walls.
- Tightening the minimum bracing provisions in NZS 3604:2011 by 50% along the perimeter bracing lines could reduce the induced lateral deflection by 43% and keep the deflection within a tolerable damage control limit.
- The seismic effect of geometrical irregularity in an irregular-shaped LTF building is similar to that of irregular bracing arrangements in regular buildings. To mitigate the adverse effects associated with irregular-shaped buildings, it is suggested that bracing designs provided to each part of a building be based on a tributary area theory.

## References

- Al-Ali, A. & Krawinkler, H. (1998). *Effects of vertical irregularity on the seismic behaviour of building structures*. Report No. 130. San Francisco, CA: Department of Civil and Environmental Engineering, Stanford University.
- Arnold, C. & Reitherman, R. (1982). *Building configuration and seismic design*. New York, NY: John Wiley & Sons.
- Bahmani, P. & van de Lindt, J. W. (2013). Direct displacement design of vertically and horizontally irregular woodframe buildings. *Proceedings of Structures Congress 2013*, Pittsburgh, USA, 2–4 May.
- Canterbury Earthquakes Royal Commission. (2012). *Final report: Volume 2: The performance of Christchurch CBD buildings*. Christchurch, New Zealand: Author.
- Carradine, D. M., Dolan, J. D. & Bott, J. W. (2004). Effect of load and construction on cyclic stiffness of wood diaphragms. *Proceedings of the 8<sup>th</sup> World Conference on Timber Engineering*, Lahti, Finland, 14–17 June.
- Chen, Z., Chui, Y., Ni, C., Doudak, G. & Mohammad, M. (2014). Load distribution in timber structures consisting of multiple lateral load resisting elements with different stiffnesses. *Journal of Performance of Constructed Facilities*, 28(6), A4014011.
- Chopra, A. K. & Goel, G. K. (2004). A modal push-over analysis procedure to estimate seismic demands for unsymmetric-plan buildings. *Earthquake Engineering and Structural Dynamics*, 33(8), 903–927.
- Christovasilis, I. P., Filiatrault, A. & Wanitkorkul, A. (2007). *Seismic testing of a full-scale two-story light-frame wood building: NEESWood benchmark test*. Buffalo, NY: Department of Civil, Structural and Environmental Engineering, University at Buffalo, State University of New York.
- Dolan, J. D. (1989). *The dynamic response of timber shear walls* (PhD thesis). University of British Columbia, Vancouver, Canada.
- Dowrick, D. J. & Smith, P. C. (1986). Timber sheathed walls for wind and earthquake resistance. *Bulletin of the New Zealand National Society for Earthquake Engineering*, 19(2), 123–134.
- Easley, J. T., Foomani, M. & Dodds, R. H. (1982). Formulas for wood shear walls. *Journal of the Structural Division*, 108(11), 2460–2478.
- Fajfar, P., Marusic, D. & Perus, I. (2006). The N2 method for asymmetric buildings. *Proceedings of First European Conference on Earthquake Engineering and Seismology*, Geneva, Switzerland, 3–8 September.
- FEMA. (2012). *Seismic evaluation and retrofit of multi-unit wood-frame buildings with weak first stories*. FEMA P-807. Washington, DC: Federal Emergency Management Agency.
- Folz, B. & Filiatrault, A. (2002a). *A computer program for cyclic analysis of shearwall in woodframe*. Richmond, California: CUREE.

- Folz, B. & Filiatrault, A. (2002b). *A computer program for seismic analysis of woodframe structures*. Richmond, California: CUREE.
- Foschi, R. O. (1977). Analysis of wood diaphragms and trusses. Part 1: Diaphragms. *Canadian Journal of Civil Engineering*, 4(3), 345–352.
- Gupta, A. K. & Kuo, G. P. (1985). Behavior of wood-framed shear walls. *Journal of Structural Engineering*, 111(8), 1722–1733.
- Gutkowski, R. M. & Castillo, A. L. (1988). Single and double-sheathed wood shear wall study. *Journal of Structural Engineering*, 114(6), 1268–1284.
- Itani, R. Y. & Cheung, C. K. (1984). Nonlinear analysis of sheathed wood diaphragms. *Journal of Structural Engineering*, 110(9), 2137–2147.
- Jacobsen, L. S. (1960). Damping in composite structures. *Proceedings of the Second World Conference on Earthquake Engineering*, Tokyo and Kyoto, Japan, 11–18 July.
- Kamiya, F. (1990). Horizontal plywood sheathed diaphragms with openings: Static loading tests and analysis. *Proceedings of the International Timber Engineering Conference*, Tokyo, Japan, 23–25 October.
- Kasal, B., Leichti, R. J. & Itani, R. Y. (1994). Nonlinear finite element model of complete light frame wood structures. *Journal of Structural Engineering*, 120(1), 100–119.
- Kirkham, W. J., Gupta, R. & Miller, T. H. (2015). Effects of roof pitch and gypsum ceilings on the behavior of wood roof diaphragms. *Journal of Performance of Constructed Facilities*, 29(1), 04014039.
- Kirkham, W. J., Miller, T. H. & Gupta, R. (2016). Practical analysis for horizontal diaphragm design of wood-frame single-family dwellings. *Practice Periodical on Structural Design and Construction*, 21(1).
- Liew, Y. L., Gad E. F. & Duffield, C. F. (2005). Modularised closed-form mathematical model for predicting the bracing performance of plasterboard clad walls. *Structural Engineering and Mechanics*, 20(1), 45–67.
- Liu, A. (2011). *Guidance for bracing design for hillside houses*. Study Report SR262. Judgeford, New Zealand: BRANZ Ltd.
- Liu, A. (2015). *Design guidance of specifically designed bracing systems in light timber-framed residential buildings*. EQC Report.  
<http://www.eqc.govt.nz/research/research-papers/390-design-guidance-bracing-systems-light-timber-framed-res-bldgs>
- Liu, A. (2017). Need for a systematic approach in damage control design for light timber-framed buildings. *Proceedings of the 16th World Conference on Earthquake Engineering*, Santiago, Chile, 9–13 January.
- Lucksiri, K., Miller, T., Gupta, R., Pei, S. & van den Lindt, J. (2012). Effect of plan configuration on seismic performance of single-storey wood-frame dwellings. *Natural Hazards Review*, 13(1), 24–33.



- McCutcheon, W. J. (1985). Racking deformations in wood shear walls. *Journal of Structural Engineering*, 111(2), 257–269.
- Moroder, D. (2016). *Floor diaphragms in multi-storey timber buildings* (PhD thesis). University of Canterbury, Christchurch, New Zealand.
- Murakami, M., Moss, P. J., Carr, A. J. & Inayama, M. (1999). Formulae to predict non-linear behaviour of sheathed walls with any nailing arrangement pattern. *Proceedings of the Pacific Timber Engineering Conference*, Rotorua, New Zealand, 14–18 March.
- Paevere, P., Foliente, G. C. & Kasal, B. (2003). Load-sharing and redistribution in a one-story woodframe building. *Journal of Structural Engineering*, 129(9), 1275–1284.
- Pang, W. C. & Rosowsky, D. V. (2010). Beam-spring model for timber diaphragm and shear walls. *Proceedings of the Institution of Civil Engineers – Structures and Buildings*, 163(4), 227–244.
- Patton-Mallory, M. & McCutcheon, W. J. (1987). Predicting racking performance of walls sheathed on both sides. *Forest Products Journal*, 37(9), 27–32.
- Paulay, T. (1996). Seismic design for torsional response of ductile buildings. *Bulletin of the New Zealand National Society for Earthquake Engineering*, 29(3), 178–198.
- Paulay, T. (1997). A review of code provisions for torsional seismic effects in buildings. *Bulletin of the New Zealand National Society for Earthquake Engineering*, 30(3), 252–263.
- Paulay, T. (2000). Understanding torsional phenomena in ductile systems. *Bulletin of the New Zealand National Society for Earthquake Engineering*, 33(4), 403–420.
- Paulay, T. & Priestley, M. (1992). *Seismic design of reinforced concrete and masonry buildings*. New York, NY: John Wiley & Sons.
- Sadashiva, V. K. (2010). *Quantifying structural irregularity effects for simple seismic design*. Christchurch, New Zealand: University of Canterbury.
- Saifullah, I., Gad, E., Shahi, R., Wilson, J., Lam, N. & Watson, K. (2014). Ceiling diaphragm actions in cold formed steel-framed domestic structures. *Proceedings of the ASEC (Australasian Structural Engineering Conference)*, Auckland, New Zealand, 9–11 July.
- Saifullah, I., Gad, E., Shahi, R. & Watson, K. (2016). Structural behaviour of ceiling diaphragms in steel-framed residential structures. *Proceedings of the Australasian Structural Engineering Conference: ASEC 2016*, Brisbane, Australia, 22–25 November.
- Salenikovich, A. J. (2000). *The racking performance of light-frame shear walls* (PhD thesis). Department of Wood Science and Forest Products, Virginia Polytechnic Institute and State University, Blacksburg, VA.
- SEAOC. (1999). *Recommended lateral force requirements and commentary* (7th ed.). Sacramento, CA: Structural Engineers Association of California.

- Shelton, R. (2004). Diaphragms for timber framed buildings. *SESOC Journal*, 17(1), 16–23.
- Shelton, R. (2010). *A wall bracing test and evaluation procedure*. BRANZ Technical Paper P21. Judgeford, New Zealand: BRANZ Ltd.
- Shelton, R. (2013). *Engineering basis of NZS 3604*. Judgeford, New Zealand: BRANZ Ltd.
- Thurston, S. (1993). Report on racking resistance of long sheathed timber framed walls with openings. BRANZ Study Report SR54. Judgeford, New Zealand: BRANZ Ltd.
- Tuomi, R. L. & McCutcheon, W. J. (1978). Racking strength of light frame nailed walls. *Journal of the Structural Division*, 104(7), 1131–1140.
- Valmundsson, E. V. & Nau, J. M. (1997). Seismic response of building frames with vertical structural irregularities. *Journal of Structural Engineering*, 123(1), 30–41.
- White, M. W. (1995). *Parametric study of timber shear walls* (PhD thesis). Department of Wood Science and Forest Products, Virginia Polytechnic Institute and State University, Blacksburg, VA.
- Winstone Wallboards. (2014). *GIB site guide*. Auckland, New Zealand: Winstone Wallboards. <https://www.gib.co.nz/assets/Uploads/LiteratureFile/GIB-Site-Guide/GIB-Site-Guide-2014.pdf>



## Appendix A: Seismic behaviour of LTF bracing walls

As stated above, residential LTF buildings in New Zealand are constructed according to NZS 3604:2011, and the seismic bracing elements are proprietary LTF walls.

Seismic performance of LTF buildings thus depends on the bracing strength/stiffness and energy-dissipating capacities of the walls. A better understanding and then adequate modelling of bracing behaviour of timber walls are logical steps to be undertaken in order to understand the expected seismic performance of LTF buildings.

Research frequently shows that bracing behaviour of LTF walls is dependent on the sheathing material and the fixing details from the sheathing sheets to the timber frames. For timber-framed houses overseas, the sheathing sheets for timber bracing walls are often engineered timber panels, such as plywood or OSB (oriented stranded board). In comparison, the sheathing materials commonly used in constructing timber bracing walls in New Zealand are plasterboard sheets, and the attachment of plasterboard to timber frame members is universally by screws.

The objectives of this appendix are to:

- clarify the seismic rating methodology of timber bracing walls used with NZS 3604:2011
- characterise the bracing performance of LTF walls sheathed by plasterboard sheet as typical of New Zealand practice
- develop a modelling technique for the bracing behaviour of plasterboard-sheathed LTF walls.

### A1 Seismic rating methodology

NZS 3604:2011 specifies not only the seismic demands but also seismic bracing provisions. NZS 3604:2011 specifies that the P21 test and evaluation procedure (Shelton, 2013), developed and published by BRANZ (Shelton, 2010) be used to evaluate the seismic bracing capacity of proprietary LTF wall elements.

The P21 test is a slow cyclic racking test on a cantilever proprietary LTF wall element, and a horizontal load is applied at the top of the wall. The test arrangement for a typical P21 test is illustrated in Figure 19.

The seismic rating of the wall element is determined from the fourth cycle force at a deflection between 15 mm and 36 mm, depending on when significant strength degradation occurs. P21 tests are often conducted on standard wall lengths 0.4 m long, 0.6 m long and 1.2 m long. For longer walls up to 2.4 m long, the seismic rating per metre length is assumed to be the same as for 1.2 m long walls. That is, the determined rating may be applied to walls up to twice the length of the tested LTF proprietary walls. If the rated LTF walls are used in taller storey height situations, the rated seismic rating of the walls should be adjusted. The adjusted seismic capacity is equal to the rated seismic capacity multiplied by the ratio of 2.4 m versus the wall height in the intended applications. P21 tests on LTF walls are mostly conducted on rectangular walls.

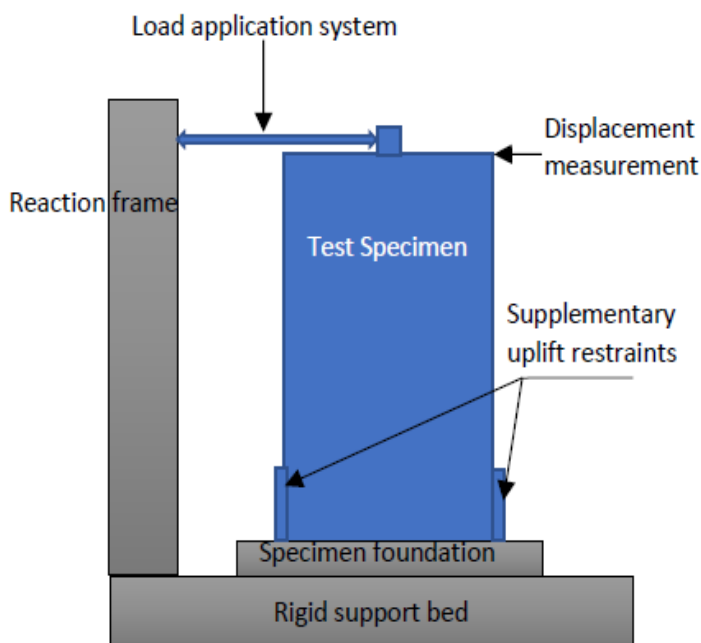


**Figure 19. P21 test arrangement.**

There are a variety of LTF proprietary timber wall bracing systems available in New Zealand. Typically, these proprietary timber wall bracing systems have identical timber frames, and the differences between these systems are the sheathing sheets and the fixing details (fastener and fixing details) from the sheathing sheets to timber frames. Over 90% of LTF proprietary bracing systems in New Zealand are plasterboard bracing walls. These vary in terms of plasterboard sheets and the fixing details, depending on the specification of plasterboard manufacturers.

## A2 Racking behaviour of plasterboard walls

As a main structural testing centre in New Zealand, BRANZ Structures Lab has conducted many P21 tests on plasterboard timber walls on either a commercial basis or a research basis. The measurements obtained during a test include the applied load, the deflection at the top of the specimen, uplifts at both ends of the specimen and the slip at the base of the wall.

In this appendix, a reasonable set of P21 test results conducted on plasterboard walls at BRANZ Structures Lab has been collated and studied. The study focuses on:

- characteristics of bracing performance of plasterboard walls
- mathematical models of LTF wall racking performance as typical of New Zealand plasterboard walls.

### A2.1 Bracing performance of plasterboard walls

Most important seismic behaviour properties of any lateral seismic-resisting systems are strength attainment and strength maintenance with the progress of imposed deformation as well as the energy-dissipating capacities. In the following, the strength degradation and energy-dissipating capacity of plasterboard walls are studied, based on test evidence.

### Strength degradation

In conducting P21 tests on proprietary LTF walls, the loading is a displacement-controlled procedure. At one specific deflection level, three cycles are applied. A common phenomenon observed during P21 tests on plasterboard walls is significant strength degradation as cyclic loading progresses at the same deflection levels, as demonstrated in Figure 20.

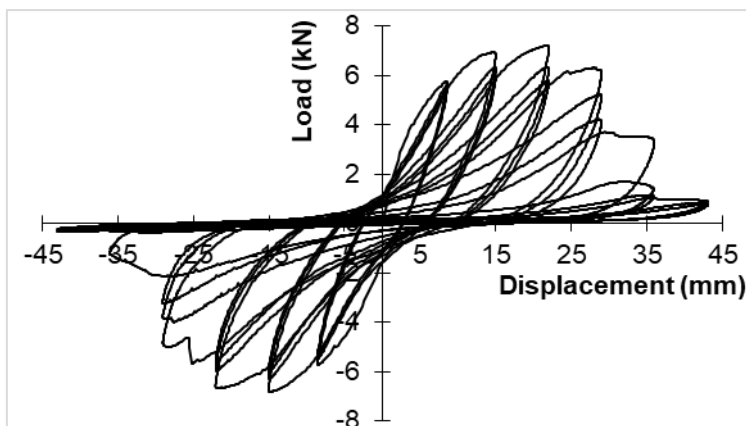


**Figure 20. Hysteresis loops of a 1.2 m long plasterboard wall.**

Table 20 lists the attained racking strengths of six P21 tests during the first cycle and the third cycle at specific deflection levels.

**Table 20. Attainment of racking strength at the same deflection level.**

| Test ID | Cycle # | Racking strength (kN) at specific deflection levels |            |            |            |            |            |
|---------|---------|---|------------|------------|------------|------------|------------|
|         |         | 8 mm  | 15 mm      | 22 mm      | 29 mm      | 36 mm      | 43 mm      |
| 1       | 1st     | 5.7 (-5.0)  | 6.1 (-5.7) | 6.5 (-6.0) | 6.8 (-5.9) | 6.8 (-5.9) | 5.9 (-5.2) |
|         | 3rd     | 4.9 (-4.6)  | 5.4 (-5.1) | 5.7 (-5.2) | 5.8 (-5.1) | 5.6 (-4.8) | 4.4 (-4.0) |
| 2       | 1st     | 3.2 (-3.1)  | 3.5 (-3.4) | 3.7 (-3.6) | 3.6 (-3.5) | 3.5 (-3.3) | 3.2 (-3.0) |
|         | 3rd     | 2.6 (-2.6)  | 2.9 (-2.9) | 3.1 (-3.0) | 2.9 (-2.9) | 2.8 (-2.6) | 2.5 (-2.3) |
| 3       | 1st     | 5.5 (-4.8)  | 6.2 (-5.1) | 6.1 (-5.2) | 6.1 (-5.1) | 6.2 (-5.1) | 6.3 (-5.0) |
|         | 3rd     | 5.0 (-4.3)  | 5.5 (-4.5) | 5.3 (-4.5) | 5.4 (-4.5) | 5.3 (-4.6) | 5.2 (-4.7) |
| 4       | 1st     | 3.3 (-3.5)  | 3.7 (-3.9) | 3.8 (-3.9) | 3.8 (-3.8) | 3.1 (-3.1) | 1.9 (-1.9) |
|         | 3rd     | 2.8 (-3.0)  | 3.1 (-3.2) | 3.2 (-3.2) | 2.8 (-2.9) | 1.9 (-1.9) | 0.6 (-0.5) |
| 5       | 1st     | 3.7 (-3.4)  | 4.1 (-4.0) | 4.2 (-4.1) | 4.1 (-3.7) | 3.5 (-3.5) | 3.2 (-3.2) |
|         | 3rd     | 3.1 (-2.9)  | 3.5 (-3.3) | 3.5 (-3.2) | 3.1 (-3.0) | 2.8 (-2.9) | 2.6 (-2.5) |
| 6       | 1st     | 1.1 (-1.1)  | 1.3 (-1.3) | 1.4 (-1.4) | 1.4 (-1.5) | 1.4 (-1.5) | 1.4 (-1.6) |
|         | 3rd     | 1.1 (-1.1)  | 1.2 (-1.2) | 1.3 (-1.3) | 1.3 (-1.4) | 1.3 (-1.4) | 1.3 (-1.4) |

Racking strengths outside brackets and inside brackets are respectively the attained racking strength in positive loading direction and in negative loading direction.

As demonstrated in Table 20, the racking strength attained at the third cycle is significantly lower than the racking strength attained at the first cycle for the same deflection level. The drops range from 15–25% and occasionally up to 70% (test 4).

### Energy-dissipating capacity of plasterboard wall elements

An apparent evidence observed during P21 tests on plasterboard walls is that the hysteresis loops become significantly pinched as the loading progresses, as illustrated in Figure 19, indicating a significant reduction in the energy-dissipating capacities.

There are many methods to calculate equivalent damping levels. Using a common method developed by Jacobsen (1960), equivalent damping is derived by equating the energy absorbed by hysteretic cyclic response to a given displacement level as follows:

$$\xi_{eq} = \frac{A_h}{2\pi F_m \Delta_m} \quad \text{Eq. 9}$$

Where:  $A_h$  is the area within one complete cycle of stabilised force-displacement response and  $F_m$  and  $\Delta_m$  are the maximum force and displacement achieved in the stabilised loops.

It needs to be appreciated that the force-displacement hysteresis loops of plasterboard walls are not stabilised as the loading cycles at the same deflection. However, Jacobsen's method is used in this study to obtain the equivalent damping of plasterboard wall bracing elements.

The equivalent damping,  $\xi_{eq}$ , in Eq. 9 is the fraction of critical damping and is related to the secant stiffness,  $K_e$ , to maximum response. It is thus compatible with the assumptions of structural characterisation by stiffness and damping at peak response.

In this study, the damping levels are estimated using the complete first cycle and complete third cycle at each deflection level. Equivalent damping levels of four selected P21 tests were calculated using the method described above, and the results are listed in Table 21. The third cycle shows significantly reduced energy-dissipating capacity in comparison with the first cycle of the same test and the same deflection level. The damping ratio derived from the first cycle of a test at a specific deflection level is about 10–15%, equivalent to a ductility of 1.5–2 in a force-based approach. In addition, damping ratio derived from the third cycle drops to about 6–10%, equivalent to a ductility of 1.25–1.5. Clearly, plasterboard walls are not expected to perform in a desirable ductile manner. Coupled with the drop of the racking strength at the same deflection level of 15–25%, the racking capacity degradation of the third cycle is about 35–50% compared with that at the first cycle.

**Table 21. Equivalent damping levels,  $\xi_{eq}$ .**

| Test ID | Cycle # | Deflection levels of cycles (mm) |     |     |     |     |     |
|---------|---------|----------------------------------|-----|-----|-----|-----|-----|
|         |         | 8                                | 15  | 22  | 29  | 36  | 43  |
| A       | 1st     | 16%                              | 14% | 13% | 12% | 11% | 10% |
|         | 3rd     | 10%                              | 9%  | 9%  | 8%  | 8%  | 6%  |
| B       | 1st     | 16%                              | 15% | 13% | 11% | 9%  | 8%  |
|         | 3rd     | 10%                              | 9%  | 8%  | 7%  | 6%  | 6%  |
| C       | 1st     | 15%                              | 14% | 13% | 12% | 10% | 9%  |
|         | 3rd     | 10%                              | 10% | 9%  | 8%  | 7%  | 7%  |
| D       | 1st     | 15%                              | 14% | 13% | 11% | 11% | 11% |
|         | 3rd     | 10%                              | 9%  | 9%  | 9%  | 9%  | 8%  |

Based on an elemental based approach, a system with a damping ratio of 6–10% would translate to an equivalent ductility of about 1.5. As observed during P21 tests, ongoing degradation would occur as loading progresses, indicating that the energy-dissipating mechanism of plasterboard walls is not reliable, especially when the earthquake duration is long. Therefore, the damping capacity of plasterboard walls at elemental level is very low.

## A2.2 Racking model of plasterboard timber walls

Commonly, racking tests on timber-sheathed walls are conducted on rectangular cantilever wall elements of certain lengths. Many people have attempted to develop models to predict racking performance of bracing wall elements of other configurations or other lengths.

A few models have been developed overseas and in New Zealand on the racking performance of timber-sheathed walls that can be classified into two main categories – mathematical models and finite element (FE) models.

A common form of mathematical model is the closed-form mathematical model. This describes the overall response of a wall of a given configuration without comprehensively analysing each component of the wall. The closed-form mathematical modelling approach was adopted by Tuomi and McCutcheon (1978), Easley, Foomani and Dodds (1982), Gupta and Kuo (1985), McCutcheon (1985), Patton-Mallory and McCutcheon (1987), Murakami et al. (1999) and Salenikovich (2000). All these studies focused on modelling timber walls with wood-based sheathing materials (plywood and OSB) as typically used in the United States. Liew, Gad and Duffield (2005) developed a modularised closed-form model for predicting the bracing performance of plasterboard walls as typical Australia practice. In Liew et al.'s model, the load-slip model of the fasteners is formulated first, and the total strain energy of the fasteners and the timber studs is set to be in equilibrium with the work done by external force. However, the model was developed based on Australian practice.

Contrary to closed-form mathematical models, FE models are more complicated but versatile. They model all the components within a wall as well as boundary conditions. Researchers including Foschi (1977), Itani and Cheung (1984), Gutkowski and Castillo (1988), Dolan (1989), White (1995), Kasal, Leichti and Itani (1994) and Folz and Filiatrault (2002a, 2002b) developed racking models of different timber walls using FE formulations. These models were essentially developed and verified for timber walls with wood-based sheathing sheets rather than for plasterboard walls.

Racking tests frequently reveal that plasterboard walls have different cyclic responses from wood-based timber walls. Typically during a racking test, the sheathing of a plasterboard wall behaves like a plate element and rotates as one unit relative to the timber perimeter frames. This is different from timber walls with plywood or other wood-based sheathing sheets where significant movements would occur between sheets during the racking test of a wall. Clearly, a mathematical model developed based on timber walls with wood-based sheathing is not suitable for timber walls with plasterboard sheathing. An appropriate mathematical model for plasterboard walls as typical New Zealand practice needs to be developed.

Since P21 testing procedure was specified, many P21 tests on plasterboard walls have been conducted in New Zealand. However, the measurements obtained during P21 tests are not enough to distinguish contributions of different mechanisms to the total deformations. As a consequence, a closed-form racking performance model is to be developed for plasterboard walls typical of New Zealand practice. It needs to be realised that LTF walls are expected to have significant degradation (strength/stiffness) as loading progresses and it is difficult to elaborate force-displacement behaviour of plasterboard walls.

### Deformation mechanisms of typical New Zealand plasterboard walls

With regard to the load-deflection mathematical model development for plasterboard walls, it is assumed that the lateral in-plane deflection at the top of a cantilever plasterboard wall consists of three components and is expressed as follows:

$$\Delta_{\text{total}} = \Delta_{\text{flexural}} + \Delta_{\text{shear}} + \Delta_{\text{slip}} \quad \text{Eq. 10}$$

Where:

$\Delta_{\text{flexural}} = 2VH^3/(3EAL^2)$  – the contribution to the horizontal deflection due to bending deformation of the wall. The primary contribution of an LTF wall to bending rigidity is attributed to the chords of the wall.

$\Delta_{\text{shear}} = VH/(GLt)$  – the contribution to the horizontal deflection due to shear deformation of a plasterboard wall where the shear resistance is primarily provided by sheathing

$\Delta_{\text{slip}}$  is the contribution to the horizontal deflection due to the slips occurring between fasteners and the sheathing.

In a typical P21 racking test on a plasterboard wall, the fastener slip is the primary source of the total lateral deflection at the wall top and the main source of non-linear performance of a plasterboard wall. The deformation mechanism due to slips between fasteners and the boards is similar to wall rocking as demonstrated in Figure 21.

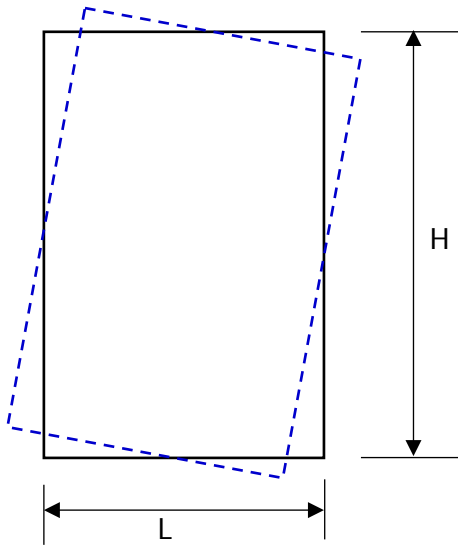


**Figure 21. Wall rocking mode.**

Mathematical expression of slip-induced deformation is again similar to that of the shear deformation mechanism because both shear-induced deformation and slip-induced deformation are proportional to the wall aspect ratio ( $H/B$ ). Based on this, development of the mathematical model of a plasterboard wall combines the shear deformation component and slip deformation component into a combined deformation,  $\Delta_{ss}$ , which becomes the non-linear deformation source, namely:

$$\Delta_{\text{total}} = \Delta_{\text{flexural}} + \Delta_{ss} \quad \text{Eq. 11}$$

$$\Delta_{\text{flexural}} = 2VH^3 / (3E A_c L^2) \quad \text{Eq. 12}$$



Where:

V is the racking load at top of the wall, H is the height of the wall assembly, E is the modulus of elasticity of the timber chord and is 8,000 MPa as per NZS 3603:1993 for SG8,  $A_c$  is the area of chord and L is length of the wall assembly.

$$\Delta_{ss} = VH / (G_e L t_e) \quad \text{Eq. 13}$$

Where:

$t_e$  is the effective thickness of plasterboard sheathing, and it is taken as the thickness of sheathing if the walls are singly lined and is taken as the sum of the thicknesses of the sheathing sheets if the walls have linings on both faces.

$G_e$  is the equivalent shear modulus of the panel wall, which combines the effects of shear deformation occurring within the plasterboard and slip deformation.  $G_e$  will degrade as loading progresses.

Based on results of many P21 tests on plasterboard walls, equivalent shear modulus is calibrated for different lateral deflection levels and is listed in Table 22 as equivalent shear modulus obtained if the contribution of uplift at wall base is not taken away.

**Table 22. Equivalent shear modulus ( $G_e$ ).**

| 8 mm cycle | 15 mm cycle | 22 mm cycle | 29 mm cycle | 36 mm cycle | 43 mm cycle |
|------------|-------------|-------------|-------------|-------------|-------------|
| 90 MPa     | 50 MPa      | 35 MPa      | 25 MPa      | 18 MPa      | 15 MPa      |

The skeleton curves derived using the mathematical model developed in this section have a reasonable match with the hysteresis loops obtained during P21 tests, as illustrated in Figure 22 for several typical P21 tests. The models developed match the test results reasonably well.

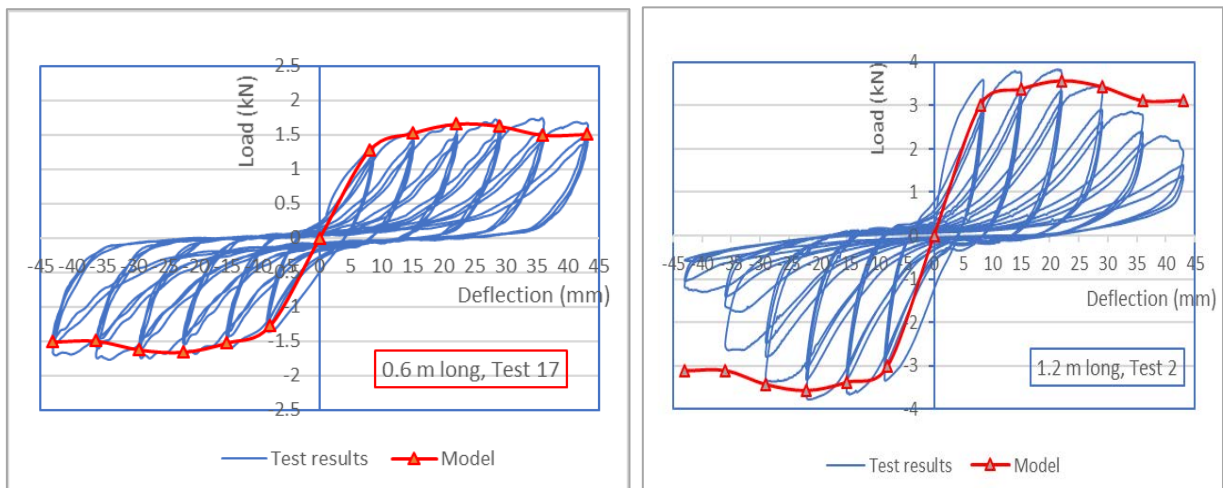


**Figure 22. Test results versus the model developed.**

Material property parameters E and G are the essential properties required in structural analysis models.

## A3 Summary

In this appendix, seismic bracing performance of plasterboard bracing walls in LTF residential buildings constructed to NZS 3604:2011 is studied. In this study, a set of racking test data on plasterboard timber walls conducted at BRANZ Structures Lab was collected and analysed. The study led to the following findings:

- The racking resistance of an LTF plasterboard wall sheathed on two opposite faces is greater than the equivalent counterpart sheathed on one face only and with the same sheath and fixing details. The enhancement of racking resistance due to the sheathing on the opposite face varies from 30–70%, and it is far less than the predictions from the direct superposition rule.
- LTF plasterboard walls are expected to have significant racking strength degradations as cyclic loading progresses at the same deflection levels. The analysis showed that the racking strength attained at the third cycle is significantly lower than the racking strength attained at the first cycle for the same deflection level. The drops in most cases range from 15–25%.
- Apart from racking strength degradation, LTF plasterboard walls are expected to have significant degradation in energy-dissipating capacity as cyclic loading progresses at the same deflection levels. The analysis showed that the energy-dissipating capacities are greater at lower deflection levels. Also the energy-dissipating capacity is greater at the first cycle in comparison with the third cycle of cyclic loading at the same deflection level.
- LTF plasterboard walls have limited energy-dissipating capacity, and the maximum damping level derived is slightly greater than 15%. This is equivalent to a ductility of 2 in a force-based approach domain.
- The main racking deformation source of a plasterboard wall was identified as slips of fasteners provided that the uplift at wall base was prevented.

Based on these findings, an appropriate model of racking behaviour of plasterboard walls typical of New Zealand practice was developed and calibrated against the collected test results. The characteristics of the developed mathematical model are:

- the developed mathematical racking model of a plasterboard wall considers the wall as a shear-flexure wall element
- the assigned shear modulus to the wall element is a degrading parameter that degrades as the lateral deflections increase to model the degradation nature inherent in plasterboard walls.

## Appendix B: Rigidity study of roof/ceiling diaphragms

This appendix summarises the study conducted on the in-plane behaviour of plasterboard ceiling diaphragms.

Section B1 outlines the review of research efforts on timber floor/ceiling diaphragms. In section B2, standards-specified requirements and construction practice of timber diaphragms are explained. Section B3 describes the test programme and results of tests on full-scale and small-scale ceiling diaphragms conducted at BRANZ. The mathematical model, which was developed for representing the in-plane rigidity of plasterboard ceiling diaphragms as typical of New Zealand practice, is presented in section B4.

### B1 In-plane behaviour of timber diaphragms

Numerous studies, mainly reported overseas, were conducted on quantifying the stiffness of timber floor and ceiling diaphragms. These studies investigated the effects of various factors on the in-plane behaviour of floor/roof diaphragms, such as the effect of sheathing sheets (used in sheet floors and/or ceilings), fixing details from sheathing sheets to the frames, aspect ratios of diaphragms and penetrations, construction details of diaphragm framings, connection details between diaphragms and vertical bracing elements and so on. Representatives of these studies are presented below.

Carradine, Dolan and Bott (2004) studied, by experimental testing, the effect of aspect ratio and fastener schedules on diaphragm stiffness. Several full-scale floor diaphragms with different nail schedules and different penetrations were constructed and tested. The study concluded that loading the diaphragm parallel to the joists provided the highest shear stiffness, but the highest global and bending stiffness values were achieved when the diaphragms were loaded perpendicular to the joists.

Kirkham, Gupta and Miller (2015) experimentally studied the effects of roof pitch and a gypsum ceiling on in-plane behaviour of roof diaphragms. Ten full-size plywood roof diaphragms were constructed using metal plate connected (MPC) common and hip wood trusses or joists. The specimens included three gable roof slopes, expressed as rise to horizontal of 4:12, 8:12 and 12:12, a hip roof with a slope of 4:12 and a flat roof with a horizontal bottom chord. These roofs were constructed and tested in duplicate to make the total of 10 roofs. Roofs were tested following the ASTM E455 standard procedures and analysis. Test results showed that

- roof pitch affected gable roof apparent stiffness significantly but had insignificant effect on gable roof strength
- hip roofs had almost the same apparent stiffness and strength as flat roofs
- apparent stiffness of gable roofs was about 50% of that of flat roofs
- gypsum provided more than one-third of the total roof apparent stiffness at slopes of less than 4:12.

Roof pitch was found to have no effect on roof strength in any configuration. All roofs exhibited approximately the same shear strength. Failure modes of roofs included nail withdrawal, nail tear-through, metal plate tear-out on trusses and chord tensile failure.

Kirkham, Miller and Gupta (2016) studied the diaphragm modelling techniques. Rigid and tributary area analysis methods were examined for different geometries of LTF buildings constructed according to US practice. These methods were applied to historical earthquake damage reports and compared using rigid, semi-rigid or flexible horizontal diaphragm analyses useful in design practice. The study suggested that semi-rigid modelling or an envelope method is prudent.

The closest study to New Zealand timber diaphragms was the research conducted in Australia by Saifullah et al. (2014) where the sheathing of the diaphragms studied contained plasterboard sheathing. Saifullah et al. experimentally studied the strength and stiffness of a typical ceiling system used in cold formed steel-framed domestic structures. In this study, two tests on ceiling diaphragms as typical of Australia practice were conducted using two different test set-ups – cantilever set-up and beam set-up.

The highlights of the findings revealed by the tests included that:

- the beam test set-up gave greater ultimate strength and stiffness of the diaphragm, in comparison with those obtained from the cantilever set-up
- unlike timber-based sheathing case, the plasterboard moved or rotated as a rigid body without relative movement between individual sheets.

However, the construction details tested were not common New Zealand residential construction practice.

For New Zealand residential buildings, the construction techniques of diaphragms are different from overseas practices. Highlights of these differences include lining sheet materials and/or fixing details from linings to the framings or at junctions of ceiling to walls. Consequently, it is expected that the in-plane behaviour of roof/floor diaphragms as typical of New Zealand construction is different from that of their overseas counterparts. As such, it is necessary that the in-plane behaviour of ceilings and floor diaphragms as commonly used in New Zealand is studied.

To this end, the requirements of NZS 3604:2011 and conventional timber diaphragm construction practices are reviewed (see section B2 and section B3). Subsequently, a series of diaphragm tests (replicas of New Zealand practices) were designed and conducted in this project to study the in-plane behaviour of New Zealand diaphragms (section B4).

## B2 Standards and typical practice in New Zealand

The governing principle in NZS 3604:2011 for dealing with lateral loads on buildings is to provide a number of load-resisting elements of moderate capacity, evenly distributed in each direction throughout the floor plan at each storey. This is achieved by requiring the designer to match the demand in each direction by distributing vertical bracing elements along notional bracing lines at regular spacing.

In theory, the buildings constructed in such a way will be simple and regular, and the horizontal elements (floors and ceilings) are only required to carry the action associated with its tributary area to the bracing lines.

As outlined by Shelton (2004), there are two types of diaphragms classified in NZS 3604:2011 – normal diaphragms and structural diaphragms. Dimensional limits for the various types of diaphragms are summarised in Table 23.

**Table 23. Dimensional limits of ceiling diaphragms in NZS 3604:2011.**

|                 |   | Maximum spacing of bracing lines |
|-----------------|---|----------------------------------|
| <b>Floors</b>   | Normal floors*  | 6 m                              |
|                 | Diaphragm floors                                      | 15 m                             |
| <b>Ceilings</b> | Any ceiling, single top plate unless:                 | 5 m                              |
|                 | • Low-density ceiling, double top plate <sup>#</sup>  | 6 m                              |
|                 | • Ordinary ceiling, single top plate                  |                                  |
|                 | • Ordinary ceiling, dragon ties at external walls     | 7.5 m                            |
|                 | • Gypsum diaphragm ceiling <25°                       |                                  |
|                 | • Plywood or other wood-based diaphragm ceiling <45°* |                                  |
|                 | • Plywood or other wood-based diaphragm ceiling <25°* | 15 m                             |

\* Floors and ceilings designated as diaphragms are limited to an aspect ratio (long dimension/short dimension) of 2.0 (or 2.5 for a floor diaphragm in a single-storey building). There are no such limits for normal floors or ceilings, although the spacing restrictions on bracing lines (and practical room sizes) effectively limits the aspect ratio to between 1 and 2.

<sup>#</sup> Low density ceilings are defined as those having a mass of less than 600 kg/m<sup>3</sup>. Thus plasterboard ceilings are ordinary ceilings.

Although any horizontal element (floor or ceiling) will be called upon to act as a diaphragm under lateral load action on the building, as described in the section above, use of the defined term 'diaphragm' in NZS 3604:2011 is restricted only to the situation where the bracing lines in the storey below are spaced at more than 6 m. This may be required, for instance, to accommodate a large room or to reduce the number of foundation bracing elements in conjunction with a continuous perimeter foundation.

The differences in details between diaphragm floors and ceilings and non-diaphragm floors and ceilings are summarised in Table 24.

**Table 24. Provisions in NZS 3604:2011 for floor and ceiling diaphragms.**

|                 |                              |   |
|-----------------|------------------------------|---|
| <b>Floors</b>   | Sheet size                   | <ul style="list-style-type: none"> <li>Minimum dimension 1200 mm for diaphragm</li> <li>900 mm for proprietary non-diaphragm</li> </ul>   |
|                 | Sheet fixing                 | Same for both   |
|                 | Framing details              | 25 mm thick continuous boundary joist for both, or <ul style="list-style-type: none"> <li>continuous 40 mm blocking for diaphragm</li> <li>40 mm blocking at 1.8 m for non-diaphragm (continuous over 1.8 m if over a foundation wall)</li> </ul>                           |
|                 | Joist fixing to plate        | <ul style="list-style-type: none"> <li>12 skew nails per 1.5 m for diaphragm (joists parallel to plate)</li> <li>2 skew nails for non-diaphragm</li> </ul>  |
|                 | End of joist fixing to plate | <ul style="list-style-type: none"> <li>Blocking between all joist ends, connected with equivalent of 15 skew nails per 1.5 m for diaphragm</li> <li>Blocking at 1.8 m between joist ends, connected with equivalent of 10 skew nails per 1.8 m for non-diaphragm</li> </ul> |
| <b>Ceilings</b> | Sheet size                   | Same for both   |
|                 | Sheet fixing                 | <ul style="list-style-type: none"> <li>Nails at 150 mm around sheet edges, 300 mm intermediate supports for diaphragm</li> <li>Nail, screws or glue at 200 mm sheet edges, 200 mm intermediate supports for non-diaphragm</li> </ul>  |
|                 | Framing details              | No specific details for either  |

## B3 Diaphragm construction practice in New Zealand

In this project, only ceiling diaphragms were studied, and the discussion here is thus limited to ceiling diaphragm practice.

There are two basic types of domestic ceiling construction used in New Zealand:

### Traditional dwanged ceiling

This is typically used with on-site built stick-framed construction and is perhaps more common today in alterations or additions to existing buildings. Ceiling joists are used to span between walls and are spaced to suit the spanning capability of the ceiling lining (for example 450 mm for 10 mm plasterboard). Dwangs (or nogs) are installed, cut between the joists, to provide fixing for the longitudinal sheet joints. The lining is direct fixed (nailed, screwed or glued) to the joists and dwangs. This type of construction was the norm when NZS 3604 was originally published in 1978.

### Battened ceiling

This is more common in new construction where it is used with prefabricated timber trusses. Battens may be timber or metal and are used in conjunction with a double top plate to provide adequate fixing of the ceiling lining at the wall junction. Battens are attached to the truss bottom chords at spacings to suit the ceiling lining and are themselves sized to suit the truss spacings. Lining sheets are fixed to the battens and upper of the top plates at the junctions with the walls.

A traditional dwanged ceiling and battened ceiling are illustrated in Figure 23.

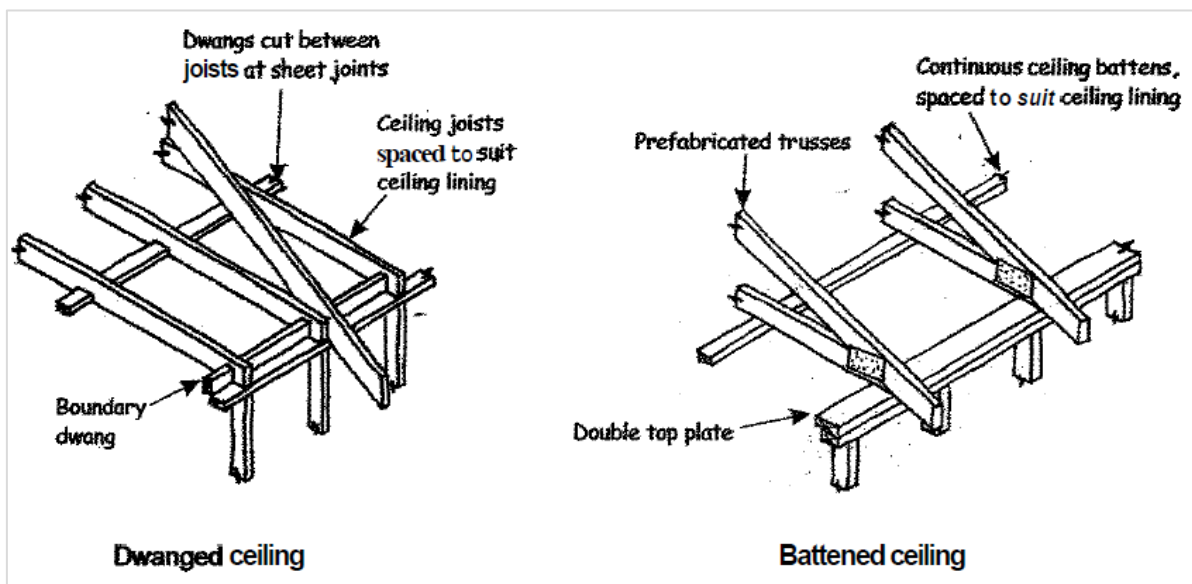


Figure 23. Construction of dwanged and battened ceilings (Shelton, 2004).

Figure 24 shows two types of common ceiling diaphragm construction practice in New Zealand, when GIB plasterboard linings are used (Winstone Wallboards, 2014).



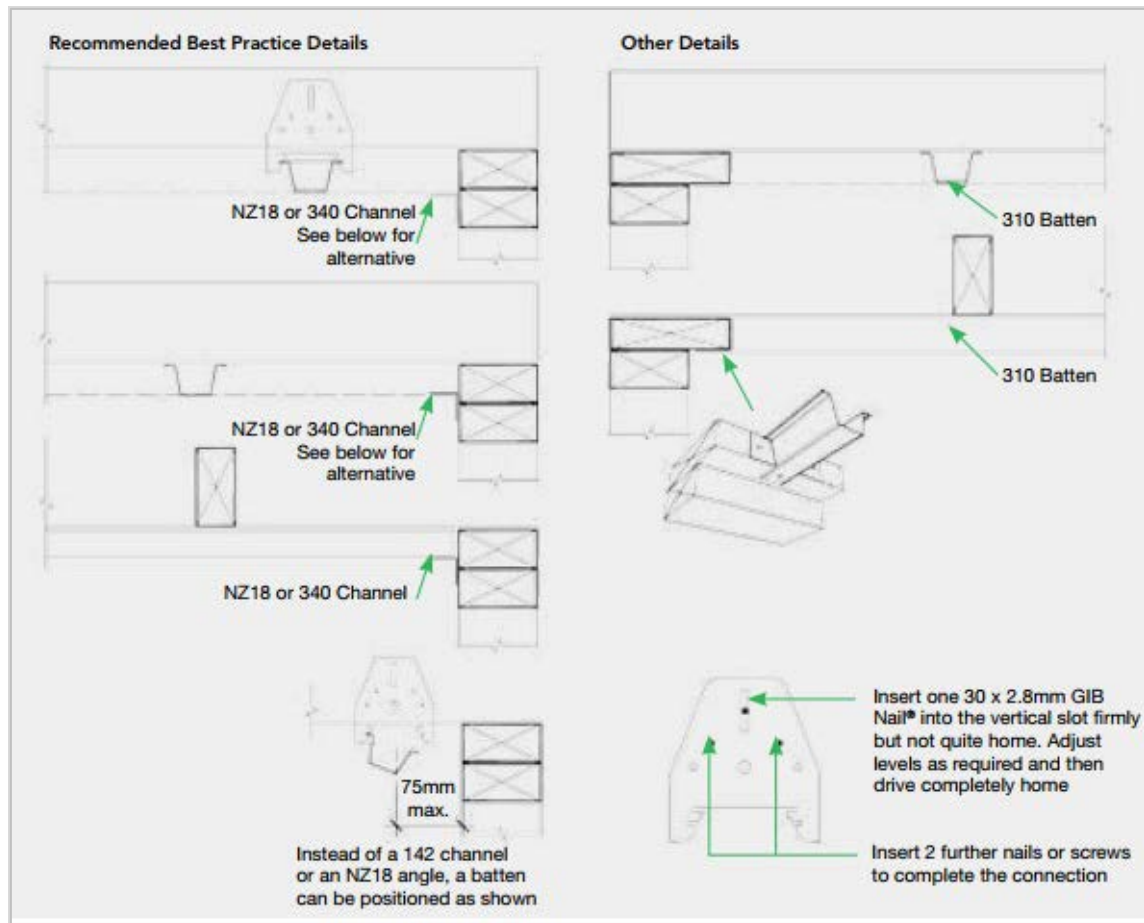


Figure 24. Common diaphragm construction practice (Winstone Wallboards, 2014).

## B4 Experimental study of ceiling diaphragm

A test programme on plasterboard ceiling diaphragms was undertaken as part of the project reported here. The objectives of the test programme were to:

- quantitatively study the in-plane rigidity of plasterboard ceiling diaphragms with different construction details (batten orientations, details at junctions, fixing details from linings to the framings and so on)
- develop a modelling technique to simulate the in-plane performance of ceiling diaphragms.

The test programme included two stages, as described below.

The first stage of the test programme included only one full-scale ceiling diaphragm test, which simulated one typical plasterboard ceiling construction technique.

The second stage of the test programme included several small-scale ceiling diaphragm tests. The small ceiling diaphragm specimens had different construction details from each other, and one of these specimens had identical edge construction details as the full-scale ceiling test. The intention of the small-scale ceiling diaphragm tests was to quantify the relative in-plane rigidity of other ceiling diaphragm details to that of the full-scale test.

## B4.1 Full-scale ceiling diaphragm test

### Construction of the test specimen

The overall specimen dimensions for the full-scale ceiling diaphragm test were 7.2 x 3.6 m, and it simulated one common batten ceiling diaphragm practice. The specimen was constructed upside down for easier viewing of the behaviour. It was considered that the performance would be no different from if it was constructed the correct way up.

It is noted that the full-scale test set-up was similar to a few commercial ceiling tests conducted on a commercial basis in the past at BRANZ Structures Lab.

A plan of the full-scale ceiling diaphragm specimen is presented in Figure 25.

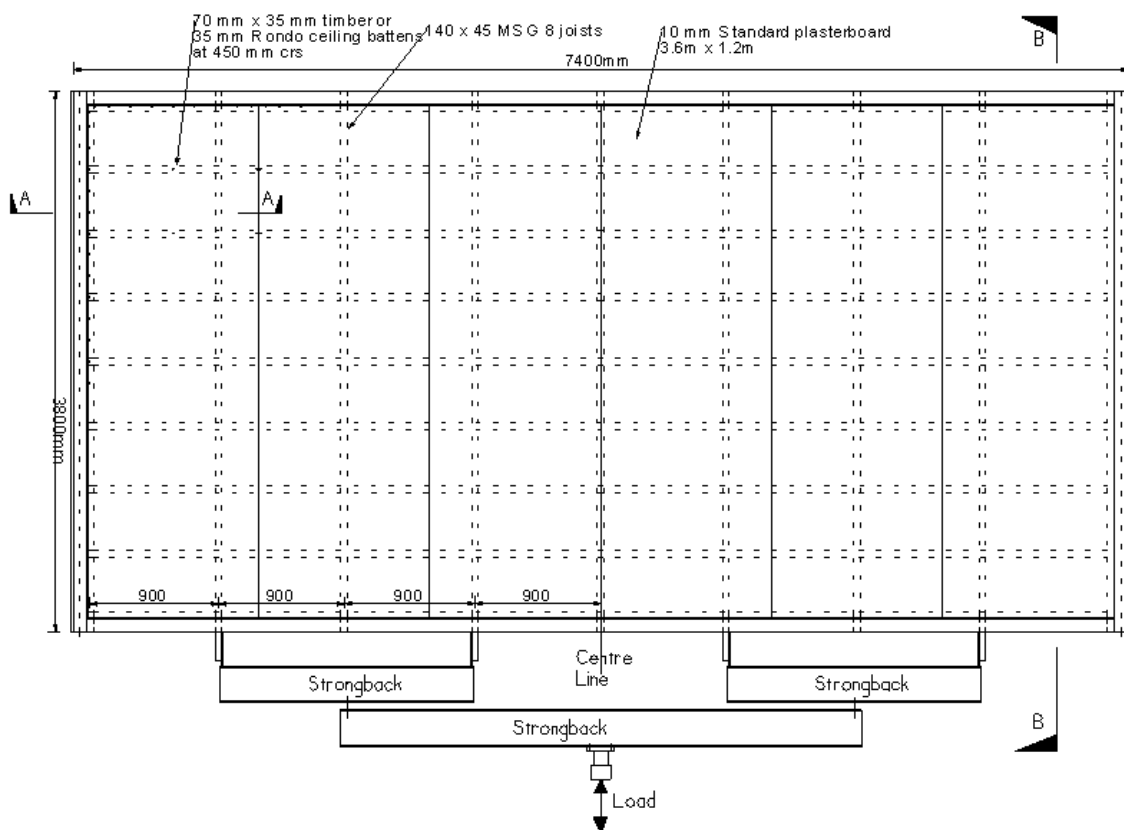


**Figure 25. Plan of the full-scale ceiling test specimen and test set-up.**

Cross-sections through the critical elements are presented in Figure 26.

The timber framing was kiln dried radiata pine, MSG8. The joists, which represented either joists or trusses in a real structure, were spaced at 900 mm centres. Around the perimeter of the diaphragm, a 140 x 35 mm top plate, simulating the top member of a double top plate as illustrated in Figure 24, was nailed to the joists with two 90 x 3.15 mm power driven nails at each joist crossing to simulate the skew-nailed connection between the rafters and the plate in normal practice.

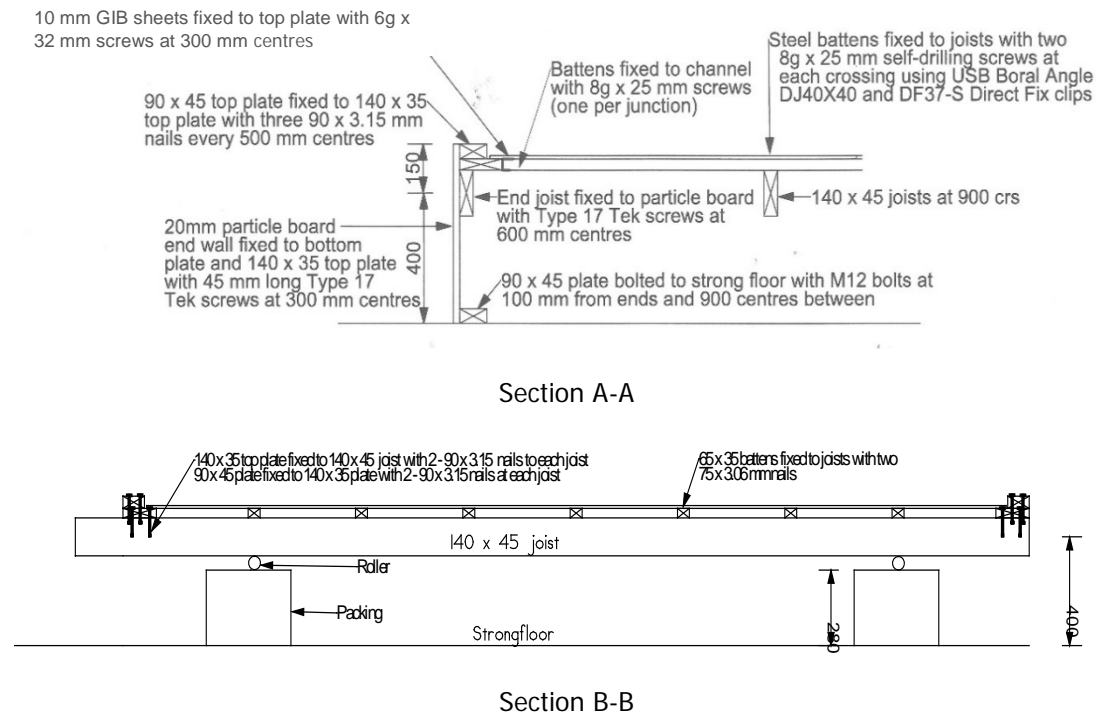


**Figure 26. Edge details of the test specimen and the support details**

At the ends of the specimen, this member was screwed directly to the particleboard transfer sheet with Type 17 Tek screws at 300 mm centres. At each corner of the diaphragm and at a butt joint on each of the two long sides, the 140 x 35 mm plates were joined with a Mitek 6T10 Tylok connector (Figure 27).



**Figure 27. Mitek 6T10 Tylok connector at corners of diaphragm.**

A 90 x 45 mm MSG8 plate was fixed on top of the 140 x 35 mm plate. This simulated the lower member of a twin top plate in normal construction. The 90 x 45 mm member was fixed to the 140 x 35 mm plate with two 90 x 3.15 mm power-driven nails at each joist crossing (i.e. 900 mm centres). At the ends of the specimen, this member was fixed with three 90 x 3.15 mm power driven nails at 500 mm centres. In normal construction, nailing between the two plates would be in the opposite direction, but the diaphragm performance was not expected to be different because of this. At the

corners and at one point along the long sides of the specimen, Mitek 6T10 Tylok connectors were used to join the 90 x 45 mm members.

The battens were top hat ceiling battens spaced at 450 mm centres. The battens were attached to the joists using ceiling clips, one at each joist crossing. The ceiling battens were also fixed through the brim of the top hat section at each joist crossing to metal angles fixed to the ceiling joists. The metal angles transferred shear loading between plasterboard and joists. The ceiling battens were located at each end in folded metal channels screwed to the edge of the timber double top plates.

Figure 28 shows the framing prior to lining.



**Figure 28. Framing of the full-scale ceiling test specimen.**

Winstone Wallboards GIB Standard 10 mm plasterboard in 3.6 x 1.2 m sheets was fixed to the joists and perimeter framing and paper tape reinforced and stopped at sheet joints. Sheet fixings were 6 g screws, spaced at 150 mm around the perimeter (50 mm and 100 mm from each corner) and 300 mm along the battens.

Figure 29 shows the completed test specimen prior to testing.



**Figure 29. Full-scale test specimen prior to testing.**



### Test instrumentation and set-up

Linear potentiometers were used to record the slips and displacements at various locations on the diaphragm. The arrangement of linear potentiometers for measuring slips (movements of the plasterboard relative to framing) is shown in Figure 30, and the arrangement of linear potentiometers for measuring the absolute displacements of frames relative to the floor is shown in Figure 31. Applied loads and ram displacements were also recorded.

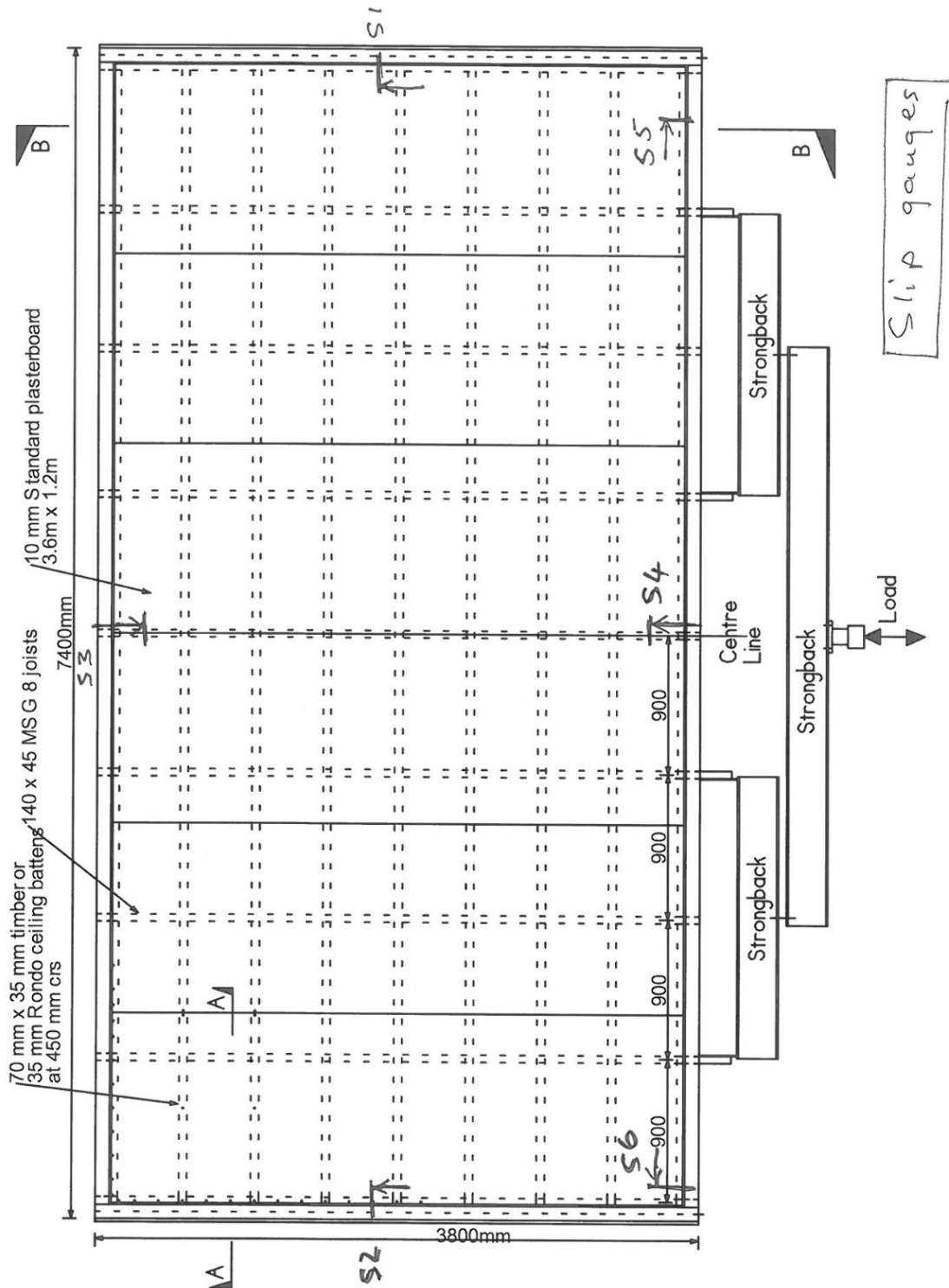
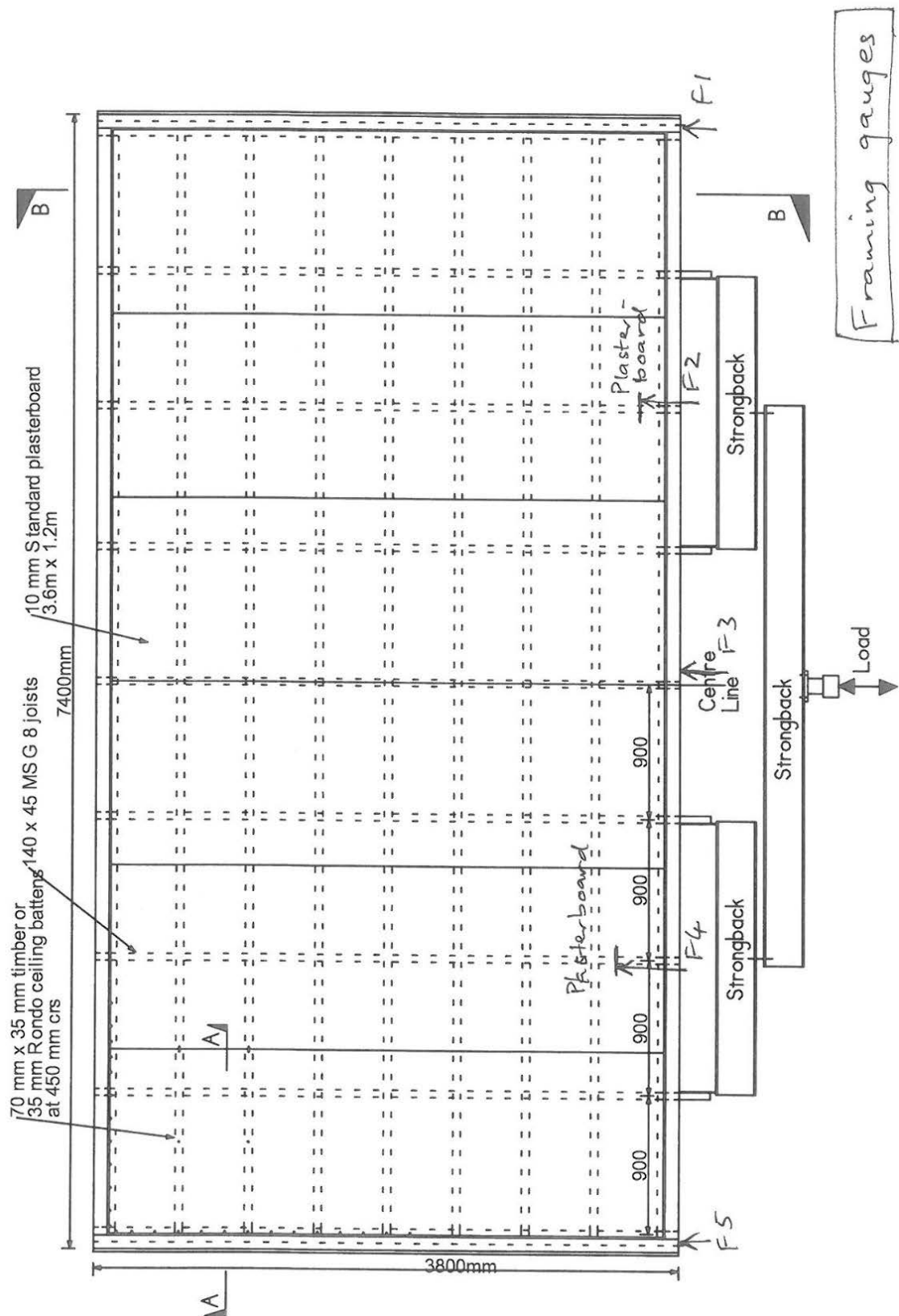


Figure 30. Arrangement of slip gauges.



**Figure 31. Arrangement of frame displacement gauges.**

### Loading procedure

The full-scale ceiling diaphragm was tested using a forced controlled quasi-static cyclic loading sequence.



The loading was applied to the specimen in-plane at four points along the long side of the diaphragm via the ceiling joists. Two cycles of loading were applied at each of the following loads:  $\pm 8$  kN,  $\pm 15$  kN,  $\pm 20$  kN,  $\pm 25$  kN,  $\pm 30$  kN,  $\pm 35$  kN,  $\pm 40$  kN,  $\pm 45$  kN or until failure occurred.

The applied load regime is shown in Figure 32.

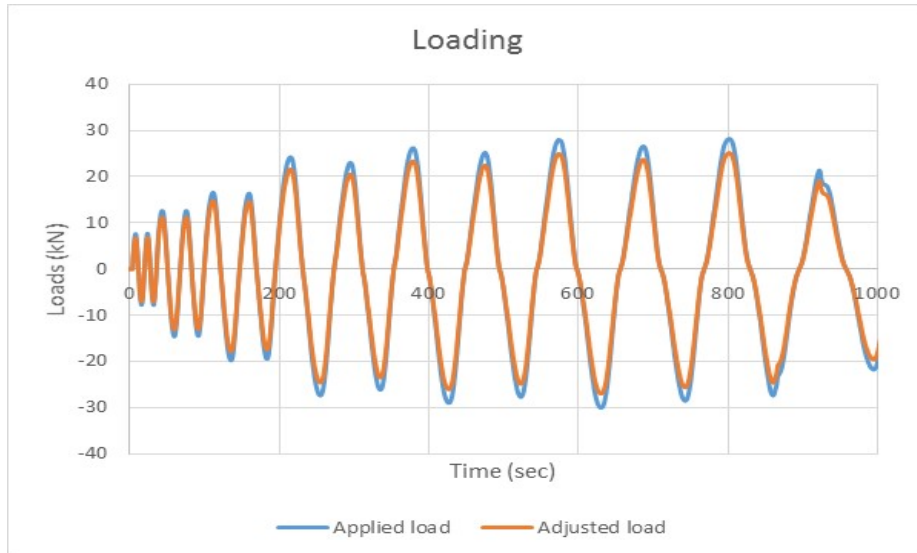


**Figure 32. Plot of applied and adjusted loads.**

### Test observations

During the entire test, there was no relative movement between the individual plasterboard sheets, and the entire plasterboard lining moved as if it was a monolithic plate. No damage was observed in the plasterboard lining except around the fixings where screw slips caused significant slotting and/or complete disengagement of fixings from linings, as illustrated in Figure 33.



**Figure 33. Damage associated with screw failures.**

The slips progressed as the loading progressed, especially around the corners and along the short sides, leading to significant degradation of stiffness/strength due to the gradual reduction of the composite action between linings and frames. Figure 34 shows the detailed damage observed at one corner of the ceiling diaphragm.

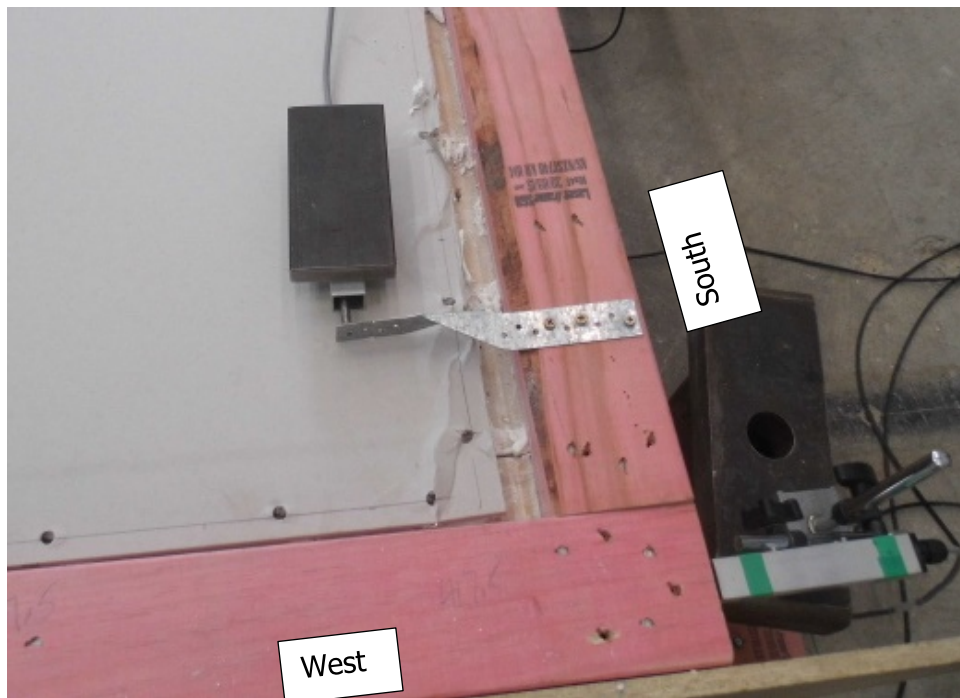
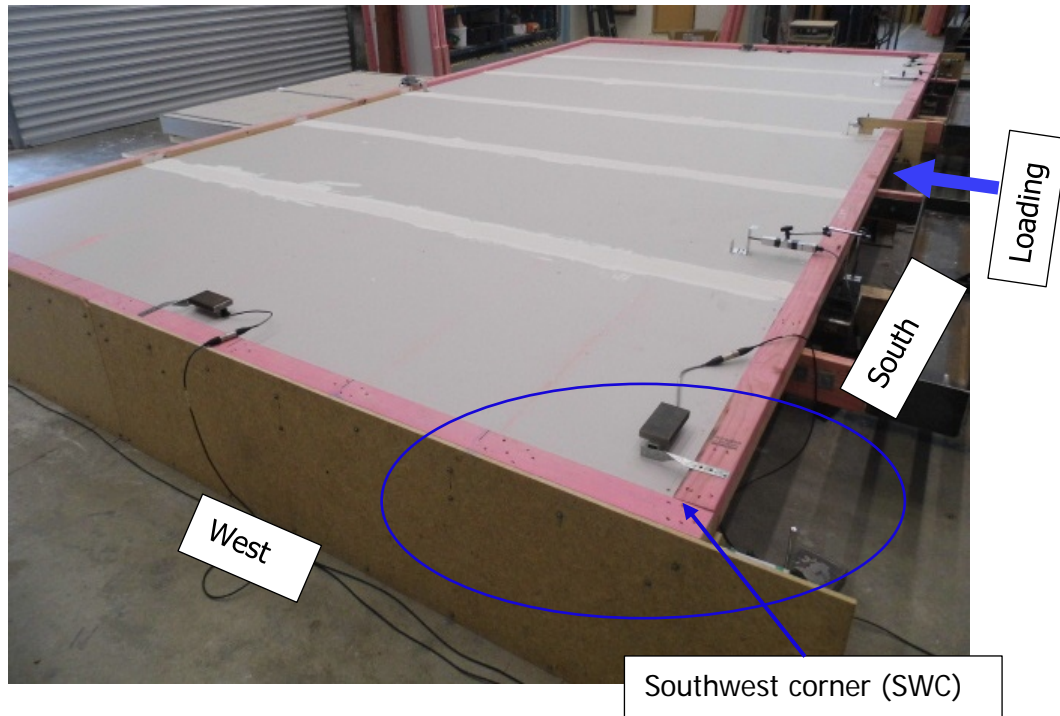
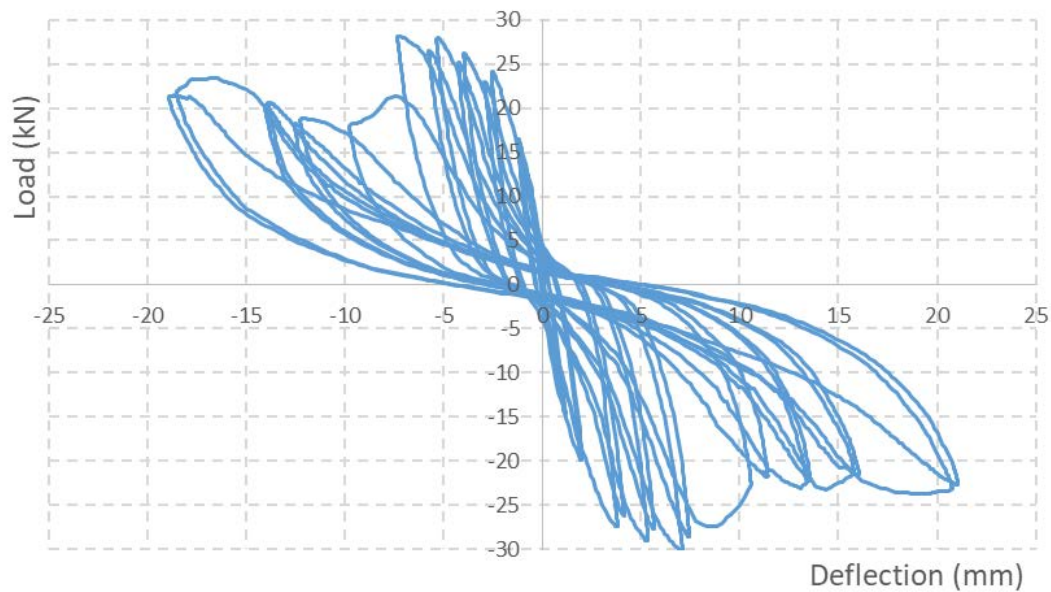


**Figure 34. Disengagement of linings at southwest corner due to screw fixing failure.**

### Deformation mechanisms

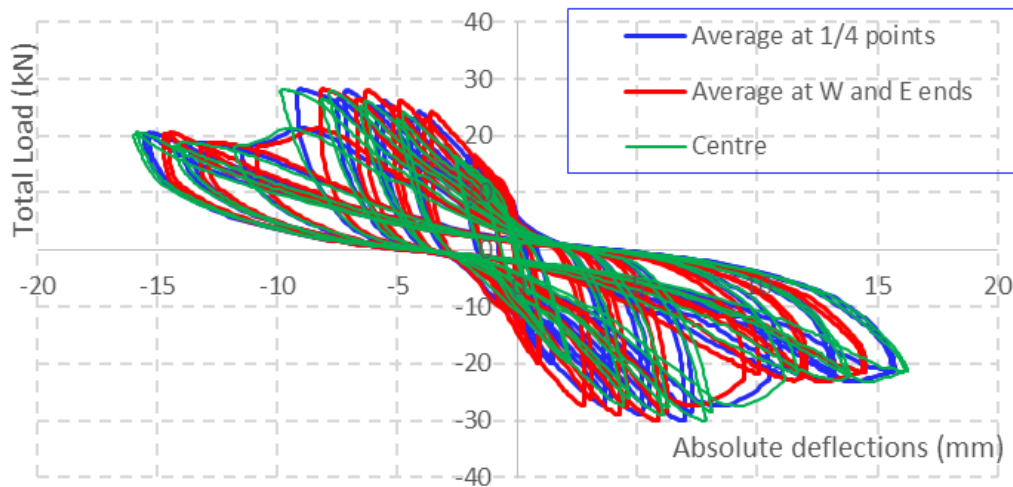
Figure 35 shows the load versus deflection (mid-span deflection) hysteresis loops, where the deflection refers to the relative deflection at the mid-span of the test specimen to the supports (namely, the deflection associated with the supports has been taken away).

As shown in Figure 35, the ceiling diaphragms had undergone significant stiffness degradation with the progress of loading.



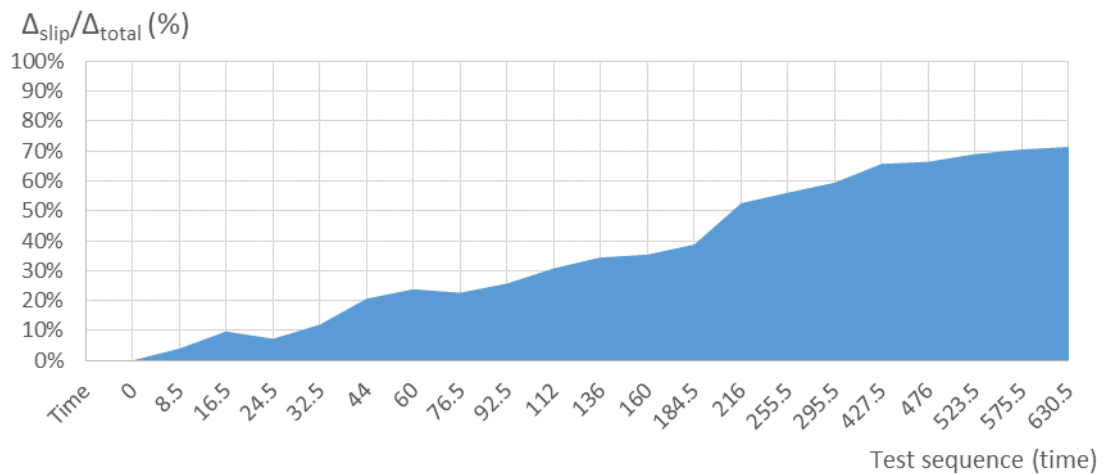
**Figure 35. Hysteresis loops obtained from the full-scale ceiling diaphragm test.**

Figure 36 shows the measured absolute deflections of the plasterboard lining at different locations. Clearly, the plasterboard movements at different locations (F2 and F4 in test specimen diagram are  $\frac{1}{4}$  span locations as illustrated in Figure 31) had negligible differences, and the sheathing as a whole moved similarly to a rigid plate.



**Figure 36. Absolute deflections at different locations of plasterboard sheet (mm)**

Figure 37 shows the contribution of screw slip to the total deformations measured during the testing. As shown in Figure 37, the slip's contribution increased as the loading progressed and it reached about 75% of total deformation. Clearly the screw slips were the dominant contribution to the flexibility of the plasterboard ceiling diaphragms.



**Figure 37. Contribution of screw slips to the total diaphragm deflection.**

### Validation of NZS 3603:1993 method for diaphragm stiffness

Timber diaphragms are normally analysed using girder analogy where the sheathing is the web of the girder and the top plate of the wall or a continuous joist is the flange. Most diaphragms are deep beams, and diaphragm analyses often consider diaphragms as simply supported beams.

For instance, NZS 3603:1993 gives a method for estimating different deflection components for timber diaphragms sheathed by timber-based panels such as plywood sheets. According to NZS 3603:1993, the total deflection of a timber diaphragm sheathed by plywood sheets could be estimated as follows:

$$\Delta_{\text{total}} = \Delta_{\text{flexural}} + \Delta_{\text{shear}} + \Delta_{\text{slip}} \quad \text{Eq. 14}$$

Where:

$\Delta_{\text{flexural}} = 5PL^3/(192EAB^2)$  – the deflection contribution due to in-plane bending deformation of the diaphragm. The primary contribution of a timber diaphragm to bending rigidity is attributed to the chords of the diaphragm.  $P$  is the applied load,  $L$  is the span of the diaphragm,  $A$  is the sectional area of one chord,  $B$  is the distance between diaphragm chord members and  $E$  is the elastic modulus of the chords.

$\Delta_{\text{shear}} = PL/(8GBt)$  – the deflection contribution due to shear deformation where the shear resistance is primarily provided by the web of the diaphragm,  $t$  is the thickness of the web (the sheathing in this case) and  $G$  is the shear modulus of the web.

$\Delta_{\text{slip}}$  is the contribution of the screw slips to the total deflection of the diaphragm.

For the validation of NZS 3603:1993 method, it was assumed that  $E = 8,000$  MPa as for SG8 timber,  $G = 700$  MPa is the shear modulus of plasterboard linings as reported by others (Thurston, 1993). The test results obtained from the full-scale plasterboard ceiling diaphragm were used to validate the possible application of NZS 3603:1993 to plasterboard ceiling diaphragms.

For slip components,  $\Delta_{\text{slip}}$ , the screw slip model derived from screw slip tests was used and the model is shown in Figure 38.

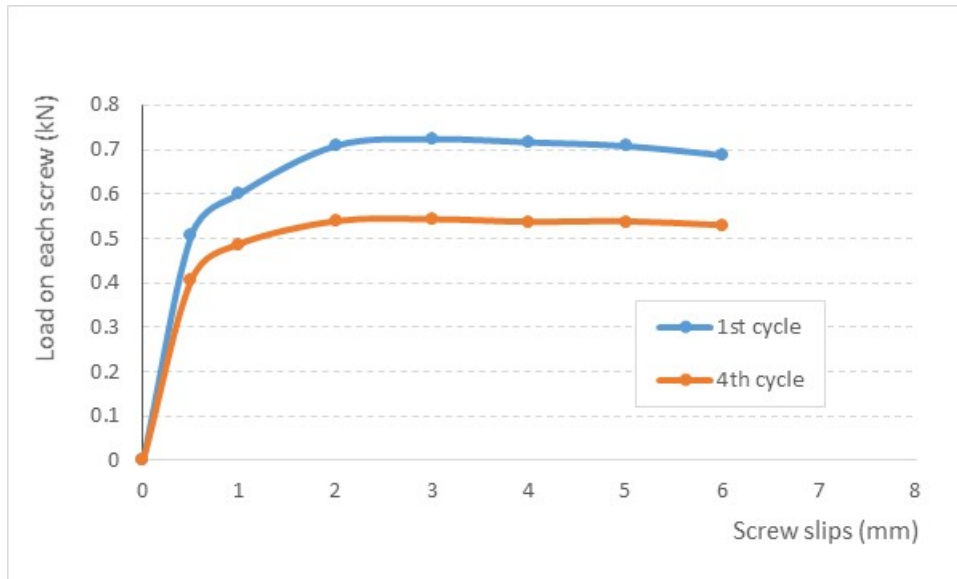


**Figure 38. Screw slip model.**

The estimated total mid-span deflections of the tested full-scale diaphragm at the peak loads were obtained, using the slip model in Figure 16 and Eq. 14. The estimated mid-span deflections were compared with the measured total deflection at mid-span, as illustrated in Figure 39, where  $\Delta_p$  and  $\Delta_m$  are respectively the predicted and measured deflections at mid-span. As shown in Figure 39, the predicted deflections match the measured deflections well.

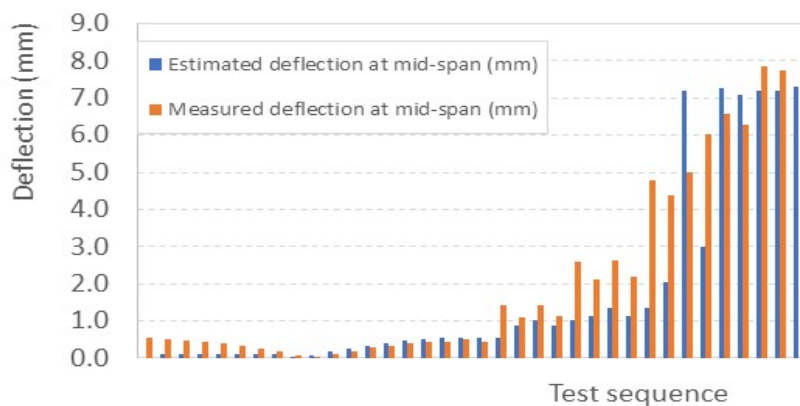


**Figure 16 Validation of predicted deflection versus measured deflection**

**Figure 39. Validation of predicted deflection versus measured deflection.**

### Summary

The experimental study on the full-scale plasterboard ceiling diaphragm has come to the following conclusions:

- The dominant contribution to the in-plane flexibility of plasterboard ceiling diaphragms is due to the slips of screws from plasterboard linings to the framing.



- The beam analogy method in NZS 3603:1993, although developed mainly based on timber-based panel sheathing, could be used for modelling the plasterboard ceiling diaphragm, provided that the screw slip model is adequate.

## B4.2 Small-scale ceiling diaphragm tests

### Test specimens

Test specimens constructed for the stage two test programme were representatives of various types of ceiling construction details. All the test specimens were 1.2 x 1.2 m in plan. A complete list of small-scale test specimens is set out in Table 25.

**Table 25. Small-scale ceiling diaphragm tests.**

| Test ID | Additional top plate<br>(on top of wall top plate) | Battens |                       | Plasterboard          |                  | Edge reinf?<br>(tape & stopped) | Structural ceiling diaphragm? |
|---------|--|---------|-----------------------|-----------------------|------------------|---------------------------------|-------------------------------|
|         |  | Type    | Orientation (to load) | Orientation (to load) | Fixings to edge  |                                 |                               |
| A       | 140x35 + Boral channel                             | Steel   | Perpendicular         | Parallel              | 6g screws at 150 | N                               | y                             |
| B       | 140x35   | Steel   | Parallel              | Perpendicular         | 6g screws at 150 | N                               | Y                             |
| C       | 140x35   | Steel   | Perpendicular         | Parallel              | 6g screws at 150 | Yes (to wall GIB)               | Y                             |
| D       | 90x45 + NZ 18 angle                                | steel   | Parallel              | Perpendicular         | 6g screws at 600 | n                               | N                             |

In Table 25, test A was designed to replicate the construction details of the full-scale ceiling diaphragm. Test A would be the benchmark test to study effects of various construction details on the stiffness of ceiling diaphragms. Tests B and C were identical to test A except test B had different batten orientation from test A and test C had tape-reinforced jointing details from wall to ceiling. Test D was identical to test B but the additional top plate was SG8 90 x 45 mm rather than SG8 140 x 35 mm as for test B.

### Test instrumentation, test set-up and test observations

Linear potentiometers were arranged in a similar way to that made for the full-scale ceiling diaphragm test. The highlight of the instrumentations is to obtain the information on the hysteresis behaviour of the screw slips along the two sides parallel to the loading direction. The applied load and ram displacements were also recorded. Figure 40 shows the schematic test set-up.





**Figure 40. Test set up for the small-scale ceiling tests.**

Load was applied in sets of reversed cycles of increasing amplitude, similar to that adopted for the full-scale ceiling diaphragm test.

During the tests on small-scale ceiling diaphragms, observed ceiling diaphragm performance confirmed that the plasterboard sheathing behaved in a similar way to a monolithic plate, and most of deformation occurred due to slip of screws along the two sides parallel to the loading direction.

#### Relative rigidities of ceiling diaphragms

When ceiling diaphragms are subjected to in-plane loading, the dominant deformation sources are from screw slips and thus slip-related rigidity could be used as an approximate indicator of ceiling rigidity.

Figure 41 compares the hysteresis loops of measured slips versus the applied loads for all the small-scale ceiling diaphragm tests.

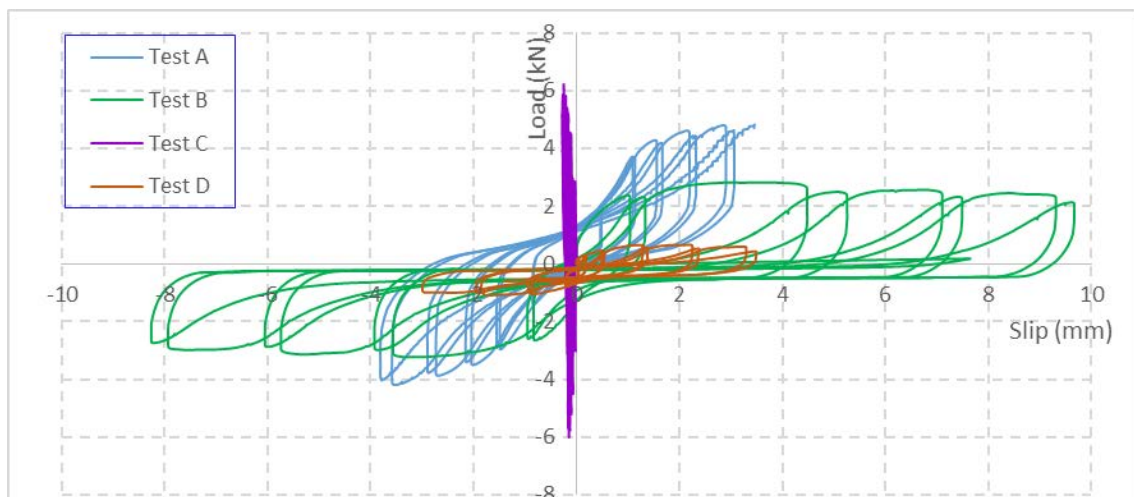


#### Figure 41. Hysteresis behaviour of screw slips of four small-scale ceiling diaphragm tests.

As shown in Figure 41, the greatest in-plane rigidity of the plasterboard ceiling diaphragms occurred when the joints between walls and the diaphragms are tape reinforced (test C). In comparison, the least in-plane rigidity of the plasterboard ceiling diaphragm occurred when the screw fixing spacing was doubled and the joints between walls and the diaphragms were not tape reinforced (test D). The in-plane rigidity of the plasterboard ceiling diaphragms with the same details as the full-scale test was in the middle range.

Slip-related ceiling diaphragm rigidities at peaks of loading are calculated for all small-scale ceiling diaphragm tests and summarised in Table 26. Calculation of the slip-related rigidity of each ceiling diaphragm is explained as follows:

$$K_s = 0.5 P / (\Delta_s B) \quad \text{Eq. 15}$$

Where:

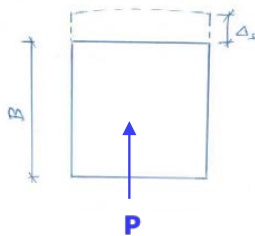
$K_s$  = rigidity parameters.

$P$  = the average maximum load (average loads of positive loading cycle and negative loading cycle) applied to the specimen.

$\Delta_s$  = the measured maximum slip (average slip values along the two sides of the ceiling parallel to the loading direction where the slips are the relative movement between ceiling and the wall top)..

$B$  = ceiling width, which is the diaphragm dimension parallel to the loading direction.

**Table 26. Slip-related ceiling diaphragm rigidity.**

| Test ID | $K_s$ (kN/mm/m) |  |
|---------|-----------------|---|
| A       | 1.02            |   |
| B       | 0.85            |   |
| C       | 17.0            |   |
| D       | 0.22            |   |

From Table 26, it is evident that the reinforced tape jointing details enhanced the ceiling diaphragm's rigidity much more significantly than the batten orientation. The spacing of screw fixing from plasterboard to framing was found to be a dominant factor of ceiling diaphragm rigidity, as revealed by comparing test A with test D.

It is noted that the spacing of screw fixings from plasterboard to framing was respectively 600 mm and 150 mm for test A and test D. It is very interesting that the increase of the screw fixing spacing is inversely proportional to the ceiling diaphragm rigidity, implying that screw slip is the major contributor to the flexibility of plasterboard ceiling diaphragm.

### B4.3 Modelling of in-plane rigidity of diaphragms

Several researchers have attempted to develop methods to model the in-plane stiffness of ceiling/floor diaphragms. The models developed are mainly in two categories – finite element models and mathematical models involving engineering formulae.

As for structural analyses of other structural systems, finite element models used for timber diaphragms model the engineering behaviour of each building component within a diaphragm (fasteners, frame members, sheathing and so on). An example of finite element models developed so far is the work by Saifullah et al. (2016) studying the stiffness of plasterboard ceiling diaphragms in light steel-framed residential structures. In this study, the finite element model of a plasterboard ceiling diaphragm was developed using ANSYS software. Non-linear deformation sources were believed to be the slips of screws from plasterboards to framing, and the load-slip models of the screws used in finite element models were obtained based on shear connection tests conducted at component level.

In comparison, mathematical models are often developed based on an analogical theory. For timber diaphragms, a common mathematical model is the deep beam analogy. A representative of mathematical models based on deep beam analogy is the method in NZS 3603:1993, which was originally developed by Dowrick and Smith (1986) for timber diaphragms with wood-based sheathing. There are also a few mathematical models developed based on shear field analogy. Examples include the truss method developed by Kamiya (1990) and the equivalent truss method developed by Moroder (2016). However, all these models were developed mainly for timber diaphragms sheathed by wood-based panels, such as plywood sheets.

There are no significant research efforts made in modelling the in-plane stiffness of plasterboard ceiling diaphragms as typical New Zealand residential construction. The intention of this section is to develop a mathematical model for the in-plane performance (stiffness/strength characteristics) of plasterboard ceiling diaphragms.

### Model development

The major contribution to plasterboard ceiling diaphragm flexibility is the contribution of screw slips, and this contribution could account for 75% of the total ceiling diaphragm deformation.

Currently, there is only one set of full-scale plasterboard ceiling diaphragm test data for each sheathing material, even when the tests conducted on a commercial basis were allowed for. It is thus impossible to develop an elaborated screw slip model. Instead, a high-level mathematical model is to be developed, similar to the model developed for LTF plasterboard walls. The method in NZS 3603:1993 is used for calculating the deflections of plasterboard ceiling diaphragms, and the shear deformation component and slip deformation component are summed as a combined deformation.

The total in-plane deformation of ceiling diaphragms is therefore expressed as:

$$\Delta_{\text{total}} = \Delta_{\text{flexural}} + \Delta_{\text{ss}} \quad \text{Eq. 16}$$

Where:

$\Delta_{\text{flexural}}$  is the deflection contribution due to in-plane bending deformation of the diaphragm. The primary contribution of a timber diaphragm to bending rigidity is attributed to the chords of the diaphragm.

$\Delta_{ss}$  is the deflection contribution due to screw slips in combination with in-plane shear deformation of the diaphragm.

The flexural deformation component is calculated using the following equation:

$$\Delta_{flexural} = 5PL^3/(192EAB^2) \quad \text{Eq. 17}$$

Where E is the elastic modulus of the chords, which is taken as  $E = 8,000$  MPa as for SG8 timber, A is the sectional area of one chord of the diaphragm, B is the distance between diaphragm chord members (plan dimension of the diaphragm parallel to the loading) and L is the plan dimension of the diaphragm perpendicular to the loading under consideration.

The combined slip-shear deformation component is calculated using the following equation:

$$\Delta_{ss} = PL/(8G_e B t_e) \quad \text{Eq. 18}$$

Where  $t_e$  is the effective thickness of plasterboard ceiling diaphragm and it is taken as the thickness of the plasterboard sheets, and  $G_e$  is the equivalent shear modulus of the diaphragms, which combines the effects of shear deformation within the plasterboard and the slip deformation of screw fixings.  $G_e$  will degrade as loading progresses, leading to non-linear performance of ceiling diaphragms.

The equivalent shear modulus at different loading peaks is derived using Eq. 16–18, based on the test result obtained from the full-scale ceiling diaphragm test. The calibrated equivalent shear modulus is listed in Table 27.

**Table 27. Equivalent shear modulus,  $G_e$ , of the full-scale ceiling diaphragm test.**

| V (kN/m) | $\Delta$ (mm) | $G_e$ (MPa) |
|----------|---------------|-------------|
| 1.1      | 0.5           | 450         |
| 1.9      | 1             | 370         |
| 2.5      | 1.6           | 300         |
| 3.6      | 2.75          | 220         |
| 3.6      | 4.5           | 160         |
| 3.6      | 5             | 140         |
| 4.0      | 6             | 110         |

- V is the shear action in the two sides of the diaphragm, parallel to the loading direction.
- $\Delta$  is the translational deflection at mid-span of the diaphragm relative to the support.

As demonstrated in Table 27, equivalent shear modulus,  $G_e$ , degrades with the deformation progresses, as revealed from the full-scale plasterboard ceiling diaphragm test.

Based on the relative rigidity values derived from the small-scale ceiling diaphragm tests, the equivalent shear modulus of plasterboard ceiling diaphragms with different details from the full-scale test are estimated. Table 28 lists the estimated equivalent shear modulus for various joint details in ceiling diaphragms.

**Table 28. Estimated equivalent shear modulus,  $G_e$ .**

| In-plane translation (mm) | $G_e$ of full-scale test (MPa) | $G_e$ (detail B) (MPa) | $G_e$ (detail C) (MPa) | $G_e$ (detail D) (MPa) |
|---------------------------|--------------------------------|------------------------|------------------------|------------------------|
|---------------------------|--------------------------------|------------------------|------------------------|------------------------|

|      |     |     |      |    |
|------|-----|-----|------|----|
| 0.5  | 450 | 397 | 7500 | 97 |
| 1    | 370 | 326 | 6167 | 80 |
| 1.6  | 300 | 265 | 5000 | 65 |
| 2.75 | 220 | 194 | 3667 | 47 |
| 4.5  | 160 | 141 | 2667 | 35 |
| 5    | 140 | 124 | 2333 | 30 |
| 6    | 110 | 97  | 1833 | 24 |

## B5 Summary

In this appendix, following a literature review of research efforts on the in-plane behaviour of floor/ceiling diaphragms, a review of New Zealand standards requirements and common practice on floor/ceiling diaphragms was undertaken. The review revealed that the majority of research conducted was based on overseas practice and bore little relevance to New Zealand applications.

A test programme was proposed and a series of tests on plasterboard ceiling diaphragms were carried out at BRANZ as part of the work in this reported project. From the tests, the characteristics of in-plane behaviour of plasterboard ceiling diaphragms were studied, and a mathematical modelling technique for plasterboard ceiling diaphragm was proposed.

Conclusions of the study as reported in this appendix:

- When the plasterboard ceiling diaphragm is subjected to in-plane loading, the entire plasterboard lining behaves like one monolithic plate.
- When plasterboard ceiling diaphragms are subjected to in-plane loading, about 80% of total in-plane deformation is due to the slips of screws from plasterboard linings to the frames.
- The beam analogical method in predicting in-plane deflection of floor diaphragms as in NZS 3603:1993 can be used in estimating the rigidity of plasterboard ceiling diaphragms if the screw slip model is adequate.
- Stiffness degradation of the plasterboard ceiling diaphragm is very significant as the loading progresses.
- A mathematical model has been developed for simulating the in-plane rigidity of a plasterboard ceiling diaphragm, and the developed model is easy to use when diaphragms are modelled as plate elements.